DESIGN AND ANALYSIS OF A VARIABLE-COMPRESSION -RATIO INTERNAL-COMBUSTION ENGINE - THE ALVAR ENGINE CONCEPT

by

MARCUS STEWART

B.S., Department of Mechanical Engineering
University of Tennessee, Knoxville
(1995)

SUBMITTED IN PARTIAL FULFILLMENT OF THE
REQUIREMENTS FOR THE DEGREE OF

MASTER OF SCIENCE
IN
MECHANICAL ENGINEERING

at the
MASSACHUSETTS INSTITUTE OF TECHNOLOGY

June 1997
© 1997 Massachusetts Institute of Technology
All rights reserved

Signature of Author____
Department of Mechanical Engineering
May 16, 1997

Certified by____
Victor W. Wong
Lecturer, Department of Mechanical Engineering
Thesis Supervisor

Accepted by____
Ain A. Sonin
Chairman, Department Committee on Graduate Studies
Department of Mechanical Engineering

MASSACHUSETTS INSTITUTE
OF TECHNOLOGY

JUL 21 1997 Eng.

LIBRARIES

Design and Analysis of A Variable-Compression -Ratio Internal-Combustion Engine - The Alvar Engine Concept

by

Marcus Stewart

Submitted to the Department of Mechanical Engineering
in Partial Fulfillment of the Requirements for the Degree
of Masters of Science in Mechanical Engineering

Abstract

The internal-combustion engine operates over a wide range of conditions. These conditions include boosted intake pressures and increased fuel rate to deliver maximum power output and, most of the time, part loads with emphasis on fuel efficiency. Inherent in the internal-combustion engine design is the compression ratio. The compression ratio affects engine efficiency and the charge temperature and pressure prior to ignition, and thus the engine's tendency to knock. Maximum power output of an engine is therefore influenced by the compression ratio.

The Alvar engine represents an attempt to capitalize on the benefits available from varying the compression ratio of the internal-combustion engine. One main advantage of the Alvar concept stems from the ability to operate at higher power output at a given engine size (power density) via a combination of higher intake pressure (boost) and lower compression ratio at the maximum load condition to avoid knock. Another advantage of the Alvar approach is the thermal efficiency gain by operating at higher compression ratios at part loads.

This work includes the design and analysis of the Alvar engine. Through a performance analysis using a quasi-dimensional four-stroke cycle engine simulation, the Alvar concept has been found to effectively extract the benefits associated with the compression-ratio flexibility.

The analysis included in this thesis reveals that close to six percent improvement of engine efficiency at very light load and 3.8 percent improvement in energy-weighted-average urban-driving-cycle efficiency are attainable by the Alvar engine. Furthermore, this work reveals a significant advantage in the reduction of knock likelihood in the Alvar engine during turbocharged operation, allowing an increase in power density.

This thesis recommends an optimal and practical design of the Alvar combustion chamber to be sized at 34.0 mm secondary bore and 39.9 mm secondary stroke, secondary connecting-rod length at 101.1 mm, and a clearance volume of 42.3 cc to fit onto an existing engine block of a Volvo 850 engine. Physical testing of the proposed design will further determine the success of the Alvar engine concept.

Thesis Supervisor: Dr. Victor W. Wong
Title: Principal Research Scientist - Sloan Automotive Laboratory
Lecturer - Department of Mechanical Engineering

Table of Contents

Cover 1

Abstract 3

Table of Contents 5

Acknowledgments 8

Definition of Symbols and Abbreviations 9

List of Figures 11

List of Tables 14

Chapter 1 Variable Compression Ratio Background 15

- 1.1 Previous Variable Compression Ratio Methods 15
- 1.2 The Alvar Variable Compression Ratio Engine Concept 16
- 1.3 Objectives of the Present Study 17
- 1.4 Scope of Work and Approach 18
- 1.5 Organization of Thesis 19

Chapter 2 Validation of Engine Simulations 21

- 2.1 Introduction 21
- 2.2 The MIT Engine Cycle Simulation 22
- 2.3 The Alvar Engine Cycle Simulation 23
- 2.4 Matching MIT and Alvar Inputs 25
- 2.5 Comparison of MIT and Alvar Simulation Results 28
  - 2.5.1 Comparison between MIT and Alvar (Hoglund) Simulations 28
  - 2.5.2 Comparison of Simulations against Experimental Data 29
- 2.6 Summary 31

Chapter 3 Parametric Studies 33

- 3.1 Approach 33
- 3.2 Effect of Secondary Bore 35
- 3.3 Effect of Phase Shift 37
- 3.4 Summary 41

Chapter 4 Alvar Engine Design 43

- 4.1 Introduction 43

4.2 Scope of Work and Approach 43

4.3 Conventional Cylinder Head 44

4.4 Phase and Nominal Compression Ratio Requirement 45

4.4.1 Determination of Knock and Compression-Ratio Constraints 45

4.4.2 Determination of Secondary Bore, Stroke, and Clearance Volume Combinations 47

4.5 Flame Travel Requirement 55

4.6 Engine Performance Constraint 61

4.7 Alvar Piston Design 64

4.8 Obtaining Clearance Volume 64

4.8.1 Existing Geometry 65

4.8.2 Modifying Piston 68

4.8.3 Modifying Cylinder Head 70

4.9 Positioning of Alvar Piston 72

4.10 Clearance Volume Change 73

4.11 Discussion 74

4.12 Summary 75

Chapter 5 Compression-Ratio Effect on Efficiency 77

5.1 Introduction 77

5.2 Alvar-Conventional Engine Comparison at Baseline Conditions 78

5.3 Compression-Ratio Schedule 80

5.4 Alvar-Conventional Engine Comparison at Various Speed-Load Conditions 81

5.5 Alvar-Conventional Engine Comparison for EPA Driving Cycle 83

5.6. Summary 87

Chapter 6 Turbocharged Alvar 89

6.1 Introduction 89

6.2 Knock Background 89

6.3 Modifications to Alvar Simulation & Test Runs 90

6.4 Analysis of Test Runs 92

6.5 Test Conditions 94
6.6 Results of Comparison 95
6.7 Summary 99
Chapter 7 Variable Engine Displacement 101
7.1 Introduction 101
7.2 Definition of Displaced Volumes 101
7.3 Mean Effective Pressures 103
7.4 Variable Engine Displacement 106
7.5 Summary 107
Chapter 8 Summary and Conclusions 109
References 111
Appendices 113
Appendix A: Alvar Simulation Variables 115
Appendix B: Alvar Patent 131

Acknowledgments

I begin this portion of my thesis by thanking God for the opportunities of life and specifically for bestowing me with the abilities necessary to accomplish the works placed in this document. Next, I extend my gratitude to my parents for serving as such inspiring role models, attesting to the benefits of perseverance and foresight. And to my brothers and other loved ones who continuously provide encouragement, I extend thanks.

To continue, I would like to acknowledge those whose direct interaction contributed positively to this thesis. I greatly appreciate John Heywood and Victor Wong for providing the academic guidance and support that created an environment that stretched my technical competency and therefore contributed to the evolution of a better engineer. Additionally, the remaining members of the Sloan Automotive Laboratory receive my thanks for contributing, in an aggregate sense, to the success of this work.

Last but not least, I would like to acknowledge Anders Hoglund, whose simulation is the foundation of this work. I thank Anders for showing me the intricacies of the simulation. I thank Prof. Gunnar Lundholm for his kindness and encouragement all along. J.R. Linna was very helpful to me personally, as a friend, with his knowledge of the Volvo engine. In the final stage of the project, I had the benefit of looking at the work of Melvin Woods with Adiabatics, Inc. To all these people, I extend my gratitude.

This project is sponsored by the U.S. Department of Energy (Prime Contract Grant #01-95EE15618) and the Swedish Board for Industrial and Technical Development (NUTEK) via a subcontract from Alvar Engine, AB.

Definition of Symbols and Abbreviations

θ - crank angle
φ - fuel air ratio
γ - ratio of specific heats
η_c - compressor efficiency
$\eta_{f,i}$ - fuel conversion efficiency
θ_o - crank angle at combustion start
η_t - turbine efficiency
τ_t - induction time
a - Wiebe function constant
A - area
A0 - spark timing
A50 - 50 % burn duration
ABDC - after - bottom - dead - center
afr - air-fuel ratio
ATDC - after - top - dead - center
B - bore
b1 = bore1 - primary bore
b2 = bore2 - secondary bore
BBDC - before - bottom - dead - center
BDC - bottom - dead - center
BMEP - brake mean effective pressure
B_{ref} - reference bore
c - mass burn rate constant
c_d - discharge coefficient
cfc1 - primary pin friction coefficient
cfc2 - secondary pin friction coefficient
cfc - camshaft friction coefficient
cgk - charge gas kappa value
clv. - clearance volume
CMBMEP - compression stroke brake mean effective pressure
conht - heat transfer coefficient
conrl - connecting rod length
cpd1 - primary crank pin diameter
cpd2 - secondary crank pin diameter
CR - compression ratio
CR_{ref} - reference compression ratio
csd - camshaft diameter
csr - crank shaft speed ratio
cra1 - primary crank radius
cra2 - secondary crank radius
crl1 - primary connecting rod length
crl2 - secondary connecting rod length
crm1 - primary connecting rod mass
crm2 - secondary connecting rod mass
csr - crank speed ratio
cvmin - minimum compression stroke volume
D90 - 10-90 % burn duration
D99 - 1-99 % burn duration
D100 - 0-100 % burn duration
deg. - degrees
DL - differential heat loss
dtburn - burn duration
egk - exhaust gas kappa value
EGR - exhaust gas recirculation
EHL - exhaust heat loss
EPBMEP - expansion stroke brake mean effective pressure
EVC - exhaust valve closing time
EVL - exhaust valve lift
evmin - minimum exhaust stroke volume
EVO - exhaust valve opening time
EXBMEP - exhaust stroke brake mean effective pressure
fhc - fuel heat of combustion
fmw - fuel vapor mole weight
gpd1 - primary gudgeon pin diameter
gpd2 - secondary gudgeon pin diameter
GIMEP - gross mean effective pressure
h - convective heat transfer constant
hlc - wall heat transfer coefficient
IBMEP - intake stroke brake mean effective pressure
IEF - indicated effective pressure
IVC - inlet valve closing time
IVL - inlet valve lift
ivmax - maximum intake stroke volume

IVO - inlet valve opening time
kat - kappa activation temperature
L - stroke
m - Wiebe function constant
mbd1 - primary main bearing diameter
mbd2 - secondary main bearing diameter
N - cylinder numbers
NCR - nominal compression ratio
n_r - number of crank revolutions per power stroke
N_{ref} - reference cylinder numbers
ncy - number of cylinders
offset2 - secondary piston offset
OR - octane requirement
OR_{ref} - reference octane number
p_1 - compressor inlet pressure
p_2 - compressor exit pressure
p_3 - turbine inlet pressure
p_4 - turbine exit pressure
Pamb - ambient pressure
P_b - brake power
pdry - dry air pressure
p_e - cylinder exhaust pressure
Pexhaust - exhaust manifold pressure
p_f - friction pressure
pfc1 - primary piston friction coefficient
pfc2 - secondary piston friction coefficient
phi - fuel - air ratio
p_i - cylinder inlet pressure
$p_{i,wot}$ - intake pressure at WOT
Pintake - intake manifold pressure
pim1 - primary piston mass
pim2 - secondary piston mass
pivc - cylinder pressure at inlet-valve-closing
Pmax - maximum cylinder pressure
p_o - stagnation pressure
p_s - static pressure at restriction
Pu - unburned cylinder gas pressure
Q_{HV} - fuel heating value
Q_w - wall heat loss
R - universal gas constant
r_c - compression ratio
$r_{c, ref}$ - reference compression ratio
rfc1 - primary top ring friction coefficient
rfc2 - secondary top ring friction coefficient
rpm - revolution per minute
s - crank pin to piston pin distance
s1 = stroke1 - primary stroke
s2 = stroke2 - secondary stroke
T_1 - compressor inlet temperature
T_2 - exit compressor temperature
T_3 - turbine inlet temperature
T_4 - turbine exit temperature
ta - Alvar induction time
Tamb - ambient temperature
tbt - transmission belt tension
T_b - brake torque
tc - conventional induction time
tcha - charge temperature
Tcw - cylinder wall temperature
TER - total energy release
Tfresh - charge temperature
T_g - gas temperature
Thead - cylinder head temperature
t_o - initial time
T_o - stagnation temperature
Tpiston - piston temperature
Tspark - spark timing
Tu - unburned cylinder gas temperature
T_w - wall temperature
V - cylinder volume
V_c - clearance volume
V_d - displaced volume
vivc - volume at inlet - valve - closing
vevo - volume at exhaust valve opening
W_c - compressor work
$w_{f,c}$ - friction work through cycle
WHL - wall heat loss
WI - indicated work
wj - water jacket
WOT - wide open throttle
w_p - pumping work
x_b - burned mass fraction
yy - piston crown to cylinder base distance

List of Figures

Figure 2.1: Mass fraction burned versus normalized crank angle 27
Figure 2.2: Comparison of MIT and Alvar simulations to experimental Volvo data - cylinder pressure versus crank angle for 900 RPM and part load 30
Figure 2.3: Comparison of MIT and Alvar simulation to experimental Volvo data - cylinder pressure versus crank angle for 900 RPM and WOT 31
Figure 3.1: Brake mean effective pressure vs. secondary bore for given geometry 36
Figure 3.2: Nominal compression ratio versus secondary bore for given geometry 36
Figure 3.3: Nominal compression ratio versus phase shift for geometry 38
Figure 3.4: Brake mean effective pressure versus phase shift for given geometry 39
Figure 3.5: Indicated fuel conversion efficiency versus phase shift for given geometry 40
Figure 4.1: Knock Requirement - compression ratio versus intake pressure extracted from Patton Thesis 46
Figure 4.2: Nominal compression ratio versus phase shift for given geometry 49
Figure 4.3: Compression ratio range versus clearance volume 50
Figure 4.4: Secondary stroke versus secondary bore combinations meeting compression-ratio range constraint 53
Figure 4.5: Secondary piston position at 15 degrees ATC and nominal compression ratio versus phase shift for b2 = 36.00 mm, s2 = 35.10 mm, crl2 = 61.78 mm and clearance volume = 42.38 cc 54
Figure 4.6: Schematic of spark plug in-cylinder chamber locations 55
Figure 4.7: Simple Alvar cylinder head side and top view with emphasis on flame travel length to secondary crevice 57
Figure 4.8: Piston position versus crank angle for phase of 0 degrees and nominal compression ratio of 13:1 58

Figure 4.9: Piston position versus crank angle for phase of 180 degrees and nominal compression ratio of 7:1 59
Figure 4.10: Secondary corner angular position at 15 degrees ATC versus secondary bore for given phase shift 60
Figure 4.11: Cylinder wall heat loss versus secondary geometry for part load and WOT operation, and engine speed of 3000 RPM 62
Figure 4.12: Torque versus secondary piston geometry for part load and WOT operation, engine speed of 3000 RPM 63
Figure 4.13: Side view of conventional piston 65
Figure 4.14: Top view of conventional piston 66
Figure 4.15: 3-Dimensional schematic of pentroof cylinder head design 66
Figure 4.16: Combined top view of cylinder head and piston top 67
Figure 4.17: Addition to piston for purpose of reducing clearance volume 68
Figure 4.18: Side view of modified conventional piston 69
Figure 4.19: Side view of modified piston and cylinder head 70
Figure 4.20: Side view of pentroof cylinder and dimensions to cut for cylinder head reduction 71
Figure 4.21: Side view of modified cylinder head with secondary piston 72
Figure 4.22: Top view of Alvar cylinder head with dual spark plug design 73
Figure 5.1: Brake power and torque versus engine speed for conventional Volvo 850 engine 79
Figure 5.2: Compression ratio versus load schedule 81
Figure 5.3: Energy-weighted brake efficiencies for conventional and Alvar engines for EPA City Driving Cycle 86
Figure 6.1: Alvar compression ratio-load schedule for turbocharged case study 95
Figure 6.2: Time required to autoignite versus boost pressure for conventional and Alvar (CR=7.3) engines at 3000 RPM, with MBT 96
Figure 6.3: Time required to autoignite versus boost pressure for conventional and scheduled (variable CR) Alvar engines at 3000 RPM, with MBT 97

Figure 6.4: In-cylinder unburned gas temperature versus brake power for scheduled Alvar and conventional engines at 3000 RPM, MBT 98

Figure 6.5: Knock induction time versus brake power for Alvar and conventional engines 99

Figure 7.1: Depiction of intake, compression, expansion, and exhaust displaced volumes for the Alvar engine at 0 degrees phase shift 102

Figure 7.2: Displaced volume versus crank angle, with phase of 0 degrees and nominal compression ratio of 13:1 104

Figure 7.3: Displaced volume versus crank angle, with phase of 180 degrees and nominal compression ratio of 7:1 104

Figure 7.4: BMEP versus phase for given displaced volumes, with engine speed of 3000 RPM, WOT operation, and MBT 106

List of Tables

Table 2.1 Simulation Inputs 25

Table 2.2 Simulation Test Cases 28

Table 2.3 Comparison Results 29

Table 3.1 Set Engine Parameters 33

Table 3.2 Connecting Rod Length Influence 41

Table 4.1 Conventional Engine Specifications 44

Table 4.2 Combinations for Nominal Compression Ratio - Phase Shift Study 48

Table 4.3 Additional Secondary Bore and Stroke Combinations 50

Table 4.4 Combinations that meet the Compression-Ratio Constraints 52

Table 4.5 Geometrical Parameters for Relative Piston Position Study 57

Table 4.6 Summations of Reductions for Modified Cylinder Head Approach 71

Table 5.1 Brake Power and Torque from Conventional Engine via Alvar Simulation 79

Table 5.2 Matching Alvar and Conventional Engines for Efficiency Comparison 80

Table 5.3 Conventional and Alvar (CR = 12.8) Engines at Low Load = 50 Nm 82

Table 5.4 Conventional and Alvar (12.5) Engines at Medium Load = 100 Nm 82

Table 5.5 Conventional and Alvar (CR = 10.1) Engines at High Load = 200 Nm 82

Table 5.6 EPA City Driving Cycle - Alvar CR Schedule 84

Table 5.7 Conventional Engine Under EPA City Driving Cycle 85

Table 5.8 Alvar Engine Under EPA City Driving Cycle 85

Table 6.1 Induction Time Comparison 96

Table 7.1 Effect of Compression Ratio on BMEP's via Alvar Simulation 105

Chapter 1

Variable Compression Ratio Background

The motivation to increase the efficiency and power density of the spark-ignition internal-combustion engine has fueled interest in the variable-compression-ratio engine. The primary advantages of a variable-compression-ratio engine are twofold. An ideal cycle analysis reveals that thermal efficiency increases with compression ratio [1]. The other advantage in changing the compression ratio of a spark-ignition (SI) engine lies in the ability to boost the intake pressure, thus the engine power output, without prematurely reaching knock limits. The compression ratio in an SI engine is limited by the knock phenomenon and fuel octane. Therefore, by reducing the compression ratio selectively at the high-load operating conditions, increased charge pressures may be used and increased power obtained without reaching the knock limit.

1.1 Previous Variable Compression Ratio Methods

Several methods have been used to vary the compression ratio of an internal-combustion engine. One method that has been cited and remains in use today is variable valve timing such as that used in the Miller Cycle [2]. Mazda has effectively used variable valve timing to change the effective compression ratio. One feature of the valve-timing approach is the ability to change the effective expansion volume by moving the opening of the exhaust valve closer to or further away from bottom-dead-center (BDC). Increasing displaced volume at part loads and decreasing it at the wide-open-throttle (WOT) condition are the results. This engine achieves a high compression ratio and high boost by delaying inlet-valve-closing (IVC) and using a specially-designed compressor. However, adequate transition times are dependent on a reliable and sophisticated control system.

Another method includes the movement of an adjustable piece of the cylinder head within a secondary chamber to nominally vary the clearance volume, thus the compression ratio. This approach has been studied extensively by Volkswagen [3]. The secondary piece recedes from the chamber to increase the clearance volume, and therefore decreases the compression ratio, during full-throttle operation. Similarly, the secondary piece moves closer towards the combustion chamber, to be flush with the cylinder head, to decrease the clearance volume, and therefore increases the compression ratio, during part-load operation. One possible problem with this technology is that consistent movement of the secondary piece may be questionable due to deposit and friction build-up.

A third method used to vary the compression ratio is to vary the crank radius in order to vary the clearance and swept volumes. A study at the Warsaw University of Technology [4] found that variation of the compression ratio could be accomplished by introducing an adjustable link between the crank and the connecting rod. However, there are foreseeable cost increases as a result of increased mechanical complexity.

Yet another method of varying the compression ratio is by varying the piston-crown height [5,6]. The complex piston has the drawback of increased weight and cost. Also, the intricacy of the piston raises concerns of production consistency and durability in operation.

Although the above methods vary in approach and application, each of the concepts attempted before has some major disadvantages. This thesis introduces an approach to achieve reliable and effective variations in compression ratio, as well as to increase the power density of the engine, hereafter called the Alvar engine, in honor of its inventor, Alvar Gustavsson.

1.2 The Alvar Variable Compression Ratio Engine Concept

The work being presented here focuses on the Alvar engine concept, which differs from the methods previously mentioned as it incorporates a moving secondary piston. The Alvar concept achieves variable compression ratios by changing the motion of a reciprocating auxiliary piston (secondary piston), which moves towards and recedes from the cylinder head. The motion of the secondary piston, in relation to that of the primary piston, is varied through a servo-control system. The control system traces a specified of combustion within 60 crank-angle degrees is critical. In general, combustion stability increases with flame speed; an optimal flame speed would be conducive to the control of NOx emissions.

Another issue of concern in designing the cylinder head is the volumetric efficiency. This design attempts to at least maintain, and not deteriorate, the current level of volumetric efficiency. Volumetric efficiency is primarily governed by the design of the engine valves and ports which generate turbulence. However, adequate turbocharging (or supercharging) of the engine can alleviate some of the concerns.

One more issue of concern in designing the Alvar engine is heat transfer. Heat transfer affects not only the efficiency of the engine but also, perhaps more importantly, the structural integrity of the cylinder head due to thermal stresses.

Finally, the knock characteristics of the engine are studied in the design of the combustion chamber. Engine knock acts to limit the compression ratio, thereby limiting the engine efficiency. The determination of the likelihood of engine knock will be addressed extensively in this work.

1.4 Scope of Work and Approach

The work presented in this thesis includes an analysis of the Alvar variable-compression-ratio engine concept and the geometric factors for one Alvar engine combustion system. This work examines the Alvar engine's ability to deliver increased efficiency at part loads and increased power density at boosted intake pressures. Other characteristics of the Alvar engine are also examined.

The material presented in this thesis is broken into two primary parts. The first part addresses the effects of individual design parameters on the Alvar engine's performance, using appropriate cycle simulations, and the development of a recommended Alvar-engine combustion-chamber design. The second part consists of a detailed engine-performance evaluation, including the effects of the special capabilities of the Alvar engine, such as variable-displacement-volume features.

load and speed schedule to attain the appropriate compression ratios. The crankshafts of the two pistons are linked through a pulley system, not unlike that connecting a crankshaft and camshaft, that allow a specified speed ratio of the two pistons to be maintained. The change in the relative piston motion serves to vary the clearance volume and the cylinder displacement volume.

Lia [7] performed a study on the Alvar engine concept and found that the idea was feasible and had the main advantage of eliminating the damage to the secondary piston due to deposit build-up. The main advantages of the Alvar concept over other variable-compression-ratio approaches are that: 1) the secondary piston is in constant motion so that soot and hydrocarbon deposits do not occur, 2) the Alvar system is mechanically simple, 3) the Alvar system allows for variable displacement volumes as well as variable compression ratios, and 4) the effective compression ratio can still be varied through valve-timing control.

1.3 Objective of the Present Study

The objective of this project is to develop a geometric design for a combustion chamber of an Alvar engine system. This project constitutes one task in a multi-tasked program to develop and demonstrate the feasibility of the Alvar engine system. The combustion chamber will be built into a modified cylinder head, which will fit onto an existing Volvo 850 engine cylinder block. Therefore, specifications for the primary chamber and piston are given. The secondary chamber specifications needed to be studied include piston bore, stroke, connecting rod length and piston offset. Additionally, outside the overall design of the cylinder-head components, the phase-shift logic as a function of speed-load schedule in achieving certain variations in compression ratio is necessary. Furthermore, these efforts attempt to achieve the proper design without introducing compromises with other factors such as combustion reliability, volumetric efficiency, heat transfer, and the increased risk of engine knock.

In terms of combustion reliability, the need to produce a cylinder-head and combustion-chamber design that maintains a moderate flame travel speed and is capable

1.5 Organization of Thesis

The next Chapter, Chapter 2, provides insight into the tools used in the analysis, namely the MIT and Alvar cycle simulations. Chapter 3 includes a parametric study of the Alvar engine concept. Next, Chapter 4 describes the design process used to develop a recommended Alvar combustion-chamber design. The subsequent chapters focus on the performance aspects of the Alvar engine. These areas include an analysis of engine efficiencies in Chapter 5 and an analysis of the turbocharged operation of the Alvar engine for higher power density in Chapter 6. In each case, comparisons with a conventional engine are made. Next, in Chapter 7, the issue of variable displacement volume is addressed with emphasis on its effect on the mean effective pressure. The thesis concludes with a summary of this work, which is just a part of a larger program in the development of the Alvar engine.

Chapter 2

Validation of Engine Simulations

2.1 Introduction

To begin the Alvar engine analysis, two four-stroke engine simulations were used: the MIT and the Alvar simulations. The two simulations were used in order to compare the outputs and thereby confirm the reliability of the simulations. Since the MIT simulation for conventional engines has been validated in many applications over the years, comparison of this simulation with the Alvar simulation serves to raise confidence in the simulations. The Alvar simulation will be used heavily in our subsequent analysis. The Alvar simulation is capable of simulating the operation of a conventional engine as well, as a special case. The outputs from both simulations were further validated by comparing both outputs with experimental data from a single-cylinder engine that has the combustion-chamber configuration of a Volvo-850 in the Sloan Automotive Laboratory.

The two simulations are similar in many respects. However, the MIT simulation takes into account gas-exchange processes and is slightly more comprehensive, while the Alvar simulation focuses on the special features of the Alvar engine.

In comparing the simulations, we examine the performance of a five-cylinder engine. The gas exchange, heat transfer, and combustion processes as well as the engine thermodynamics are described here. The approaches to calculating the friction work are also included.

2.2 The MIT Engine Cycle Simulation

The MIT simulation code is designed to simulate the spark-ignition four-stroke internal-combustion engine over a large range of operating conditions and geometric specifications. This simulation is a quasi-dimensional model in that it is designed to describe changes in the bulk properties of the cylinder contents. However, it does have a flame propagation model that describes the development of the flame front across the combustion chamber.

The cycle consists of the intake, compression, expansion (combustion), and exhaust processes which are treated as a sequence of processes within a multi-cylinder engine. The gas-exchange process calculates the mass flow rate across the valves, given the opening area, discharge coefficient, and the pressure ratio across the valves. The gas-exchange process is governed by the following relation,

$$dm/dt = [c_d A p_o/(RT_o)] * (\gamma R T_o)^{1/2} * [2/(\gamma-1) * (p_s/p_o) * (2/\gamma) - (p_s/p_o) * (\gamma+1)/\gamma]^{1/2}$$

where c_d represents the discharge coefficient, A represents the valve opening area, p_o represents the stagnation pressure upstream of the restriction, p_s represents the static pressure at the restriction, T_o represents the stagnation temperature upstream of restriction, γ represents the ratio of specific heats, and R represents the gas constant.

The heat transfer to the cylinder walls is governed by the following relation,

$$dQ_w/dt = hA(T_g - T_w)$$

where h represents the convective heat transfer coefficient, A represents the cylinder wall surface area, T_g represents the gas temperature, and T_w represents the wall temperature. The heat transfer coefficient is derived from a Nusselt-versus-Reynolds-number correlation.

In terms of combustion, the MIT simulation allows the use of a motoring-operation mode, a phenomenological flame-propagation model, or a specified burn-rate curve, which is the Weibe function and will be addressed in detail later in this chapter.

The MIT simulation incorporates friction losses in terms of rubbing and pumping losses. The MIT simulation also includes a turbulent flow model since the combustion and heat transfer models of the cycle simulation require estimates of a characteristic velocity and length scales. The turbulent flow model, which consists of a zero-dimensional energy cascade, is used to estimate these scales while including the physical mechanisms affecting charge motion in the cylinder.

The friction work over the cycle is calculated by summing over the pressure volume curve as shown below,

$$W_{f,c} = \int p_f * dV$$

where $W_{f,c}$ represents the friction work over one cycle, p_f represents the frictional pressure, and dV is the swept volume. Similarly, the pumping work is obtained by calculating the net work to the piston over the exhaust and intake strokes and is reduced as shown below,

$$W_p = (p_i - p_e)\,(\Delta V)$$

where W_p represents the pumping work, p_i and p_e represent the intake and exhaust pressures respectfully, and ΔV represents the change in the volume over the compression or expansion stroke.

2.3 The Alvar Engine Cycle Simulation

The Alvar simulation, otherwise called the Hoglund simulation, also addresses the thermodynamics of the combustion process, gas exchange, heat transfer, and friction processes. The combustion process differs from that of the MIT simulation in that there is no option to operate in a motoring or phenomenological flame-propagation mode . The Alvar simulation uses a cosine function to specify the mass burn rate. This approach is described in more detail later in this chapter. The gas-exchange process of the Alvar simulation differs from that of the MIT simulation in that it is significantly simpler. The Alvar simulation merely takes into account the volume available in the cylinder as a function of crank angle.

The heat transfer mechanism used in the Alvar simulation does not differ from that used in the MIT simulation significantly. The heat transfer approach in the Alvar simulation relies on a First Law energy balance that includes the heat loss through exhaust (EHL), heat loss through the cylinder wall (WHL), and energy responsible for producing the indicated work (WI). These values must continuously match the total energy released (TER) throughout the course of the four-stroke cycle. The simulation provides that the following sum must hold.

$$\mathrm{TER} = \mathrm{EHL} + \mathrm{WHL} + \mathrm{WI}$$

The cylinder-wall heat loss is calculated continuously as conditions change in the combustion chamber per crank angle. The equation below illustrates the iterative response used in the simulation,

$$\mathrm{WHL} = \mathrm{WHL} + \mathrm{DL}$$

where the differential heat loss is represented by DL. The heat loss coefficient is also treated as an input into the simulation. This value must be calibrated to produce correct heat loss values.

The friction analysis implemented in the Alvar simulation includes the frictional characteristics of both the primary and secondary chambers separately. The relationships between the brake, indicated, gross, and friction work terms are conventional. The distinguishing features of the friction calculations in the Alvar simulation are: 1) the introduction of the secondary chamber friction characteristics of the Alvar simulation, and 2) the exclusion of a turbulent flow model by the Alvar simulation. Note that the friction coefficients of the secondary chamber can be scaled from those of the primary piston since there are no novel additional sources of friction to be considered, such as a swirl effect created by the presence of the secondary piston due to the introduction of the secondary chamber.

After the Alvar simulation was checked against the MIT simulation, it was used to gain an understanding of the Alvar engine performance as a function of geometric changes and compression ratio shifts. These studies set the stage for a design analysis of the Alvar engine.

2.4 Matching MIT and Alvar Inputs

The Volvo 850 engine specifications that were input into both simulations are shown below in Table 2.1. The specifications below were extracted from the MIT simulation input file.

Table 2.1 Simulation Inputs

* rpm = 1600
fuel type = propane
phi = 1.00
EGR = 0.00
* Pintake = 0.65 atm
Pexhaust = 1.00 atm
Tfresh = 300. 00 K
Tpiston = 403.00 K
Thead = 373.00 K
Tcw = 363.00 K
conht = 0.04
fire = t (spark ignition)

IVO = 0.00 deg.
IVC = 228.00 deg.
EVO = 488.00 deg.
EVC = 720.00 deg.
Tspark = 340.00 deg.
bore = 83.00 mm
clv. = 53.28 cc
stroke = 90.00 mm
conrl = 158.00 mm
Tamb = 300.00 K
Pamb = 1.00 atm
dtburn = 60.00 deg.

Table 2.1 shows the specifications that were input into both simulations. Note that the marked variables (*) were varied throughout the comparison and that miscellaneous parameters were excluded.

One important difference in the two four-stroke simulations is the means by which the combustion process was simulated. The MIT code relies on a burn-fraction curve called the Weibe function, while the Alvar simulation uses a cosine function. The Wiebe is shown below.

$$x_b = 1 - \exp[-a((\theta-\theta_0)/\,\Delta\theta)^{m+1}]$$

The cosine function used for the mass burn rate of the Alvar simulation is of the form,

$$m_b = c\{1-\cos[\pi(\theta-\theta_0)/\,\Delta\theta]\}$$

where θ is the crank angle, θ_0 is the start of combustion, $\Delta\theta$ is the total combustion duration, a, c and m are constants.

The burned-fraction curves of both programs were matched. This was accomplished by constructing a specified burn-fraction curve (curve in which the percent of mass burned was specified over a crank angle interval) and placing this specification into both simulations. The burn fraction curve is shown in Figure 2.1.

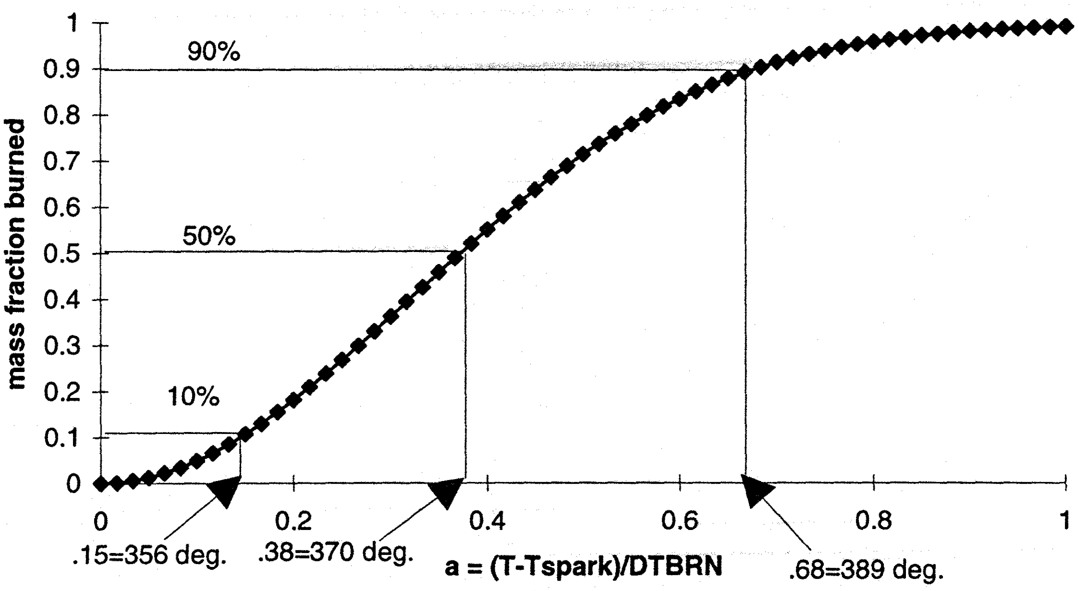

Figure 2.1: Mass fraction burned versus normalized crank angle

As shown in Figure 2.1, the mixture mass is 10 percent burned at 356 degrees of the crank angle, 50 percent burned at 362 degrees and 90 percent burned at 381 degrees. This burned-fraction curve was placed in both simulations. Also note that the heat loss coefficient of the cylinder wall is 0.08 for the Alvar simulation, and 0.04 for the MIT simulation. This coefficient is a soft constraint in that it is varied to create a reasonable heat loss percentage at a reference point. Additionally, the programs were run at stoichiometric fuel-air ratio. Note that the following Volvo 850 geometric specifications were entered into both simulations.

stroke = 90.00 mm   bore = 83.00 mm

conrl = 158.00 mm   clv. = 53.28 cc

Eight cases were run with data from this conventional engine. The varied parameters are listed next in Table 2.2.

Table 2.2 Simulation Test Cases

test	engine speed, rpm	intake press., kPa
case1	900	37.60
case2	900	102.70
case3	1600	37.60
case4	1600	102.55
case5	2400	57.80
case6	2400	101.33
case7	3200	54.10
case8	3200	102.40

2.5 Comparison of MIT and Alvar Simulation Results

2.5.1 Comparison between MIT and Alvar (Hoglund) Simulations

The indicators used here to determine the correlation between the two simulations were the indicated mean effective pressures, maximum cylinder pressure and heat release results. The percent difference in values were calculated for each case. The average percent differences for the gross indicated mean effective pressure (GIMEP), heat loss, and net indicated efficiency are 5.9, 4.8, and 0.9 percent, respectively. Table 2.3 shows impressive agreement exists for heat loss values, as these numbers do not reflect percent heat loss of chemical energy. See Table 2.3.

Table 2.3 Comparison Results

test	GIMEP, kPa	GIMEP, kPa	differ-ence	Ht Loss,J	Ht Loss,J	differ-ence	Net Ind.Eff	Net Ind.Eff	differ-ence
	Hoglund	MIT	%	Hoglund	MIT	%	%, Hogl.	%, MIT	%
case1	364.80	416.50	12.40	28.28	29.51	4.17	34.30	34.20	0.26
case2	1337.50	1274.10	4.97	75.89	67.59	12.28	41.40	41.20	0.44
case3	366.20	410.60	10.81	25.39	27.22	6.72	34.40	34.30	0.41
case4	1339.80	1283.40	4.40	67.95	63.65	6.76	41.50	41.40	0.24
case5	669.40	666.70	0.41	36.70	37.12	1.13	38.90	38.30	1.46
case6	1322.80	1256.90	5.24	62.15	60.25	3.15	41.50	41.30	0.58
case7	614.80	600.50	2.39	32.54	33.51	2.89	38.40	37.50	2.51
case8	1340.90	1255.10	6.84	59.39	58.65	1.26	41.60	41.10	1.27

2.5.2 Comparison of Simulations against Experimental Data

Next, the simulations were compared to experimental cylinder pressure data from the single-cylinder configuration of the Volvo 850. The MIT simulation burn duration of 60 degrees was translated to a 10-90 percent burn duration of 35 degrees and met the experimental pressure curve well. The Alvar simulation maintained the 60 degree duration and visually lags behind the experimental curve slightly more than the MIT simulation as a result. In noting the pressure curves for both part-load and wide-open-throttle operation, there exists a closer agreement at the wide-open-throttle condition is apparent.

Propane was used at 900 rpm and part-load operation in making comparisons between the simulations and against the experimental pressure curve. See Figure 2.2 below.

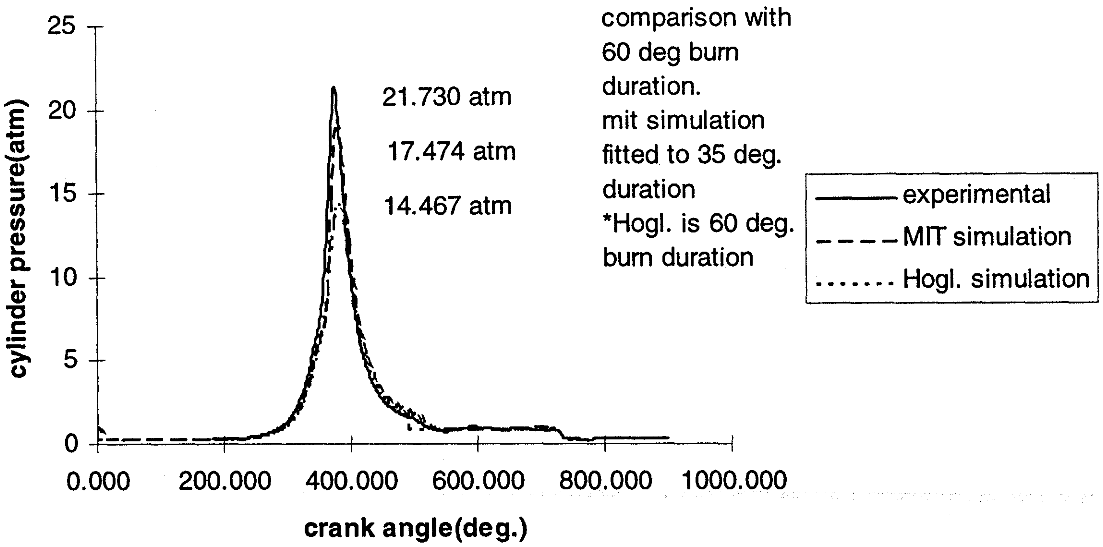

Figure 2.2: Comparison of MIT and Alvar simulations to experimental Volvo data - cylinder pressure versus crank angle for 900 RPM and part load

An equivalent match was made between the simulations and the experimental curve with all constraints maintained except intake pressure, which was increased to WOT. See Figure 2.3 below.

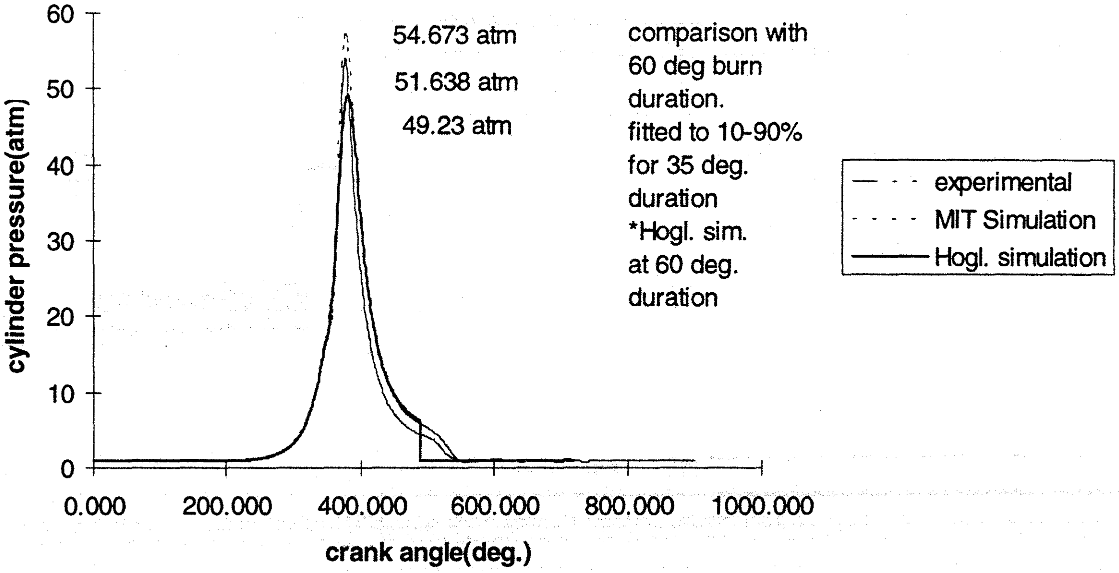

Figure 2.3: Comparison of MIT and Alvar simulations to experimental Volvo data - cylinder pressure versus crank angle for 900 RPM and WOT

2.6 Summary

The comparison between the Alvar and MIT internal combustion simulations proved that the two simulations sufficiently matched. The simulations were also found to match reasonably well with the experimental data. The differences in the approaches of the simulations produced anticipated differences in the results of the models, but despite the small discrepancies, the engine models correlate well. Therefore the Alvar (Hoglund) simulation should be a powerful tool in the analysis and design of the Alvar engine. Hereafter the Alvar simulation will be used.

Chapter 3

Parametric Studies

The parametric study serves to gain insight into the performance characteristics of the Alvar Engine. Any trends identified here would help in understanding the behavior of the Alvar engine and thereby aid in the design process.

3.1 Approach

The approach used in the parametric study is to identify relevant parameters and vary these parameters individually from a set of baseline parameters. The studies were performed with the set of baseline parameters shown in Table 3.1. However, the two asterisks (*) denote changes at some point.

Table 3.1 Set Engine Parameters

Geometry:

bore1(bor1) = 83.00 mm
crank rad.1(cra1) = 45.00 mm
con.rod length1(crl1) = 158.00 mm
crankshaft offset(cso1) = 0.00 mm
clearance vol.(clv) = 58.28 cc
effective compression ratio(ecr) = 10.00

*bore2(bor2) = 40.00 mm
*crank rad.2(cra2) = 2.00 mm
con.rod length2 (crl2) = 80.00 mm
crankshaft offset(cso2) = 0.00 mm
crankshaft speed ratio(csr) = 0.50

Masses:

primary piston mass (pim1) = 700.00 g
primary con.rod mass(crm1) = 700.00 g
secondary piston mass(pim2) = 200.00 g
secondary con.rod mass(crm2) = 200.00 g
no. of cylinders (ncy) = 5

Diameters:

gudgeon pin diameter1(gpd1) = 23.00 mm
crank pin diameter1(cpd1) = 53.00 mm
main bearing diameter1(mbd1) = 64.00 mm
gudgeon pin diameter2(gpd2) = 12.00 mm
crank pin diameter2(cpd2) = 38.00 mm
main bearing diameter(mbd2) = 53.00 mm
camshaft diameter(csd) = 48.00 mm

Friction:

piston friction coeff.1(pfc1) = 0.05
top ring friction coeff.1(rfc1) = 0.18
gudgeon pin friction coeff.1(gfc1) = 0.05
crank pin friction coeff.1(cfc1) = 0.01
main bearing friction coeff.1(mfc1) = 0.01
camshaft friction coeff.(cfc) = 0.20
valve spring force(vsf) = 800.00 N

piston friction coeff.2(pfc2) = 0.05
top ring friction coeff.2(rfc2) = 0.18
gudgeon pin friction coeff.2(gfc2) = 0.10
crank pin friction coeff.2(cfc2) = .01
main bearing friction coeff.2(mfc2) = .01
transmission belt tension(tbt) = 200.00 N

Heat Release:

spark timing(A0) = 340.00 deg.
50% burn fraction(A50) = 367.00 deg.
10 - 90% burn duration(D90) = 18.73 deg.
1 - 99% burn duration(D99) = 47.00 deg.
0 - 100% burn duration(D100) = 54.00 deg.

fuel heat of combustion(fhc) = 46.30 J
fuel vapor mole weight(fmw) = 114.23 g/mole
air fuel ratio(afr) = 14.50
stoichiometric A/F(afr) = 14.50
equivalence ratio = 1.00

Conditions:

engine speed(esp) = 2400 rpm
ambient pressure(pamb) = 101.33 kPa
dry air pressure(pdry) = 101.33 kPa
cylinder pressure @IVC(pivc) = 101.33 kPa
exhaust back pressure(pexb) = 100.33 kPa
ambient temperature(tamb) = 300.00 K

charge temperature(tcha) = 300.00 K
wall temperature(twal) = 300.00 K
cylinder wall heat transfer coeff.(hlc) = 0.08
exhaust gas recirculation(egr) = 0.00
charge gas kappa value(cgk) = 1.38
exhaust gas kappa value(egk) = 1.34
Kappa activation temp(kat) = 1500.00 K

3.2 Effect of Secondary Bore

The first study focused on the effect of secondary bore on indicated mean effective pressure, brake mean effective pressure, maximum cylinder pressure, and nominal compression ratio. Note that the set parameters included clearance volume, secondary bore-stroke ratio, phase (for this section of the study), secondary connecting rod length, secondary-stroke ratio, intake pressure and engine speed. See list below for a summary of set parameters.

clearance volume
phase
secondary connecting rod length (crl2) / secondary stroke (s2)
intake cylinder pressure (Pintake)
engine speed

Note that the effective compression ratio differs from the nominal compression ratio because the valve timing is set to IVC at 56 degrees after BDC and EVO at 48 degrees before BDC as extracted from conventional engine specifications. Each case differs by a secondary bore-stroke ratio which ranged from 0.4 to 1.6.

Figure 3.1 illustrates the effect of secondary bore on brake mean effective pressure. Note that the shorter stroke (higher secondary bore-stroke ratio) serves to increase the mean effective pressure as anticipated since the clearance volume remains constant as displaced volume is decreased.

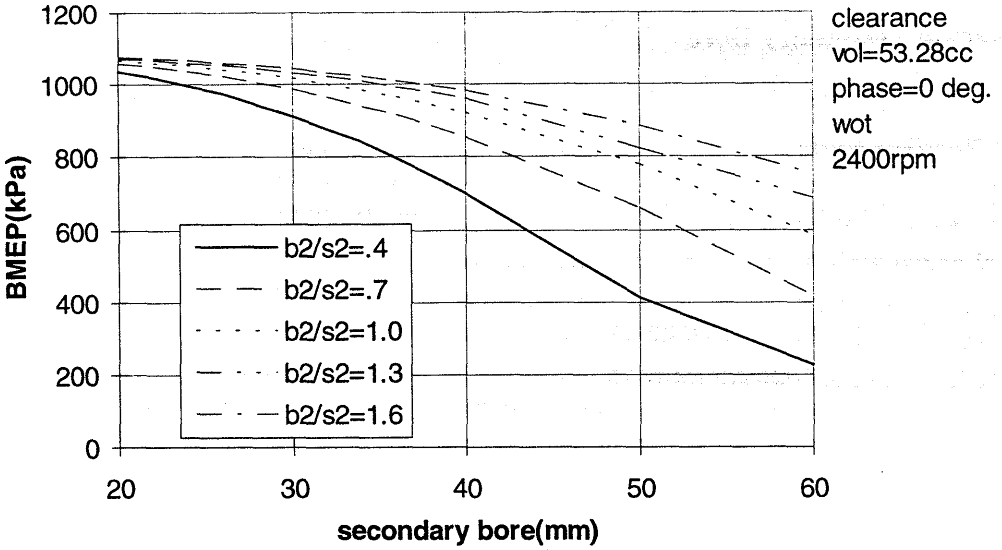

Figure 3.1: Brake mean effective pressure versus secondary bore for given geometry

Next, the geometrical relation between secondary bore and nominal compression ratio is illustrated as clearance volume and phase are held constant. Figure 3.2 shows that in order to maintain the clearance volume with increasing secondary bore, the compression ratio must be increased. This is intuitive since NCR = (Vc + Vd)/Vc. Also note that decreasing stroke serves to minimize this effect.

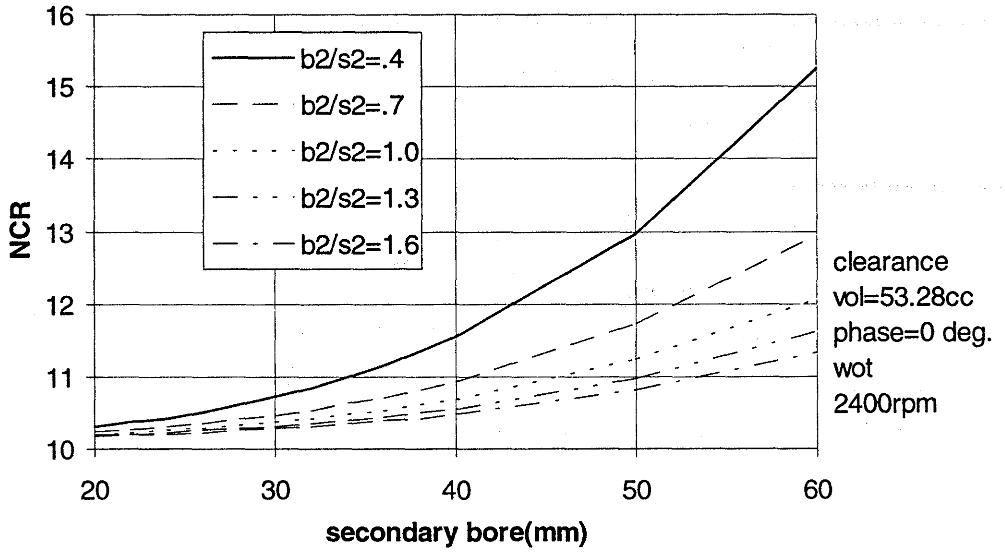

Figure 3.2: Nominal compression ratio versus secondary bore for given geometry

3.3 Effect of Phase Shift

The next relation covered in the parametric study is the effect of phase shift on indicated thermal efficiency (IEF), brake mean effective pressure (BMEP), maximum cylinder pressure (Pmax), and compression ratio. Recall that the phase shift is used solely for the purpose of changing the compression ratio by changing the relative motions of the two pistons, and that this is achieved by adjusting the timing of the secondary piston. Again this study uses conventional primary chamber geometry. For each case, the secondary bore, stroke, and therefore clearance volume is set, and the ratio of secondary connecting rod length to secondary stroke is set to 1.76. Moreover, the engine operates at WOT, 2400 rpm, and the clearance volume is set for a nominal compression ratio of 14 at a phase of 0 degrees. The following list of set and varied parameters was used.

clearance volume
secondary bore (b2)
secondary stroke (s2)
secondary connecting rod length (crl2)
intake cylinder pressure (Pintake)
engine speed

The phase was varied from 0 to 180 degrees for each case. Below is a list of secondary bore and stroke combinations for each case.

b2 = s2

b2 = s2 = 45.0 mm

b2 = s2 = 30.0 mm

b2 = s2 = 20.0 mm

b2 = s2 / 1.5

b2 = 40.0 mm, s2 = 60.0 mm

b2 = 30.0 mm, s2 = 45.0 mm

b2 = 20.0 mm, s2 = 30.0 mm

Figure 3.3 shows how the change in phase varies the nominal compression ratio. Note that the dependence of nominal compression ratio (NCR) on phase must be calibrated into the mechanical system. Also note that the NCR rebounds to a compression ratio of 14 when phase is allowed to sweep from 180 to 360 degrees.

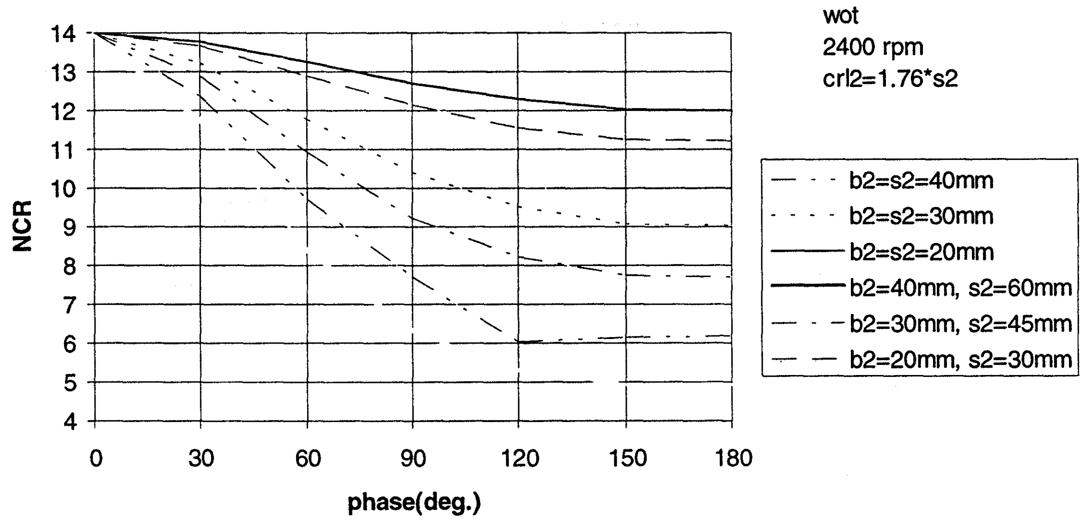

Figure 3.3: Nominal compression ratio versus phase shift for given geometry

Next, the effect of phase on BMEP is shown in Figure 3.4. Again, note the symmetry as the BMEP reaches a minimum at a phase of 90 degrees. Note that the secondary piston has swept half the stroke at combustion when operating at a phase of 90 degrees.

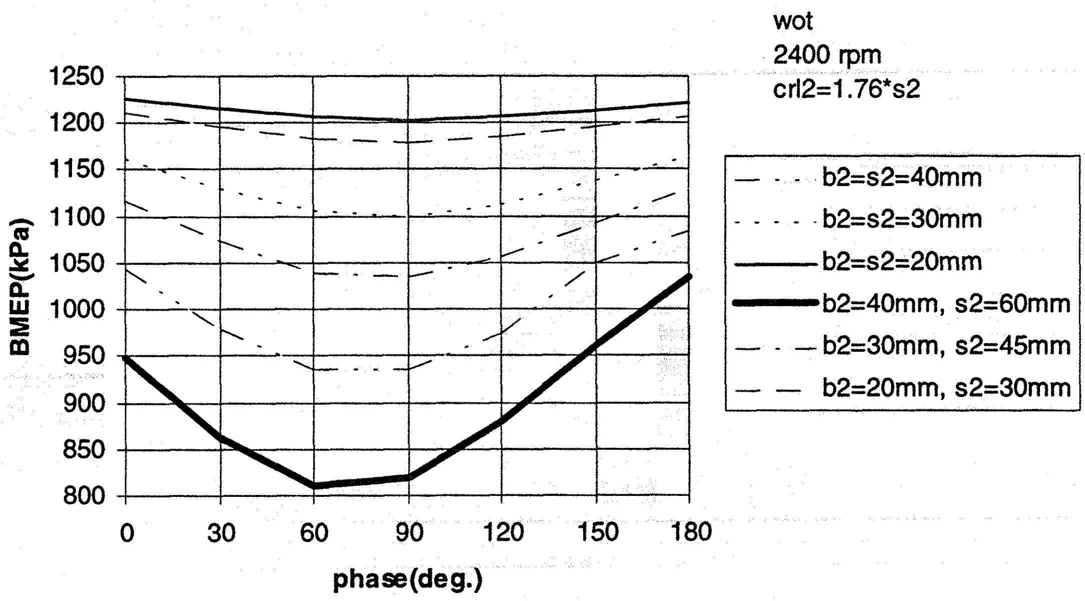

Figure 3.4: Brake mean effective pressure versus phase shift for given geometry

Next, in viewing Figure 3.5, note that the variance of indicated thermal efficiency as a result of phase variance is a direct result of the variance of the nominal compression ratio with phase.

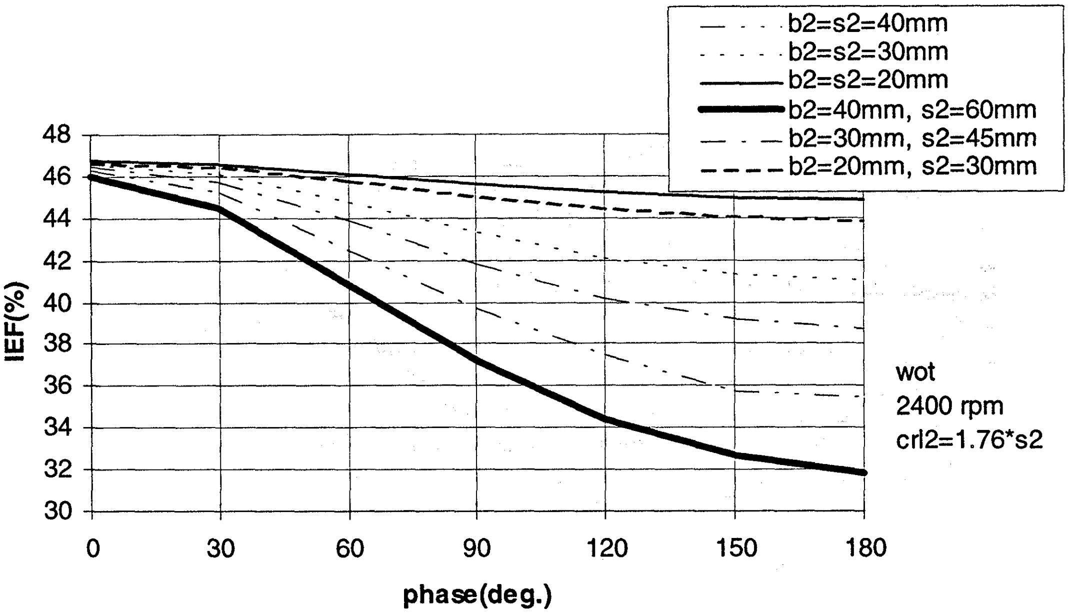

Figure 3.5: Indicated fuel conversion efficiency versus phase shift for given geometry

Finally, the effect of secondary connecting rod length is minute, as anticipated. While secondary bore and stroke were held at 30 mm, WOT operation, an engine speed of 2400 rpm, and a phase of 60 degrees, the secondary connecting rod length was varied from a length of 40 mm to 140 mm. See Table 3.2 for results.

Table 3.2 Connecting Rod Length Influence

CRL2 mm	NCR	IEF %	BMEP kPa
40	11.83	44.83	1106.26
60	11.97	45.98	1111.87
80	12.03	45.06	1114.58
100	12.07	45.10	1116.19
120	12.10	45.13	1117.25
140	12.12	45.15	1118.01

3.4 Summary

The parametric studies in this chapter illustrate the effect of secondary bore and phase on the performance characteristics of the Alvar engine, such as efficiency and mean effective pressure. This study serves to confirm that the mechanisms that motivate this project do exist and that the secondary chamber geometry (i.e. secondary bore and stroke) play a role in optimizing these effects.

Chapter 4

Alvar Engine Design

4.1 Introduction

One of the objectives of this project is to design the geometries of the primary and secondary (Alvar) chambers that will fit into a cylinder head of a single-cylinder version of a Volvo 850 engine.

The Alvar engine design is to meet the following specifications.

intake pressure = 2.0 bars absolute
primary piston speed = 3000 rpm
maximum cylinder pressure = 100.0 bars
compression ratio range = 13 - 7

4.2 Scope of Work and Approach

This thesis includes the analysis and the proposed geometric design of a single cylinder head that includes the Alvar piston shape, size of the combustion chamber, and locations of valves and spark plug(s), etc. The design considered constraints of compression ratio range, flame travel concerns, and secondary-bore fit into the conventional cylinder head.

4.3 Conventional Cylinder Head

To begin the description of the Alvar design process it is necessary to note that the design is a derivative of the Volvo 850 cylinder head. In noting this, the existing conventional cylinder head and piston geometry must be briefly described. The standard Volvo 850 engine has four valves per cylinder. The number of cylinders used in the engine is not a design concern as the project calls for the construction of a single-cylinder engine. See Table 4.1 for specifications of the conventional engine from which the Alvar engine design is derived.

Table 4.1 Conventional Engine Specifications

Displaced Volume (dm^3)	(5 - cylinders) 2.50
Stroke (mm)	90.00
Bore (mm)	83.00
Connecting Rod Length (mm)	158.00
Head Gasket Diameter (mm)	85.00
Head Gasket Thickness (compressed-mm)	1.40
Piston Protrusion @ TDC (mm) (relative to top of liner)	0.40
Clearance Volume (cc)	53.28
Intake Valve Diameter (mm)	31.00
Max Inlet Valve Lift (mm)	8.45
Exhaust Valve Diameter (mm)	28.00
Max Exhaust Valve Lift (mm)	8.45

These specifications make up the existing Volvo 850 cylinder head, hereby called conventional head. These specifications make up what is referred to in this work as the primary specifications. The Alvar therefore has a primary bore of 83 mm. A secondary (or auxiliary) bore is determined as part of the design task.

4.4 Phase and Nominal Compression Ratio Requirement

4.4.1 Determination of Knock and Compression-Ratio Constraints

It is well understood that the compression ratio of the spark ignition (SI) engine is limited by the autoignition, or knock, phenomenon. Knock is a necessary concern in the design process of this engine. A referenced knock model was used to help determine the appropriate compression ratio range [8]. The model, shown below, relies on several empirically-based relations between the spark-ignition octane requirement (OR), piston bore (B), engine speed (N), cylinder intake pressure (p_i) and compression ratio (r_c).

$$OR = OR_{ref}\,(N/N_{ref})^{-0.076}\,(B/B_{ref})^{0.29} + 0.561(p_i - p_{i,wot}) + 6.0(r_c - r_{c,ref})$$

This relation was then used to correlate the compression ratio requirement with cylinder intake pressure. It should be noted that this knock model was used here in an approximate manner to develop a reasonable compression ratio range within the knock limits.

Next, Figure 4.1 shows the relation between the knock-limited nominal compression ratio and cylinder intake pressure.

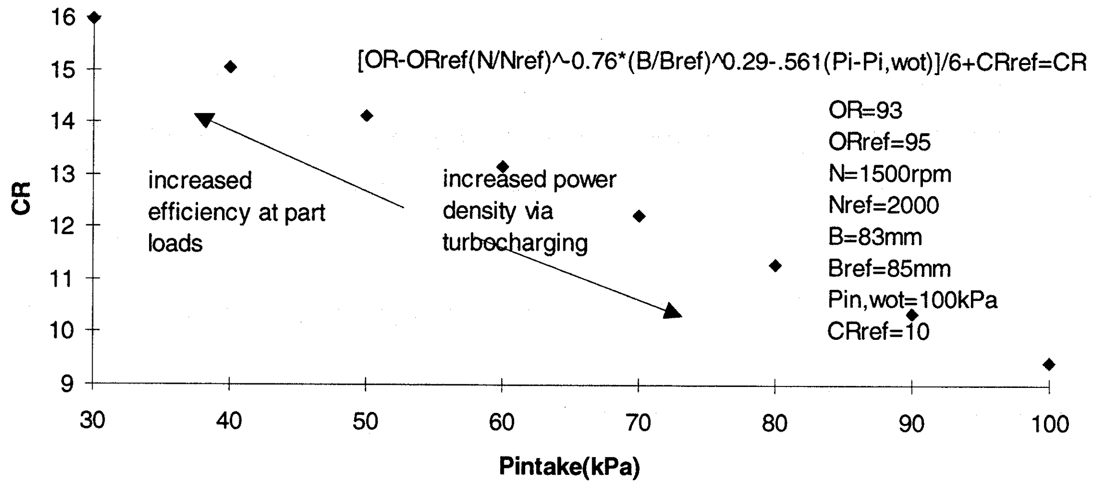

Figure 4.1: Knock Requirement - Compression ratio versus intake pressure extracted from Patton thesis

From Figure 4.1, a conservative range of 13 to 7 was extracted for the compression ratio. A linear extrapolation in the direction of decreasing compression ratio suggests that a boosted pressure is applicable for a compression ratio of 7:1. Note that the reference parameters of bore, engine speed, cylinder intake pressure, and compression ratio are originally based on a typical four-valve spark ignition engine [8]. The reference parameters were chosen to be reasonable values for a slightly smaller vehicle operating at the world-wide-operating point.

world-wide-operating point

engine speed = 1500 rpm

brake mean effective pressure = 325.00 kPa

gross indicated mean effective pressure = 450.00 kPa

net indicated mean effective pressure = 400.00 kPa

cylinder intake pressure = 50.60 kPa

As Figure 4.1 illustrates, these parameters produce a compression ratio range from 16.0 to 9.7. Note that the conventional engine (unmodified) operates at a compression ratio range of 10.1. The plan to operate with more conservative compression ratios at turbocharged conditions led to the decision to design the Alvar engine for a compression-ratio range of 13 - 7.

4.4.2 Determination of Secondary Bore, Stroke, and Clearance Volume Combinations

Once the compression ratio range was chosen, parametric studies were performed to determine the appropriate secondary geometry. At this stage the secondary bore (b2), stroke (s2), and phase shift were the focus, while the secondary connecting rod length (crl2) and offset were maintained as soft constraints. To that point the secondary connecting rod length was taken in the same proportion to the secondary stroke as the following relation of the primary stroke and connecting rod length of the conventional engine.

$$crl1 / s1 = 1.76 = crl2 / s2$$

Also note that the secondary offset was assumed to be half of the secondary crank radius or a quarter of the secondary stroke distance. This offset was chosen as it was decided that an offset would benefit the performance of the engine, particularly by reducing friction. Later studies would serve to determine the necessity of a secondary offset.

The first Alvar parametric tests were used to identify secondary bore and stroke combinations that would satisfy the compression ratios (13 to 7) specifications. To narrow the possibilities, the nominal compression ratio was plotted against the phase shifts. Note that the phase shift serves the sole purpose of controlling the phase of the secondary piston, or its motion relative to that of the primary piston. The need to work within the constraints of the conventional cylinder head suggested that a secondary bore less than approximately 40 mm, and a secondary stroke not exceeding approximately 50 mm would fit. Therefore, the upper-most case was taken as a secondary bore of 40 mm and a secondary stroke of 50 mm. Similarly, structural integrity motivated a lower limit on the secondary bore of 20 mm. An corresponding lower limit for the secondary stroke was taken as 10 mm. A lower combination was therefore taken with a secondary bore of 20 mm, and secondary stroke of 10 mm. The combinations of the secondary geometry used in this study are shown below in Table 4.2. Note that the clearance volume for each secondary bore and secondary stroke combination is determined by the constraint that CR = 13 at phase shift = 0.

Table 4.2 Combinations for Nominal Compression Ratio-Phase Shift Study

bore2	stroke2	conrl2	offset2	clearance vol.
mm	mm	mm	mm	cc
20.00	10.00	17.60	2.50	40.74
20.00	20.00	35.20	5.00	40.89
20.00	30.00	52.80	7.50	41.05
30.00	20.00	35.20	5.00	41.29
30.00	30.00	52.80	7.50	41.65
30.00	40.00	70.40	10.00	42.01
40.00	30.00	52.80	7.50	42.49
40.00	40.00	70.40	10.00	43.14
40.00	50.00	88.00	12.50	43.79

Figure 4.2 illustrates how the Alvar nominal compression ratio varies with phase shift, given these geometric parameters.

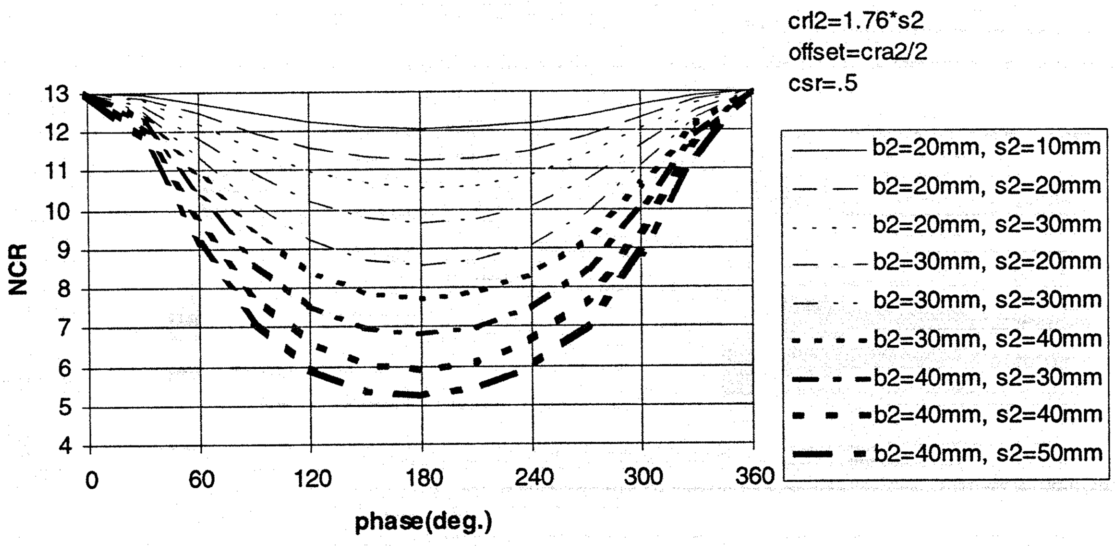

Figure 4.2: Nominal compression ratio versus phase shift for given geometry

It appeared that the clearance volume varied over a narrow range, in contrast to the compression ratio, for various combinations of secondary bore and stroke. The difference in compression ratio at a phase of 0 and a phase of 180 is related to the clearance volume, which is chosen for each secondary bore and stroke combination such that NCR (0 phase) = 13. It can also be interpreted that a small change in clearance volume strongly affects the achievable compression-ratio range.

The correlation is shown below.

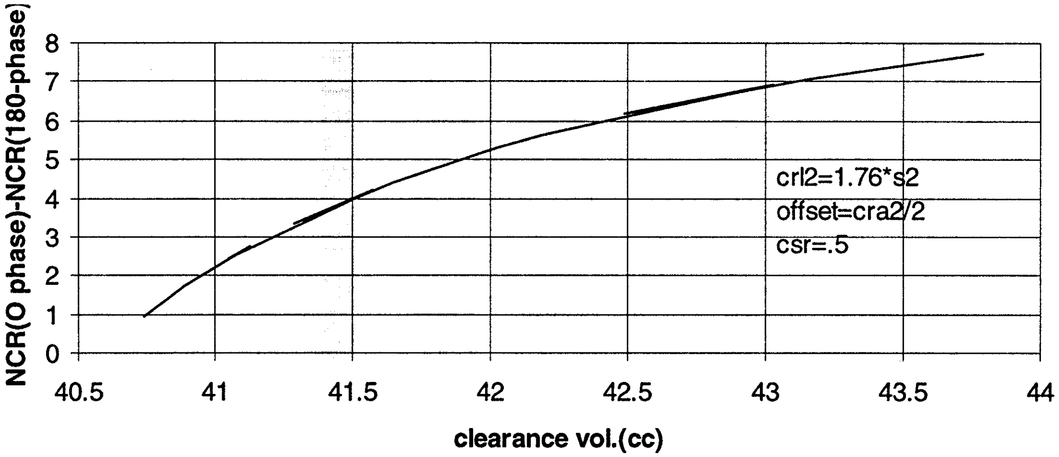

Figure 4.3: Compression ratio range versus clearance volume

Table 4.3 lists the additional bore and stroke combinations that have been added to the above chart in an effort to confirm the clearance volume variation.

Table 4.3 Additional Secondary Bore and Stroke Combinations

bore2 mm	stroke2 mm	conrl2 mm	offset2 mm	clearance vol. cc
20.00	35.00	61.60	8.75	41.13
25.00	40.00	70.40	10.00	41.57
30.00	45.00	79.20	11.25	42.19
35.00	50.00	88.00	12.50	43.03

These studies provide a general depiction of the available geometry that would meet the compression ratio requirement. To set the constraint that the compression ratio range is (13 - 7), it was found that each secondary bore between 20 and 40 mm could be matched with a secondary stroke that met this requirement. As secondary bore is increased, the secondary stroke must be decreased and the relation is non-linear. These added combinations contributed to the following correlation between the nominal compression ratio difference and the cylinder head clearance volume. See Figure 4.3.

$$\Delta ncr = 0.2(clv)^3 - 24.1(clv)^2 + 1046.2(clv) - 15150.0$$

The following studies narrow the scope of the combinations that meet the compression ratios within +/- 0.02. It now becomes apparent that each of these combinations require a clearance volume of approximately 42.38 cc. The variance from this clearance volume is small, (+/- 0.01). It was found that each secondary stroke between the range of 21 and 40 mm could be matched with a corresponding secondary bore that would achieve the first constraint of spanning the nominal compression ratio range of 7 to 13, if the following secondary geometrical parameters were held constant.

connecting rod length = 1.76*secondary stroke
secondary offset = 1/2 secondary crank radius
clearance volume = 42.38 cc
piston speed ratio = 1/2

The limiting factor of this range was the secondary stroke that would not reasonably fit within the cylinder head. This became the case at a secondary bore under 21 mm.

Table 4.4 below lists the combinations that were found to work. The stroke was iteratively matched to produce the desired compression ratio range of CR =13 at phase = 0 and CR = 7 at phase = 180.

Table 4.4 Combinations that meet the Compression-Ratio Constraints

bore2 mm	stroke2 mm	cnrl2 mm	offset mm
21.00	103.20	181.60	25.80
22.00	94.20	165.80	23.60
23.00	86.00	151.40	21.50
24.00	79.00	139.00	19.80
25.00	72.80	128.10	18.20
26.00	67.40	118.60	16.90
27.00	62.40	109.80	15.60
28.00	58.00	102.00	14.50
29.00	54.20	95.30	13.50
30.00	50.60	89.10	12.70
31.00	47.40	83.40	11.90
32.00	44.40	78.10	11.10
33.00	41.80	73.60	10.50
34.00	39.40	69.30	9.90
35.00	37.20	65.50	9.30
36.00	35.10	61.80	8.80
37.00	33.20	58.40	8.30
38.00	31.50	55.40	7.90
39.00	29.90	52.60	7.50
40.00	28.40	50.00	7.10

Next, Figure 4.4 relates the secondary stroke and secondary bore combinations that meet the CR constraint. This figure also illustrates the tradeoff as increasing secondary bore size mandates decreasing secondary stroke in order to maintain the clearance volume.

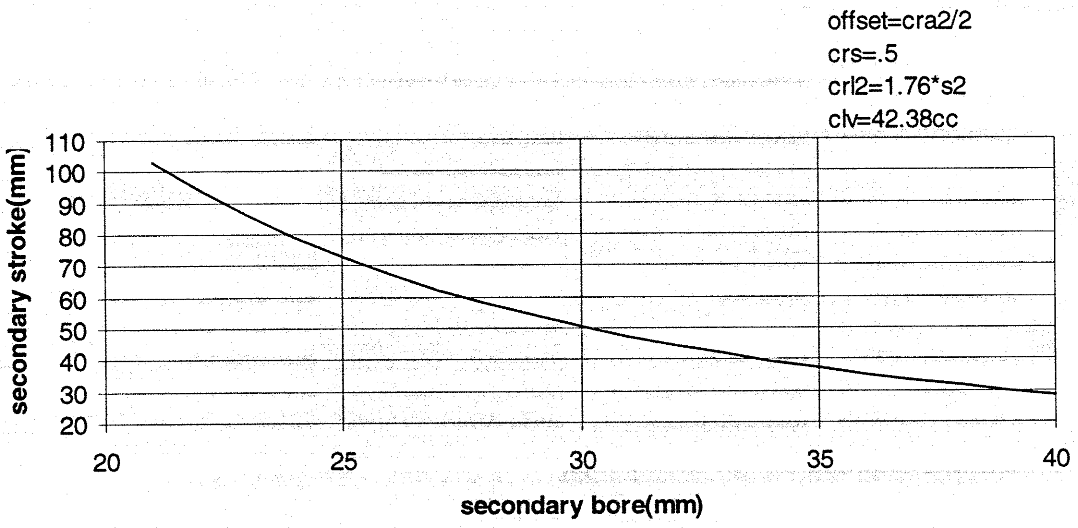

Figure 4.4: Secondary stroke versus secondary bore combinations meeting compression ratio range constraint

While this relation may be intuitive, it is a direct result of the following relationship between the cylinder bore and stroke at a given clearance volume (v_c), cylinder volume (v), connecting rod length (conrl), and distance between crank shaft axis and piston pin axis (s).

$$8(v-v_c)/\pi B^2 - 2(\text{conrl}) + 2s = L,$$

In order to illustrate that the current selected geometries meet the CR constraint, the nominal compression ratio is plotted against the phase for the following derived combination.

bore2 = 36.00 mm

stroke2 = 35.10 mm

connecting rod length2 = 61.80 mm

clearance volume = 42.38 cc

offset2 = 8.80 mm

It's worth noting that any other combination of secondary bore and stroke given in Table 4.4 will sweep the same relation between the nominal compression ratio and the phase. A variance from the noted clearance volume, however, will alter the relation and create a combination that does not fall in line with the combinations shown in the earlier figure. This relation between nominal compression ratio, phase and piston position at 15 degrees ATC is shown below in Figure 4.5. Note that the introduction of a secondary offset is responsible for the asymmetry, and therefore causes the minimum nominal compression ratio to occur at a phase slightly under 180 degrees.

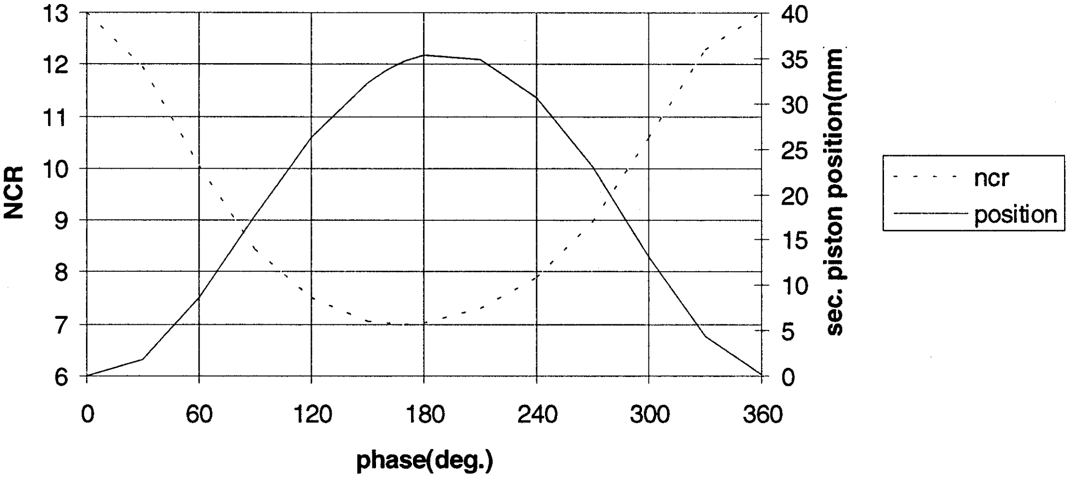

Figure 4.5: Secondary piston position at 15 degrees ATC and nominal compression ratio versus phase shift for b2 = 36.00 mm, s2 = 35.10 mm, crl2 = 61.78 mm and clearance volume = 42.38 cc

4.5 Flame Travel Requirement

Of general concern during the design of the Alvar spark ignition engine is the effect of the addition of the secondary piston on the combustion process. The combustion -chamber geometry and the placement of the spark plug dictate the behavior of the flame. The flame propagation influences combustion stability, and while this area is not extensively addressed in this project, it was taken into consideration. For instance, the combustion quality improves with increased flame speed. And while the quality of the unburned mixture plays an integral role in determining the speed of the flame propagation, the geometric effects are of concern here. The flame front area, dictated by chamber geometry and spark plug location, has significant influence on flame speed. Figure 4.6 illustrates flame propagation from three different spark plug arrangements.

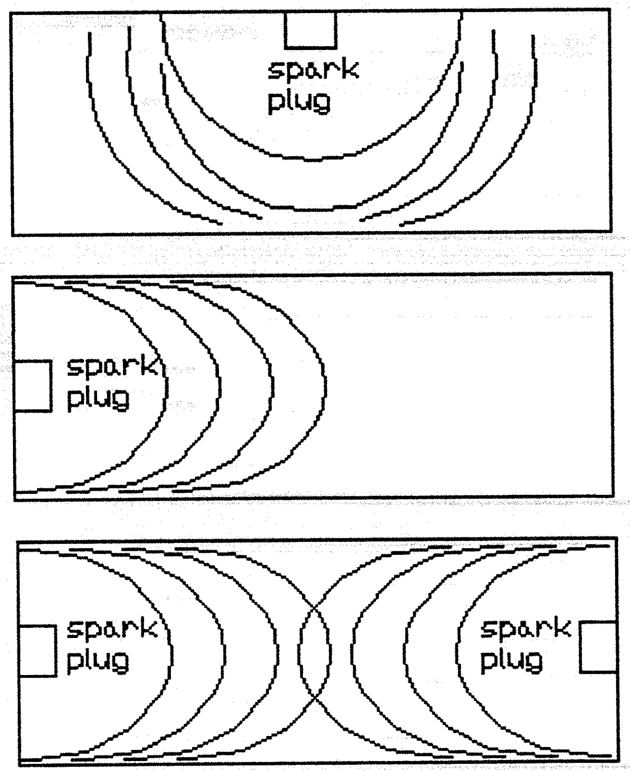

Figure 4.6: Schematic of spark plug in-cylinder chamber locations

Due to the accessibility of the flame to the unburned gases, the center location of the spark plug produces a faster burn time. The center location allows roughly twice the flame front area than that of the side location, with the flame radii equal, and therefore burns roughly twice as fast. Note also that the flame exposure area of a roughly rectangular chamber is approximately the same as that of the centrally located chamber. [1]. Each of these options would be a consideration for the Alvar chamber, however the chamber was designed with the capability to function with one centrally located spark plug to remain in-line with the geometry of the conventional pentroof geometry. There is a clear advantage in developing a chamber that allows fast burning. The faster burning engines are less susceptible to typical thermodynamic variations within the chamber than slower burning engines.

These trends motivated the flame travel distance issue. The objective of the flame travel study was to insure that the Alvar engine combustion chamber did not create a flame travel distance that would cause combustion stability problems. Additionally, the effect of increasing the flame travel length in one direction as a result of adding the Alvar piston would affect the knock likelihood, as well as, the propensity to emit unburned hydrocarbons. To this effect the need to maintain a flame travel distance into the secondary chamber that would not exceed the travel distance from the spark plug to the primary piston corner became apparent. The chamber geometry that created a symmetry (in terms of travel distances) was therefore sought. Figure 4.7 illustrates the distance from a centrally-spaced spark plug to the corner of a secondary piston.

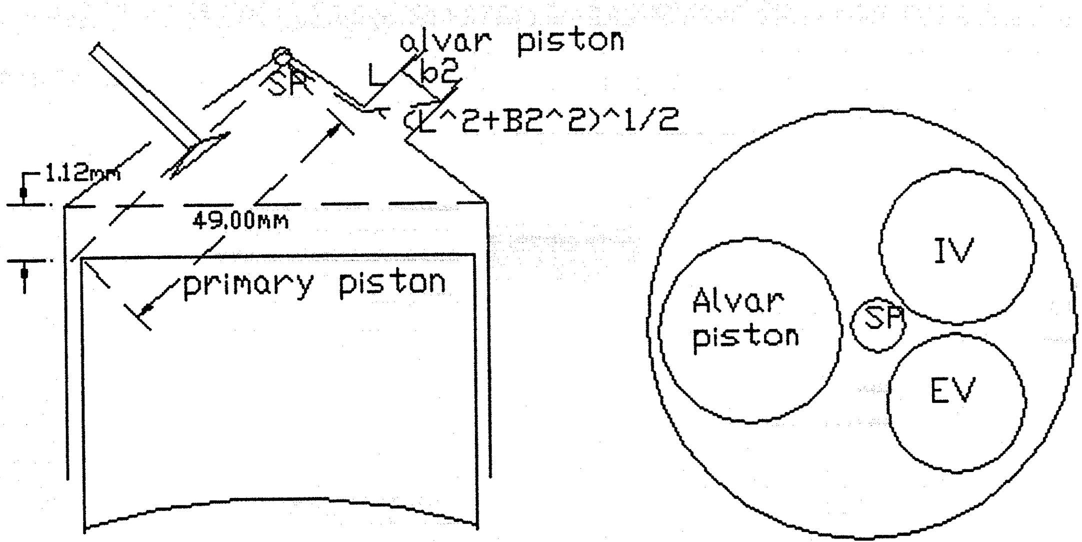
alvar piston
SP
L
b2
(L^2+B2^2)^1/2
1.12mm
49.00mm
primary piston
Alvar piston
IV
SP
EV

Figure 4.7: Simple Alvar cylinder head side and top view with emphasis on flame travel length to secondary crevice

In order to meaningfully assess the flame travel distance over the course of a cycle, the relative positions of the Alvar and primary pistons must be taken into consideration. The relative piston positions are demonstrated using the geometrical parameters listed in Table 4.5.

Table 4.5 Geometrical Parameters for Relative Piston Position Study

Primary	Secondary
bore1 = 83.00 mm	bore2 = 34.00 mm
stroke1 = 45.00 mm	stroke2 = 39.80 mm
crl1 = 101.13 mm	crl2 = 158.00 mm
offset1 = 0.00 mm	offset2 = 2.60 mm

clearance volume = 42.38 cc

piston speed ratio = ½

Figure 4.8 shows the relative piston positions for a phase shift of 180 degrees, and compression ratio of 13 (applicable to part load operation) as a function of primary crank angle.

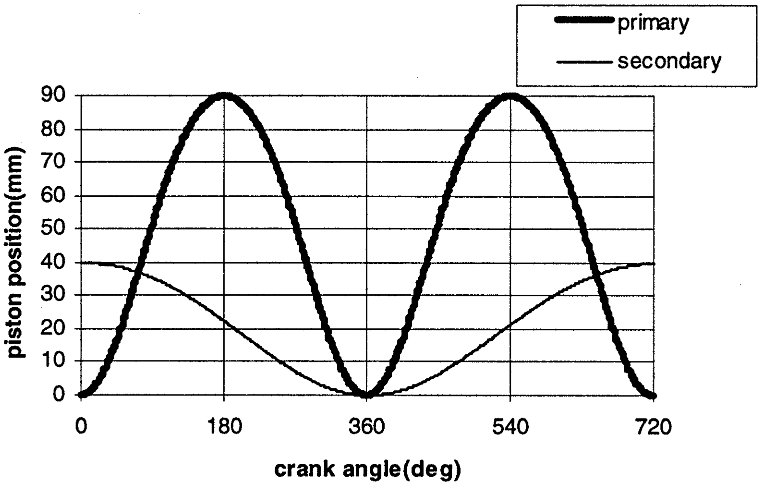

Figure 4.8: Piston position versus crank angle for phase of 0 degrees and nominal compression ratio of 13:1

Figure 4.9 shows the relative piston positions for a phase shift of 180 degrees - compression ratio of 7, applicable to full load operation, again as a function of primary crank angle.

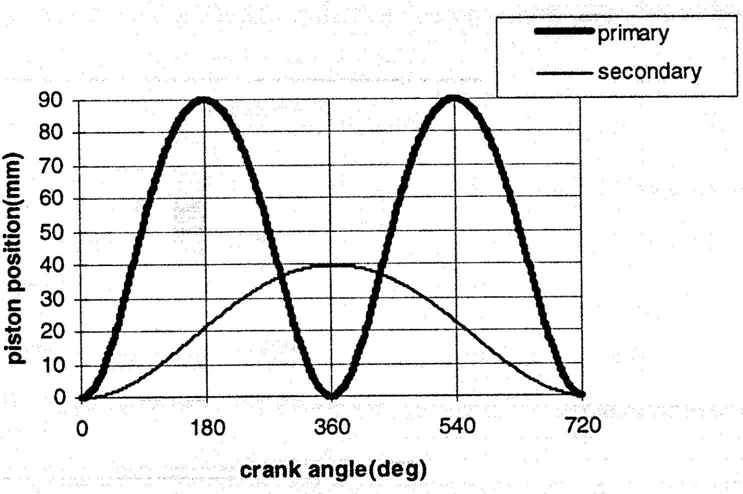

Figure 4.9: Piston position versus crank angle for phase of 180 degrees and nominal compression ratio of 7:1

The limiting flame travel distance was graphically determined by confirming the primary geometrical configuration at the point of maximum in-cylinder pressure; 15 degrees ATC. By determining the distance from the centrally located spark plug to the corner (piston-liner interface) of the primary piston, the limiting distance to the corner of the secondary piston is found. The purpose here is to design the secondary geometry so that the worst case travel (longest) distance into the secondary geometry is no longer than the travel distance to the primary corner (i.e corner of primary piston). The worst case, or furthest distance upon combustion into the secondary chamber, occurs at a phase of 180 degrees and was determined geometrically. By finding the location of the primary piston at 15 degrees ATC, and noting the geometry of the primary chamber, a travel distance of 47.6 mm was calculated.

Once the tolerated distance was determined, the issue of distance variance from the spark plug was addressed. Recall that the nature of the Alvar mechanism varies the distance of the secondary piston from the primary cylinder chamber with phase shift. The goal here was to produce a secondary geometry in which variance in phase or relative position of secondary piston, translated into a tolerable variance in "angular" position. The "angular" position is defined as the square root of $b2^2 + l^2$ where l is the depth, or axial position, of the secondary piston from the cylinder head plane, and b2 is the secondary piston bore. The angular position was significant since herein lay the longest flame travel distance in the secondary cylinder. The "angular" distance is roughly the slanting depth of the secondary chamber from the "top-right" position to the "bottom-left" position when the primary piston is at 15 degrees ATDC. Intuitively, the variance of this angular distance decreases with increasing bore for two reasons.

1) The distance becomes longer with increasing bore and thus variations are a smaller percent for a given stroke.
2) Decreasing stroke with increasing bore serves to reduce the variance in the secondary piston from the spark plug, thus decreasing angular position variance.

Figure 4.10 illustrates how the angular position varies with selection of secondary bore.

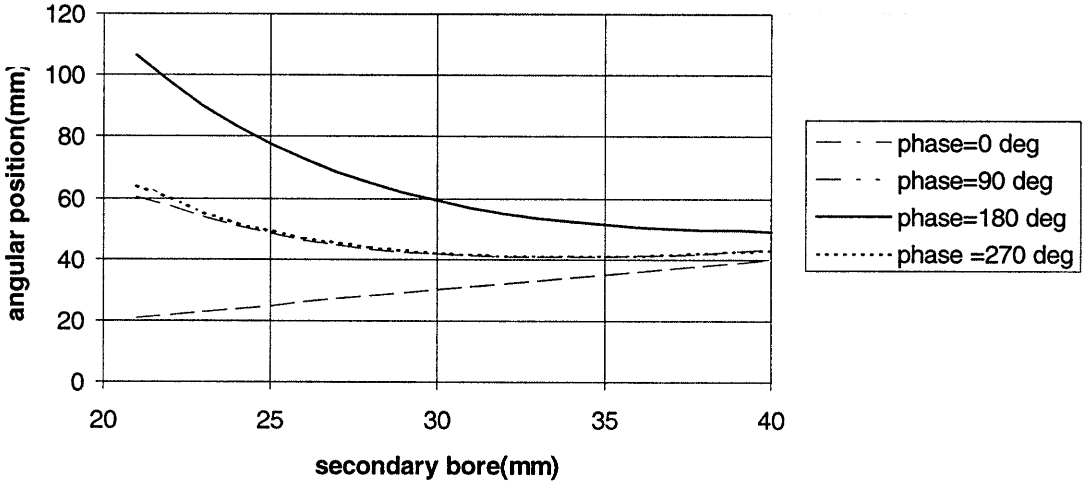

Figure 4.10: Secondary corner angular position at 15 degrees ATC versus secondary bore for given phase shift.

Although larger bore limits variances of secondary angular position, conventional cylinder head size limits the size of the secondary bore or water jacketing. Concisely, bore2↑, wj(water jacketing space)↓, within the global constraint of the material available when exhaust valves are extracted. The bore chosen as a result of this work was 34 mm which served to maximize the size of the bore without unduly restricting the ability to water jacket. In fact, anywhere beyond a secondary bore of 33 mm in the flat region of Figure 4.10 will not make a substantial impact on flame propagation into the secondary chamber. The exhaust valves are typically at high temperatures related to other areas of the cylinder chamber (i.e. intake valves) and the secondary piston will be designed with this same tendency in mind. Small modifications can be made to the conventional cylinder head to create an available secondary chamber space of 36 mm. Therefore, the selected 34 mm bore will work but requires careful design of the water jacketing flow channel.

4.6 Engine Performance Constraint

Next, the secondary bore and stroke combinations were compared on the merit of engine performance. The primary variables of interest were maximum cylinder pressure, mean effective pressures, torque, and cylinder wall heat loss. The secondary piston geometry used in this engine performance comparison included each combination that was found to meet the knock requirements of constraint #1 (compression ratio range of 13 - 7). Secondary geometry combinations were not limited based on constraint #2 (flame travel), therefore, the entire range of bore from 21 mm to 40 mm was used to produce performance results. Note that the secondary parameters of connecting rod length and offset remain defined as previously stated.

$$(crl2 = 1.76*s2 \ \& \ offset2 = 1/2cra2)$$

The performance tests were run with all combinations at a nominal compression ratio of 7:1, with a phase of 180 degrees, wide-open-throttle. Tests were also run at nominal compression ratio of 13:1, with phase of 0 degrees, part load. The engine speed was held at 3000 rpm with ignition at MBT timing.

Figure 4.11 illustrates that the performance parameters varied modestly over the range of secondary bore and stroke combinations; at part load. Note that the cylinder wall includes both the primary and secondary chambers, which justifies the modest variance of total heat loss as a result of secondary bore geometry. Below, the cylinder head heat loss as a function of secondary bore is shown.

The heat loss is shown to decrease slightly in response to an increase in the secondary bore. The variance is less than 1%. This effect, however small, is attributed to the increase of volume/area ratio associated with the increased bore.

Figure 4.11 also shows the cylinder wall heat loss at wide-open-throttle. It is well documented that heat loss decreases with increasing load, or intake pressure, while modestly [1]. The magnitude of heat loss is reduced by 5.7% as load increases from part load to wide-open-throttle.

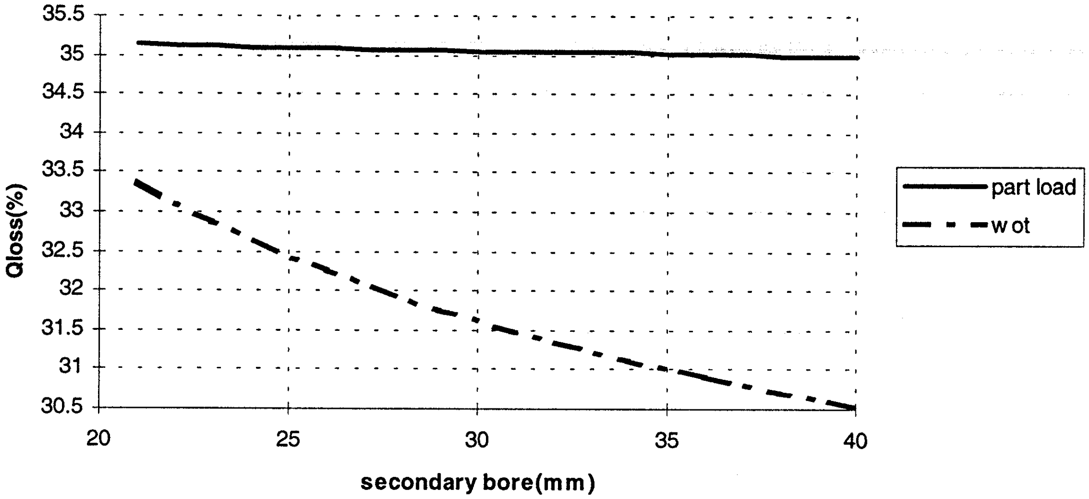

Figure 4.11: Cylinder wall heat loss versus secondary geometry for part load and WOT operation, and engine speed of 3000 RPM

Again note the variance of percent heat loss for wide-open-throttle; 33.5 to 30.5% of fuel energy, a 3.0% change due to an almost 50% change in secondary bore. Refer forward to Figure 7.2 & 7.3 to note the relative volumes as a means of visualizing the spatial significance of the secondary cylinder. Additionally, we know that heat loss varies modestly with compression ratio. In a typical spark ignition engine an increasing compression ratio serves to decrease the percent heat loss up to a compression ratio of approximately 10:1, at which point the heat loss begins to rise [1]. Note the magnitude difference in the two curves in Figure 4.11 is a direct result of the intake pressure difference.

Next, Figure 4.12 shows the effect of secondary bore size on brake torque.

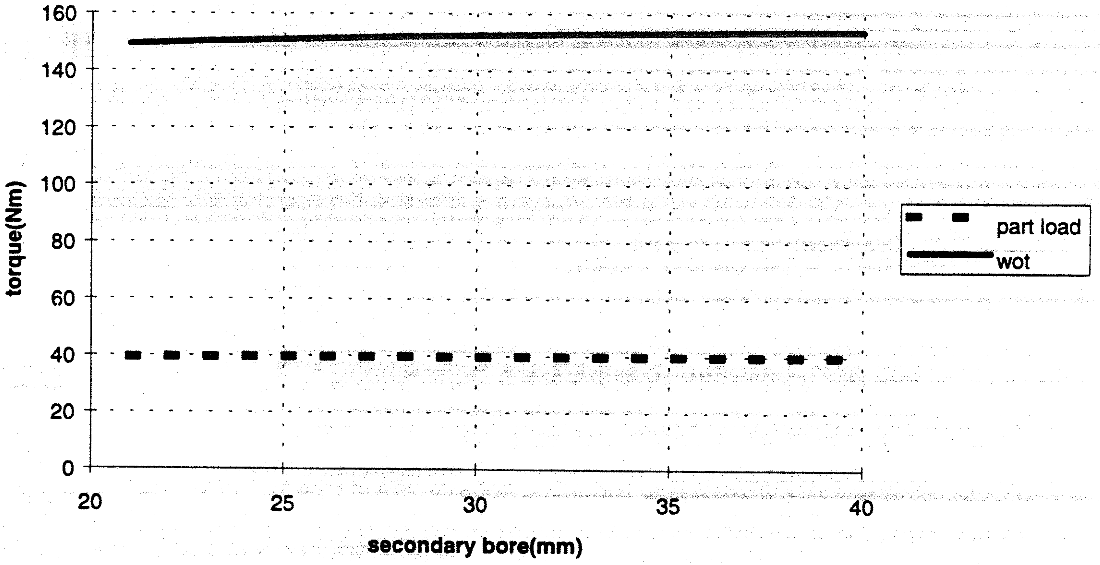

Figure 4.12: Torque versus secondary piston geometry for part load and WOT operation, engine speed of 3000 RPM

For both cases the variance is small with a difference of less than 1% for almost a 50% change in secondary bore.

4.7 Alvar Piston Design

After noting that the performance parameters varied modestly within the range of interest, the flame travel constraint became the more significant factor in determining the best selection of the Alvar piston. Since the conventional design was modified to accommodate the Alvar cylinder, some geometrical questions still remained to be answered. The two geometry considerations of concern were,

1) obtaining the clearance volume of 42.38 cc
2) fitting the Alvar piston to the conventional cylinder head in a way that ensures accurate interfacing with the exhaust valve camshaft.

4.8 Obtaining Clearance Volume

The first constraint (compression ratio range of 13 - 7) mandated modification of the existing geometry to obtain the necessary clearance volume of 42.38 cc. In order to justly modify the geometry to meet the specification needs, it was necessary to approximate the existing clearance volume. Note that the standard Volvo 850 clearance volume was found to be 53.28 cc and that the geometry of the pentroof cylinder head design holds a volume of 49.00 cc. With a volume of 4.30 cc outside the cylinder head and a necessary reduction of 42.38 - 53.28 cc by lowering the cylinder head (i.e. solely decreasing head gasket thickness was not sufficient). Three approaches were possible to reduce the clearance volume.

1) piston modification by adding material to the top of the primary piston
2) cylinder head modification by reducing gasket thickness and/or cutting from the base of the pentroof.
3) a combination of option 1 and 2.

The first two options are addressed in succession.

4.8.1 Existing Geometry

In order to modify the conventional piston, the existing geometry must be confirmed. Figure 4.13 shows a schematic of the side view of the existing piston.

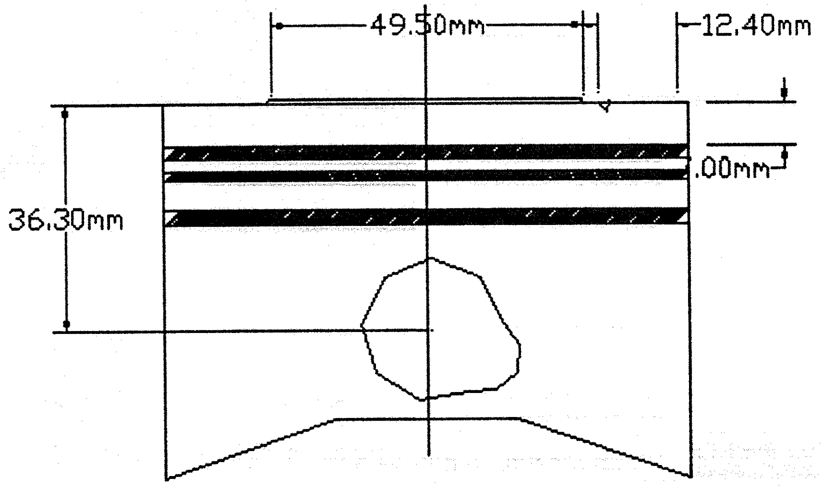

Figure 4.13: Side view of conventional piston

Note that the mass of the primary piston was estimated at 700 grams for the Alvar studies. The piston parts most relevant to the design project are the 0.40 mm piston protrusion and the indentations into the piston for valve clearance. These parts were used to account for the makeup of the chamber volume. Once this accounting was known, modification approaches were evaluated on merit. The top view of the existing piston is shown in Figure 4.14 to contribute to the understanding of the existing conventional geometry.

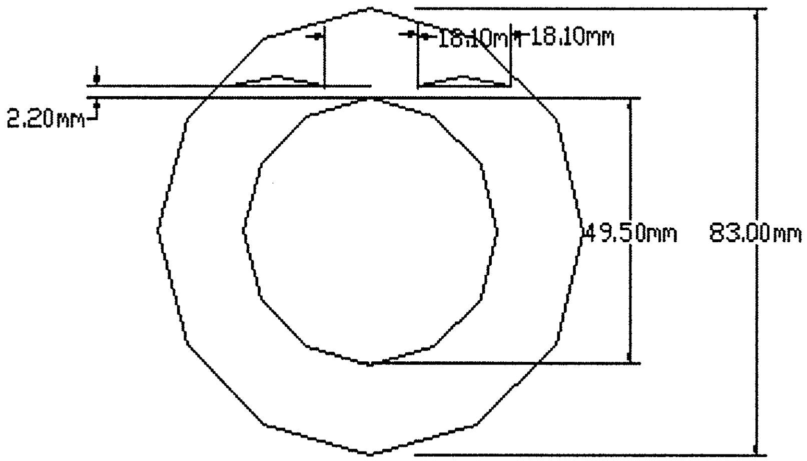
18.10mm
18.10mm
2.20mm
49.50mm
83.00mm

Figure 4.14: Top view of conventional piston

It is also important to understand the conventional geometry of the pentroof design. Figure 4.15 shows the 3-dimensional view of the conventional pentroof design. The complex details of the pentroof are approximated here.

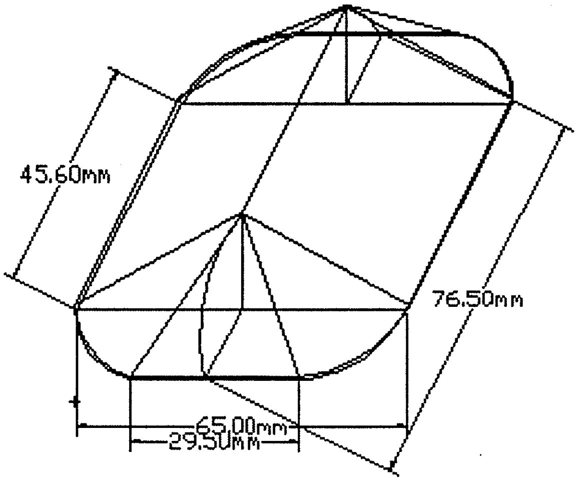
45.60mm
76.50mm
65.00mm
29.50mm

Figure 4.15: 3-Dimensional schematic of pentroof cylinder head design

View of the piston and cylinder head together enables one to obtain insight into the potential for effective solutions to reducing the clearance volume. Figure 4.16 shows a schematic of the top view of the cylinder head pentroof as it fits with the conventional piston.

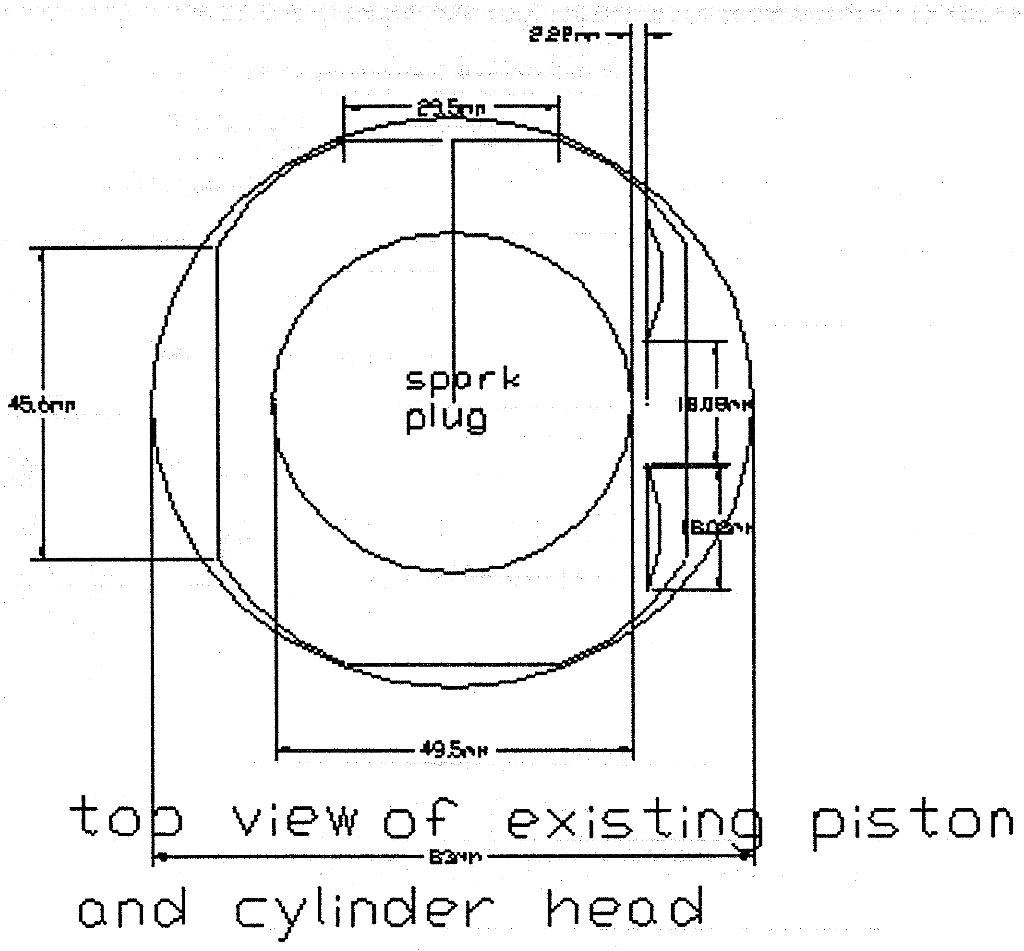
2.29mm
23.5mm
45.6mm
spark plug
18.08mm
18.02mm
49.5mm
83mm
top view of existing piston
and cylinder head

Figure 4.16: Combined top view of cylinder head and piston top

4.8.2 Modifying Piston

The first approach to obtaining the desired clearance volume is modifying the existing piston by adding a piece to the piston crown. This approach is not an unusual task and has the advantage of allowing flexible clearance volume through additional future pistons. Any addition to the piston must be compatible with the dimensions of the piston, cylinder head, and the relative motions of the valves. Note that the Alvar design includes the exhaust and intake valves on the same side of the pentroof.

The interfacing between the valves and the piston crown is dependent on the valve timing and the lift of the valves. Variations in valve timing and lift have been excluded from this study as the conventional maximum valve lift values of 8.45 mm are maintained for the exhaust and inlet valves. Any piston addition must match piston crown cutouts in angle to prevent collision of piston crown and valves. Below is a rough design for the piston addition as it excludes curvatures needed to ensure against disruption of the combustion process. Note that the volume of 11.67 cc was required for the piston addition to encompass the protrusion volume of .77 cc and provide the clearance volume of 42.38 cc. See Figure 4.17, below.

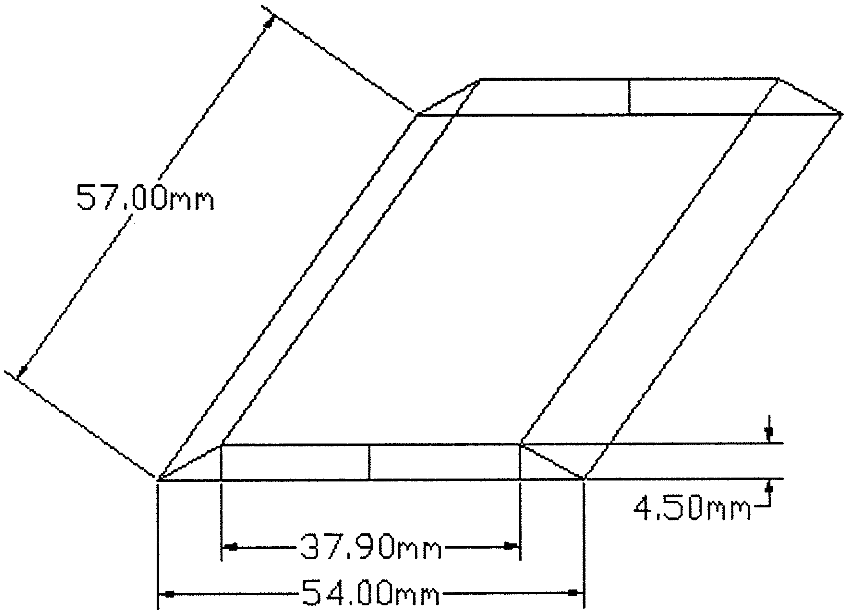

Figure 4.17: Addition to piston for purpose of reducing clearance volume

Next, Figure 4.18 illustrates how the volume addition fits on the primary piston. Note that the additional volume piece encompasses the 0.40 mm piston crown protrusion. This figure shows the placement of the piston protrusion inside the piston addition. Also note that the piston addition raises the crown 4.50 mm from the base. The addition inclines from 12.40 mm from the edge at an angle of 29 degrees.

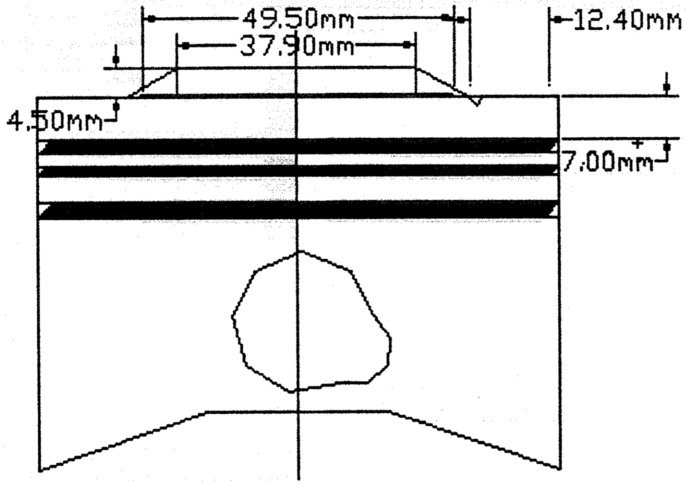

Figure 4.18: Side view of modified conventional piston

A more informative view of this design is the side view shown in Figure 4.19. Here the 1.40 mm gasket thickness can be seen. Additionally, the clearance of the piston crown and the cylinder head center (spark plug location) is apparent. See Figure 4.19 below.

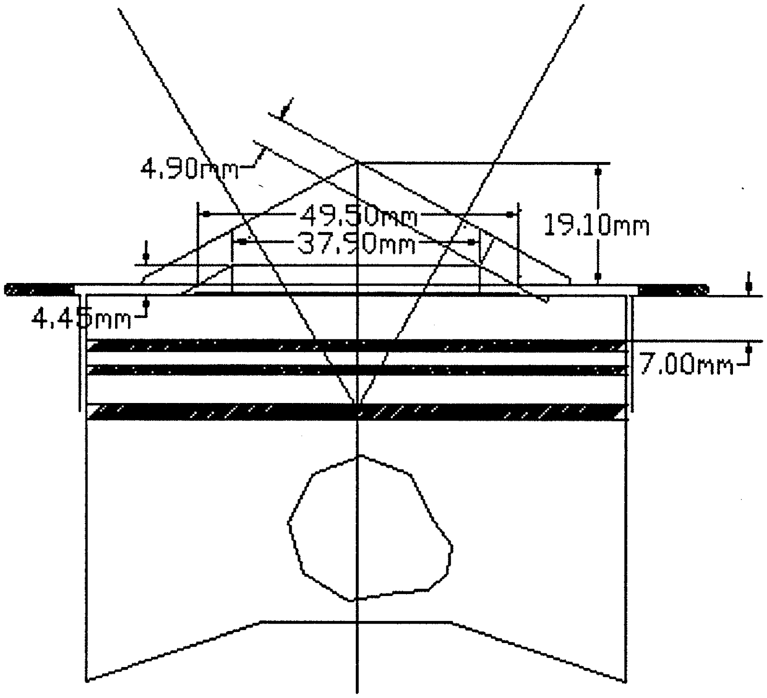

Figure 4.19: Side view of modified piston and cylinder head

4.8.3 Modifying Cylinder Head

The second approach investigated was the method of reducing the clearance volume by modifying the pentroof. This would be a plausible method if the gasket height is also reduced. By noting that the reduction necessary is 53.28 cc - 42.38 cc = 10.90 cc and that approximately 5.67 cc can be deleted by reducing the compressed gasket height from 1.40 mm to 0.40 mm and that approximately 3.01 cc can be deleted by cutting 1.0 mm from the base of the pentroof, and finally noting that taking an additional 0.75 mm from the base will delete an additional 2.25 cc. These numbers sum to 10.93 cc. Note that this approach requires a total of 1.76 mm removed from the pentroof base. The valve seat is therefore moved 1.50 mm towards the piston crown. For clarity, this modification is summarized in Table 4.6.

Table 4.6 Summations of Reductions for Modified Cylinder Head Approach

cylinder reduction mm	volume reduction cc
1.00 mm (gasket)	5.67
1.00 mm (pentroof base)	3.01
0.75 mm (cont. base)	2.25

The side view of the resulting geometric combination is shown in Figure 4.20. Concerns surrounding incorporating the structural requirement of the cylinder head around this design will be address by the cylinder head designer.

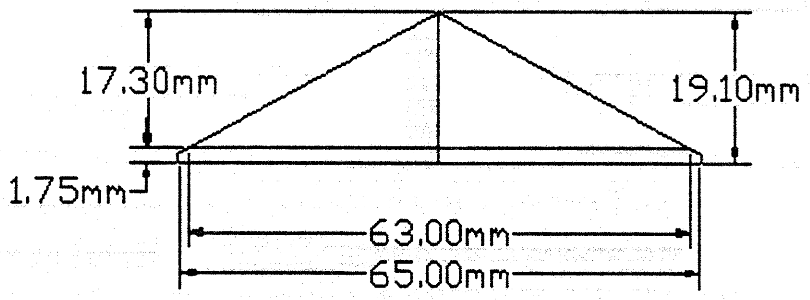

Figure 4.20: Side view of pentroof cylinder and dimensions to cut for cylinder head reduction

The modified cylinder head and conventional piston is shown in Figure 4.21. Note that the modified piston is not necessary in this model due to the focus on reducing cylinder head volume.

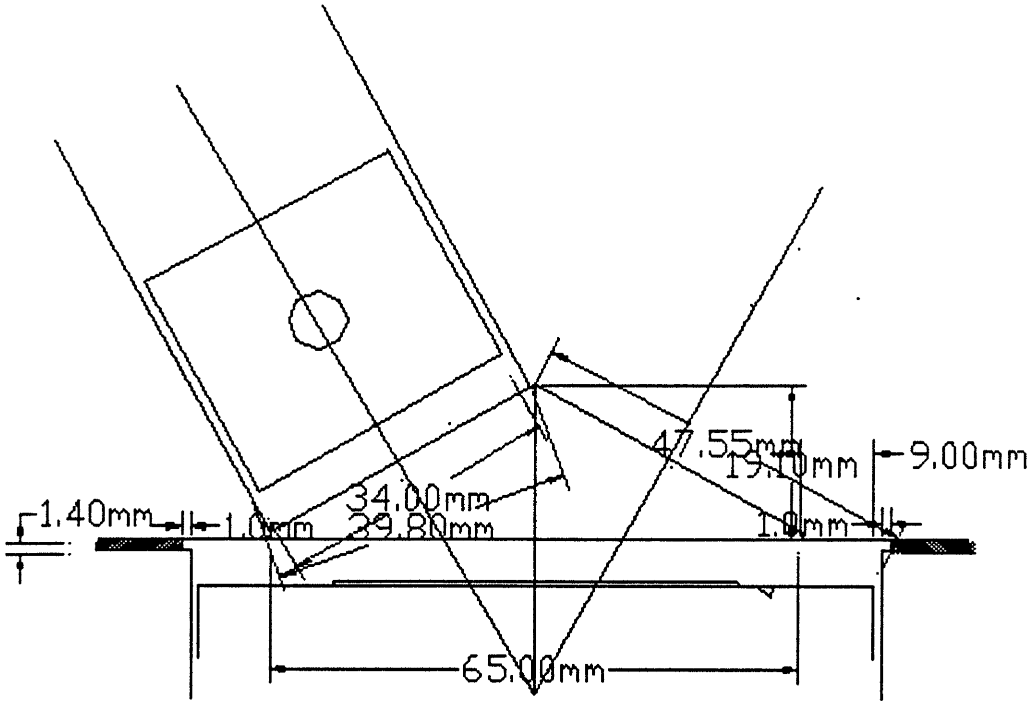

Figure 4.21: Side view of modified cylinder head with secondary piston

4.9 Positioning of Alvar Piston

The positioning of the Alvar piston is dictated by the position of the existing exhaust valve camshaft in relation to the chamber geometry surrounding the exhaust valve seats. The chamber geometry therefore restricts the secondary piston combinations within 36 mm of available space. A detailed layout that shows the positioning of the secondary piston to the cylinder head is shown in Figure 4.22. The following list includes the recommended design of the Alvar geometry to this point.

bore2 = 34.00 mm
cra2 = 19.70 mm
conrl2 = 91.00 mm
offset2 = 0.00 mm

bore1 = 83.00 mm
cra1 = 45.00 mm
crl1 = 158.00 mm
offset = 0.00 mm

Since one of the inlet valves will be used as an exhaust valve, the exhaust valve is increased to 31 mm diameter, that of the inlet valves. Note that the structural details of the water jacket are not shown and will be addressed more thoroughly during the cylinder head structural design.

It was decided that the cylinder chamber design would incorporate the potential to house two spark plugs, Figure 4.22 illustrates this effort.

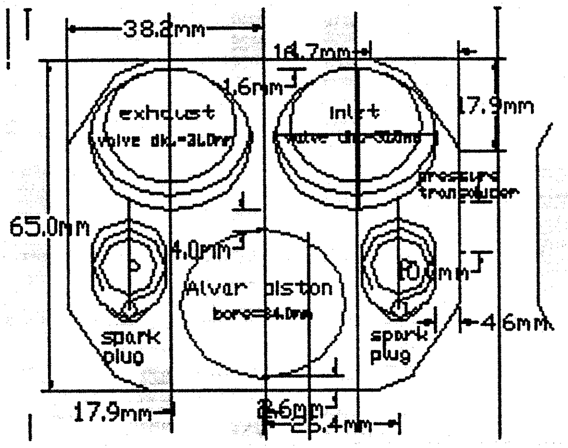
38.2mm
18.7mm
1.6mm
17.9mm
exhaust
valve dia.=31.0mm
inlet
pressure
transducer
65.0mm
4.0mm
10.0mm
Alvar piston
bore=34.0mm
spark
plug
spark
plug
4.6mm
17.9mm
2.6mm
25.4mm

Figure 4.22: Top view of Alvar cylinder head with dual spark plug design

4.10 Clearance Volume Change

The change in clearance volume was motivated by a preliminary friction analysis that revealed that there existed only a modest improvement in friction as a result of offset variance. It was also determined that the secondary connecting rod length had negligible effects on each of the previously studied constraints (i.e. bore2, stroke2). With a secondary offset of 0 mm, the appropriate clearance volume, one in which allowed compression ratio variance of 13 - 7, was determined via the Alvar simulation to be 42.27 cc. The difference in the clearance volumes of 42.38 cc and 42.27 cc required an increase in the additional volume from 11.67 cc to 11.78 cc.

The analysis shown to this point suggests a range of secondary bore from 34 mm to 36 mm would be suitable. From this study it is suggested that a secondary bore of 34 mm be used for the Alvar piston since this selection is the smallest secondary bore that will fit in the cylinder head and still maintain a cross chamber flame travel length (at 15 degrees ATC) that does not vary by more than 20 mm over the full phase range. The stroke of 39.90 mm proves to be compatible with the given geometry of the conventional cylinder head when the connecting rod length is extended from 69.34 mm to 101.13 mm. The offset that was recommended initially was ½ of the crank radius. Note that a refined friction analysis showed that an offset of 20 mm would minimize friction. It is worth noting that a piston of the size recommended is accessible.

4.11 Discussion

The design approach used in this work developed alternative secondary cylinder geometrical combinations. This will allow the cylinder-head designer flexibility in terms of modularity. Note that the information provided in this work will enable additional designs that meet the criteria advanced by the Alvar group. More importantly, the approach itself, while iterative, is conducive to developing such an engine from a variance in the constraints set forth by this group.

Moreover, in submitting the design recommendations included in this chapter, it is further advised that any changes made in the recommended design be done so with the consequences illustrated here in mind. The approach used and outlined in this chapter not only promotes the recommended design, but also provides foresight into the tradeoffs resulting from changes in design parameters such as secondary bore and stroke. This allows exploration of varied designs which may be encouraged by the accessibility of hardware, such as a secondary piston, etc.

4.12 Summary

The design results shown in this chapter meet the four constraints of: (a) compression ratio range of 13 - 7, (b) appropriate flame travel lengths, (c) avoiding deterioration in performance, and (d) physical space limits. The phase and compression ratio requirement allows a design that would be able to avoid knock for a given fuel octane. This compression ratio range will allow efficient operation at part loads and increased power density at boosted pressures, while the flame travel requirement will allow stable combustion. Of equal concern in these matters is the need to avoid introduction of poor performance characteristics. The work shown in this chapter reveals that the design options shown here would not adversely affect the overall performance of the engine. Finally, the design was configured within the geometrical constraint of the conventional cylinder head geometry. This should aid in the design of various design aspects not directly addressed here, such as the cylinder-head coolant passages, so critical to the consistent operation of the Alvar system. This work should supplement physical testing as to confirm that the advantages of the design (i.e. combustion stability, total friction tolerance) are maintained.

The proposed design includes the primary specifications from the conventional Volvo engine. The proposed secondary chamber geometry includes a bore of 34.0 mm, stroke of 39.9 mm, and a connecting rod length of 101.1 mm. A secondary offset is not included since this analysis did not reveal any significant advantages.

Chapter 5

Compression-Ratio Effect on Efficiency

5.1 Introduction

The objective of this study is to evaluate the advantages of the Alvar engine in terms of engine-efficiency gain over that of a conventional spark-ignition engine. By comparing the performance of the engines at identical speed-load conditions and a combination of these speed-load conditions over a driving cycle, any advantages offered by the Alvar engine will be apparent.

The effect of variable compression ratio on the indicated efficiencies of spark-ignition engines is well documented. The compression ratio is again defined as the ratio of the maximum cylinder volume to the minimum cylinder volume. Idealizations of isentropic processes enable the following derivation of the direct relation between the compression ratio and the indicated thermal efficiency [1],

$$\eta_{t,i} = 1 - 1/cr^{\gamma-1} ,$$

where $\eta_{t,i}$ is the indicated thermal efficiency, γ is the ratio of specific heats, and cr is the compression ratio.

This ideal relation may not be reached in practice due to the influence of other variables, such as combustion rate and stability, heat transfer, and friction [1]. Another factor that enters into this relation is valve timing, which affects the effective compression ratio. However, in this study the valve-timing effect is removed by setting the inlet-valve-closing (IVC) at top-dead-center (TDC) and the exhaust-valve-opening (EVO) at bottom-dead-center (BDC) in the Alvar simulation for each engine configuration.

5.2 Alvar-Conventional Engine Comparison at Baseline Conditions

The approach used in the Alvar versus conventional engine comparison begins by matching the engine's performance at some reference point. The brake power at wide-open-throttle and brake torque at part load were matched between the two engines. Because of the extra secondary-chamber volume in the Alvar engine, the stroke of the Alvar engine was adjusted to produce the same brake power at the wide-open-throttle (WOT) condition. The primary stroke of the Alvar engine was changed from 90.0 mm to 95.2 mm, so that both engines have the same brake power. This allowed the brake powers of the engines to match at wide-open-throttle and a speed of 5000 rpm.

Table 5.1 shows the performance of the conventional engine, as produced from the Alvar simulation. This trace, as shown in Figure 5.1, was used to match the Alvar engine at maximum rated power @ 5000 rpm and maximum torque @ 2500 rpm against the conventional engine for use in this analysis. Note that the maximum rated torque and brake power of the conventional engine, as produced from the Alvar simulation, is applicable to a compression ratio of 10.14 and clearance volume of 53.28 cc, wide-open-throttle. The maximum torque occurs at 2500 rpm, while the maximum brake power occurs at 5000 rpm.

Table 5.1 Brake Power and Torque from Conventional Engine via Alvar Simulation

Speed rpm	P_b (Brake Power) kW	T_b (Brake Torque) Nm
5000	105.34	201.18
4500	96.26	204.26
4000	86.60	206.73
3500	76.42	208.51
3000	65.82	209.52
2500	54.89	209.64
2000	43.78	209.04
1500	32.60	207.55
1000	21.43	204.64

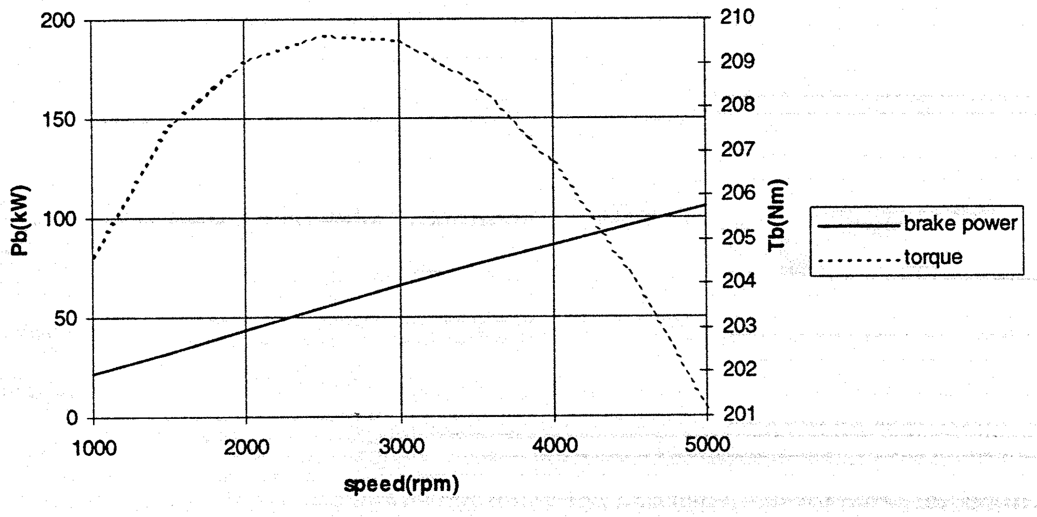

Figure 5.1 Brake power and torque versus engine speed for conventional Volvo 850 engine

With the engine output power and torque matched, the engine geometries were configured as listed in Table 5.2.

Table 5.2 Matching Alvar and Conventional Engines for Efficiency Comparison

Alvar	Conventional
bore 1 = 83.00 mm	bore = 83.00 mm
stroke 1 = 95.20 mm (extended to match)	stroke = 90.00 mm
connecting rod length 1 = 158.00mm	connecting rod length = 158.00 mm
offset = 0.00 mm	offset = 0.00 mm
bore 2 = 34.00 mm	brake power @ 5000 rpm, WOT = 105.3 kW
stroke 2 = 39.90 mm	compression ratio = 10.1
connecting rod length 2 = 101.13 mm	indicated thermal efficiency = 36.3 %
offset 2 = 0.00 mm	
phase = 69.00 degrees	
brake power @ 5000 rpm, WOT = 105.3 kW	
compression ratio = 10.1	
indicated thermal efficiency = 36.6 %	

5.3 Compression-Ratio Schedule

The Alvar engine varies its compression ratio depending on engine load. A lower compression ratio is used at high load to avoid knock, while higher compression ratios are used at lower loads. The compression ratio versus load schedule in Figure 5.2 is used for the following studies. This schedule was selected to reflect the strong decrease in knock likelihood away from the full load condition. For the purpose of comparison, the compression ratio is assumed to be the same for the Alvar and conventional engines at WOT. In the Alvar engine, compression ratio reaches 13 at the very light load condition. The precise shape, minimum and maximum compression ratios, and curvature are only estimated for the purpose of this study. In the final implementation in a vehicle, the actual schedule ought to be optimized. The compression ratio is allowed to increase steeply as the load is reduced from full load. The EPA driving cycle covered later in this chapter will use the compression-ratio schedule in Figure 5.2. Note that the schedule is independent of the driving cycle. The compression ratio for the conventional engine is held constant at 10.1. See Figure 5.2 below.

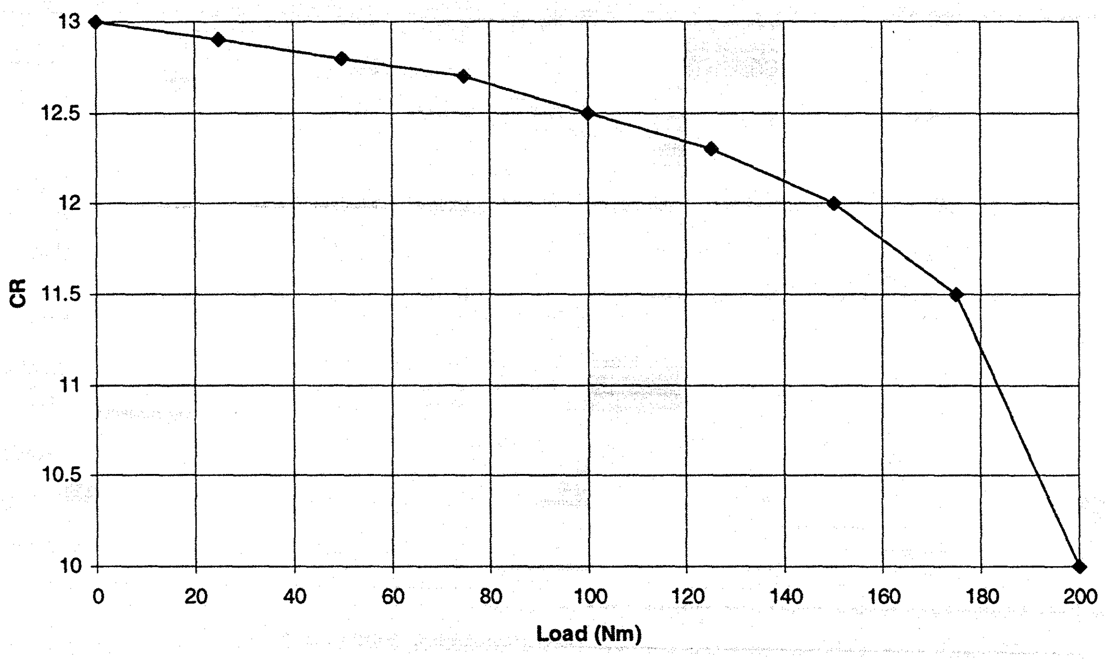

Figure 5.2 Compression ratio versus load schedule

5.4 Alvar-Conventional Engine Comparison at Various Speed-Load Conditions

First, the engines were compared with no standard driving cycle referenced. Instead three set engine speeds of 1500, 3000, and 5000 rpm were used at high, medium, and low loads of 200 Nm, 100 Nm, and 50 Nm respectively, producing nine conditions which are shown below in Table 5.3, 5.4, and 5.5. The corresponding compression ratios for the Alvar engine were 10.0, 12.5, and 12.8.

Table 5.3 Conventional and Alvar (CR=12.8) Engines at Low Load = 50 Nm

	Alvar	Conventional		Alvar	Conventional	
	(indicated)			(brake)		
Engine Speed(rpm)	$\eta_{t,i}$ (%)	$\eta_{t,i}$ (%)	Eff. Gain = (Alvar-Conv.)/Conv. x 100 % (%)	$\eta_{t,b}$ (%)	$\eta_{t,b}$ (%)	Eff. Gain = (Alvar-Conv.)/Conv. x 100 % (%)
1500	29.37	27.96	5.04	21.64	20.93	3.39
3000	30.80	29.26	5.26	20.90	20.28	3.06
5000	33.02	31.19	5.87	17.88	17.61	1.53

Table 5.4 Conventional and Alvar (12.5) Engines at Medium Load = 100 Nm

	Alvar	Conventional		Alvar	Conventional	
	(indicated)			(brake)		
Engine Speed(rpm)	$\eta_{t,i}$ (%)	$\eta_{t,i}$ (%)	Eff. Gain = (Alvar-Conv.)/Conv. x 100 % (%)	$\eta_{t,b}$ (%)	$\eta_{t,b}$ (%)	Eff. Gain = (Alvar-Conv.)/Conv. x 100 % (%)
1500	33.26	31.68	4.99	27.33	26.31	3.88
3000	34.35	32.69	5.08	27.06	26.12	3.60
5000	35.62	33.81	5.35	24.88	24.26	2.56

Table 5.5 Conventional and Alvar (CR=10.1)Engines at High Load = 200 Nm

	Alvar	Conventional		Alvar	Conventional	
	(indicated)			(brake)		
Engine Speed(rpm)	$\eta_{t,i}$ (%)	$\eta_{t,i}$ (%)	Eff. Gain = (Alvar-Conv.)/Conv. x 100 % (%)	$\eta_{t,b}$ (%)	$\eta_{t,b}$ (%)	Eff. Gain = (Alvar-Conv.)/Conv. x 100 % (%)
1500	34.86	34.60	0.75	30.52	30.40	0.04
3000	35.75	35.48	0.76	30.68	30.63	0.16
5000	36.55	36.25	0.83	29.46	29.62	0.54

The results in the initial investigation shown in Table 5.3, 5.4, and 5.5 favor the Alvar engine. However, this advantage is shown primarily at part loads, reflecting the strong influence of compression ratio on efficiency. For instance, note that there exists a 5 percent improvement in the indicated thermal efficiency at the low load and medium load operation condition for the Alvar and conventional engines, and a 0.8 percent improvement at the high load operation condition where the compression ratios are the same, each at a speed of 1500 rpm. The sharp drop in the efficiency advantage of the Alvar engine is due to the sharp drop in compression ratio towards that of the conventional engine as high load is approached.

5.5 Alvar-Conventional Engine Comparison for EPA Driving Cycle

Once the engines were configured geometrically for matched power output and the schedules were arranged for the Alvar engine, an EPA city driving cycle was chosen that would help identify any advantages in practice one engine might have in terms of efficiency.

The EPA city driving cycle is divided into three city driving conditions carried out in a total of 1372 seconds. The first scenario makes up the first 505 seconds after cold starting. The remaining 867 seconds constitutes a city cycle scenario with the engine temperature fully stabilized. A third scenario repeats the first 505 seconds with the engine temperature fully stabilized. The second and third scenarios are combined to constitute the total city time and a distance of 7.45 miles. The driving cycle can be approximated by five operating conditions shown in Table 5.6 for an engine comparable to the Volvo 850. The vehicle speed has been translated to engine rpm using a vehicle simulation program. The comparison procedure for the EPA cycle focused on these five conditions that specify engine speed and load. At each speed and load, a corresponding compression ratio was used for the Alvar engine. These five conditions were also used for the conventional engine, but note that the compression ratio remains constant in this case. The compression ratio schedules used for the Alvar engine reflect the variance of the Alvar engine over the partial range (10-13) and was extracted from Figure 5.2. The condensed driving cycle with the compression ratio schedule is shown next in Table 5.6.

Table 5.6 EPA City Driving Cycle-Alvar CR Schedule

Engine Speed (rpm)	Engine Load (Nm)	CR schedule	Phase (deg)	Time (%)
1000	27.12	12.8	26.0	51.9
1400	54.24	12.7	28.0	22.7
1500	84.07	12.6	30.0	16.4
1800	120.68	12.4	33.0	7.0
2000	158.65	11.7	44.0	2.0

Note that a 13-7 compression ratio range (full range) would leave the engine less susceptible to knock for the turbocharged Alvar (next chapter), however, the range of 10 - 13 is more applicable to this study on the naturally-aspirated engine. For each case, the indicated and brake thermal efficiencies were calculated using the Alvar simulation. By determining these thermal efficiencies and noting that the thermal efficiency is related to the brake power, and fuel mass flow rate in the following manner,

$$\eta_t = P/(m_f * Q_{HV}),$$

where P is the brake work, m_f is the fuel mass flow rate, and Q_{HV} is the fuel heating value, the power generation and mass flow rates can be calculated. From these calculations, the fuel-rate-weighted averages of efficiency, in addition to the simple time-average, can be calculated.

Table 5.7 and 5.8 show the compression ratio-load schedule used to illustrate the weighted efficiencies of the conventional and Alvar engines over the EPA driving cycle, including the accompanying phases necessary through use of the Alvar simulation. The tables further show both the time weighted average and the energy weighted average. The energy weighted average is more exact in that it takes into account the energy release variance during the driving cycle and is shown for the two engines in Figure 5.3.

Table 5.7 Conventional Engine Under EPA City Driving Cycle

CR	Engine Speed (rpm)	Load (Nm)	Time (%)	Time (seconds)	$\eta_{t,i}$ (%)	$\eta_{t,b}$ (%)	Work (Wb) (MJ)	Fuel Energy ($Wb/\eta_{t,b}$) (MJ)
10	1000	27.12	51.9	712.07	23.83	15.54	2.02	13.01
10	1400	54.24	22.7	311.44	28.33	21.59	2.48	11.47
10	1500	84.07	16.4	225.01	30.81	25.07	2.97	11.86
10	1800	120.68	7.0	96.04	32.80	27.65	2.18	7.90
10	2000	158.65	2.0	27.44	32.93	27.68	0.91	3.29
Total	**for**	**cycle:**	**100**	**1372**			**10.56**	**47.53**
time	**weighted**	**average:**	**$\Sigma[(time\%)*\eta)/100]$**		**26.81**	**19.57**		
energy	**weighted**	**average:**	**$100\%*\Sigma Wb/(\Sigma Wb/\eta_{t,b})$**			**22.23**		

Table 5.8 Alvar Engine Under EPA City Driving Cycle

CR	Engine Speed (rpm)	Load (Nm)	Time (%)	Time (seconds)	$\eta_{t,i}$ (%)	$\eta_{t,b}$ (%)	Work (Wb) (MJ)	Fuel Energy ($Wb/\eta_{t,b}$) (MJ)
12.8	1000	27.12	51.9	712.07	24.97	15.96	2.02	12.67
12.7	1400	54.24	22.7	311.44	29.73	22.32	2.48	11.09
12.6	1500	84.07	16.4	225.01	32.35	26.01	2.97	11.43
12.4	1800	120.68	7.0	96.04	34.41	28.72	2.18	7.61
11.7	2000	158.65	2.0	27.44	35.42	30.26	0.91	3.01
Total	**for**	**cycle:**	**100**	**1372**			**10.57**	**45.81**
time	**weighted**	**average:**	**$\Sigma[(time\%)*\eta)/100]$**		**28.13**	**20.23**		
energy	**weighted**	**average:**	**$100\%*\Sigma Wb/(\Sigma Wb/\eta_{t,b})$**			**23.07**		

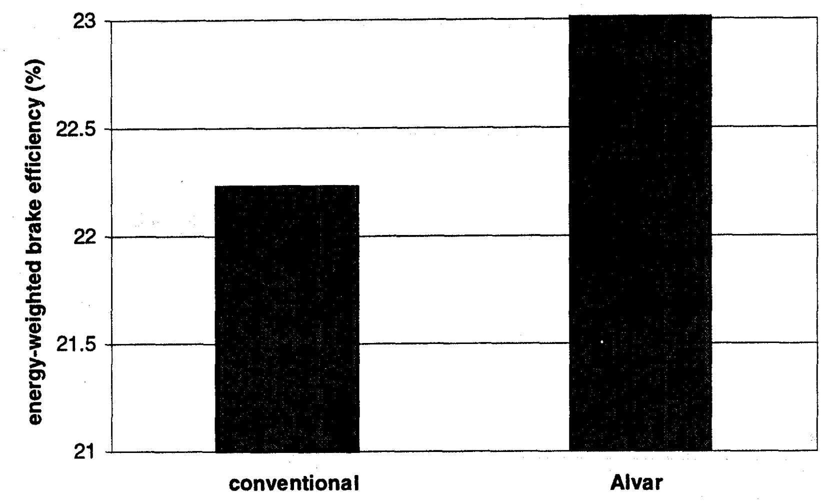

Figure 5.3: Energy-weighted brake efficiencies for conventional and Alvar engines for EPA City Driving Cycle.

Tables 5.7 and 5.8 show the advantage of the Alvar engine in indicated and brake thermal efficiencies of 5.0 percent and 3.4 percent respectively. The energy weighted average reveals an advantage of the Alvar engine in brake efficiency of 3.8 percent.

The comparison trend for the brake efficiency of the engine is similar to that of the indicated efficiency as the engine performance is dominated by compression ratio. However, the difference in the indicated and brake efficiency values for both engines reveals the friction effect.

5.6 Summary

This analysis shows that the effect of compression ratio on the thermal efficiency of the Alvar engine can be used to conserve fuel through increased efficiencies at part loads. However, this benefit is quite modest for the naturally-aspirated operation of the engine. For example, the ideal textbook relation between compression ratio and thermal efficiency indicates that a difference in compression ratio of 10 to 13 yields an increase in efficiency of 6.0 percent, while the EPA driving cycle included in this text, yields a time-weighted-average advantage in indicated efficiency of 5.0 percent, and a energy-weighted-average advantage in brake efficiency of 3.8 percent. However, substantial investment has been made in industry to improve fuel economy by even a few percentage points.

This analysis shows that the real benefit of the Alvar compression ratio variance is the flexibility. For instance, the compression ratio can be reduced as the engine is turbocharged at high load to increase the power of the engine while avoiding knock. The next chapter addresses the boosted operation of the Alvar engine.

Chapter 6

Turbocharged Alvar

6.1 Introduction

The objective of the knock analysis is to evaluate the advantages of the turbocharged Alvar engine in terms of power density over that of a conventional engine. As maximum power is often limited by knock, which relates to end-gas temperature and pressure, we can begin by investigating whether the use of the Alvar mechanism reduces in-cylinder unburned gas temperature and pressure. By making this investigation, it can be determined if the Alvar system decreases the likelihood of knock at boosted intake pressures. Furthermore, in determining the tolerance to knock, it can be determined if the Alvar mechanism has the advantage of increased power density.

6.2 Knock Background

The performance of the internal combustion engine is reduced, in part, by two mechanisms that disturb the combustion process. These include surface ignition and knock. Surface ignition is the ignition of the fuel-air mixture as a result of heat transfer from the cylinder wall or other components inside the cylinder. Components that typically cause such reactions are spark plugs, chamber deposits, or exhaust valves, all of which tend to be hotter than other parts of the cylinder chamber. The issue of reducing this effect is addressed during the design process by following typical techniques for insuring the minimization of such effects. No novel approach is used here for this purpose as surface ignition is not the focus of the current study.

However, knock is an issue of concern, which involves the state of the end gas. Knock is the title given to the noise that is transmitted through the engine block resulting from the autoignition of a portion of the end-gas, or mixture ahead of the progressing flame front. The occurrence of knock in the internal combustion engine results in the rapid release of energy, causing large pressure increases. Aside from detracting from performance, this phenomenon can cause severe damage to the engine. Two theories on the development of knock in the spark ignition engine exist: the autoignition theory and the detonation theory. The latter theory asserts that knock occurs when the flame front accelerates to sonic velocity and consumes the end-gas at a much higher rate than the normal flame front. The former theory asserts that knock occurs when portions of the end-gas spontaneously ignite without being reached by the flame front. The end-gas self ignites because it reaches a pressure and temperature that facilitates ignition. The properties of the fuel-air mixture are important in determining at what point this autoignition will occur and are described by the octane number. The theory of autoignition is more widely accepted and is used here for a comparison between the likelihood of knock occurring in the Alvar engine versus the conventional engine.

6.3 Modifications to Alvar Simulation and Test Runs

In order to compare the turbocharged performance of the Alvar engine with that of a standard Volvo 850 engine, the Alvar simulation used was a modified version to accommodate boosted intake pressures. The addition of a turbocharging unit entails the addition of a compressor and a turbine to the engine intake and exhaust respectively. The simulation was modified to reflect this addition by quantifying temperatures and pressures of an ideal gas exiting and entering both compressor and turbine and maintaining consistency with a total system energy balance.

The pressures and temperatures involving the compressor are characterized using the following efficiency relation for a compressor,

$$\eta_c = [(p_2/p_1)^{(\gamma-1)/\gamma} - 1]/[T_2/T_1 - 1] ,$$

where η_c is the compressor efficiency, γ is ratio of specific heats for unburned gases, p_1 and T_1 are the compressor inlet pressure and temperature respectively, p_2 and T_2 are the compressor exit pressure and temperature respectively.

Similarly, the pressures and temperatures involving the turbine are characterized using the following efficiency relation for a turbine,

$$\eta_t = [1 - (T_4/T_3)]/[1-(p_4/p_3)^{(\gamma-1)/\gamma}],$$

where p_3 and T_3 are the turbine inlet pressure and temperature respectively, and p_4 and T_4 are the turbine exit pressure and temperature respectively.

For a given turbocharger, the turbine and compressor are linked by an energy balance which, for an ideal gas, evolves into

$$c_{p,c}(T_2 - T_1) = \eta_m c_{p,T}(T_3 - T_4)$$

where $c_{p,c}$ and $c_{p,T}$ are the specific heats for the gases associated with the compressor and turbine respectively, and η_m is the mechanical efficiency of the turbocharger shaft arrangement. The last three relations combine to form the following energy balance:

$$(p_2/p_1)^{(\gamma c-1)/\gamma c} - 1 = \eta_c \eta_t \eta_m (c_{p,T}/c_{p,c})[1 - (p_4/p_3)^{(\gamma T-1)/\gamma T}](T_3/T_1)$$

The usual turbocharging mapping techniques involve determination of the compressor and turbine efficiencies consistent with certain pressure ratios, mass flow, and turbocharger speeds. In any case, the above relation still holds for a generic turbocharger. An iterative method was used for the turbocharged performance runs. From the *conditions* menu of the Alvar simulation, the back pressure was varied until the desired intake pressure was achieved. The code produces values for the intake pressure and temperature, both possible inputs through the *conditions* menu. Also note that the energy balance of the system, which includes the cylinder chamber, turbine, and compressor, dictates that an increase in the back pressure results in an increase in the cylinder intake pressure and temperature.

6.4 Analysis of Test Runs

The turbocharging test runs from the modified Alvar simulations using a preliminary compression ratio schedule show that the Alvar mechanism produces lower unburned gas temperatures and pressures than the conventional engine. Noting this, the issue then becomes whether the difference in these temperatures and pressures will translate into a significant difference in knock likelihood. The knock likelihood of typical SI engines is sensitive to the unburned gas temperatures and pressures. It is therefore, a goal of this analysis to illustrate a relationship between the unburned gas properties and the likelihood of knock, in order to quantitatively determine any advantage in reducing the unburned cylinder temperature and pressure.

As stated previously (6.2), the concern of the turbocharging analysis is engine knock. In developing a method for quantifying any decrease in knock likelihood, two approaches were studied and one chosen. One approach is to model the detailed chemical mechanisms that describe the autoignition process for hydrocarbon fuels. This model consists of describing the autoignition process in stages that include a large number of simultaneous and interdependent chain reactions. In this model, the knock phenomenon is induced by an increase in reaction rates [1].

Another model relies on the method used for determining the fuel ignition delay time in spark-ignition or diesel engines. Finally, the likelihood of knock can be modeled from the density trace of the unburned gas. The density of the unburned gas rises as the flame front sweeps across the combustion chamber.

The numerical correlation between the unburned gas properties and the knock likelihood, as illustrated by Douard and Ezyat [9], was chosen for this analysis. This model utilizes empirical induction time correlations that are derived by matching an Arrhenius function to induction (autoignition) time data. The assumption used in this work is that the cylinder pressure is uniform throughout the chamber during flame travel (i.e. burned and unburned gases have the same pressure). Additionally, it is assumed that the compression of the end-gas is isentropic, therefore allowing the following unburned temperature and pressure relation,

$$T_u/[p_u^{(\gamma-1)/\gamma}] = \text{constant}$$

where γ represents the ratio of specific heats for the unburned gas. T_u and p_u represent the unburned temperature and pressure, respectively. This model assumes that induction occurs when

$$\int (dt/\tau) = 1,$$

where τ is the induction time (ms) at the instantaneous temperature and pressure for the end-gas, and the finite limits of this integral are ti (time at beginning of compression by flame front) and t (time of autoignition). Because the pressure and temperature traces of the in-cylinder gases are accessible from the Alvar simulation, the induction time relation was discretionized to

$$\sum \Delta t / \tau = 1,$$

where Δt represents the time interval between crank angle degrees.
The most extensive correlation for induction time was performed by Douaud and Ezyat and produced the following relation,

$$\tau = 17.68(ON/100)\text{^}3.402 * P\text{^}(1.7)*e\text{^}(3800/T),$$

where ON is the octane number, P is pressure in atm, and T is temperature in Kelvin, and τ is induction time in milliseconds.

In theory, an advantage, in terms of decreased knock likelihood, will be apparent if the time necessary for end-gas to autoignite is extended. By comparing the time necessary to autoignite in the Alvar engine with that of the conventional engine, any advantage can be seen. The induction times of the Alvar and conventional engines are of concern only if knock induction conditions exist (i.e. gas properties are above knock limit); during most conditions there is no knock. These times can also be compared to the allowable flame travel times given the engine speed and combustion duration. Note that, in practice, flame travel speeds should allow combustion completion before this burn duration time.

6.5 Test Conditions

The induction-time comparison approach was implemented by comparing the induction times for the conventional and the Alvar engines. The in-cylinder temperature, and pressure at the start of combustion (343 degrees) are used to solve for the induction time for the two engines. These induction times are then compared against each other and against a flame travel time that is calculated for a speed of 3000 rpm and burn duration of 60 degrees. Note that a speed of 3000 rpm and 60 degrees burn duration yields an available flame travel time of 3.3 milliseconds, while a speed of 4000 rpm and 60 degrees burn duration yields a flame travel time of 2.5 milliseconds. If the induction time, or time required for knock to occur, is less than the flame travel time it is assumed that knock occurs since we assume that knock conditions exist.

While the conventional engine maintains a set compression ratio of 10.1, the Alvar test includes two cases. One case assumes that the compression-ratio-load schedule was set for the Alvar engine so that four boosted intake pressures use the same compression ratio of 7.3. The second case considers these same four loads but looks up the compression-ratio-load schedule and allows the compression ratio to be adjusted correspondingly. Figure 6.1 shows the compression-ratio-load schedule used in this second case. Note that the matched Alvar specifications shown in Table 5.2 are also used in this turbocharged-Alvar analysis.

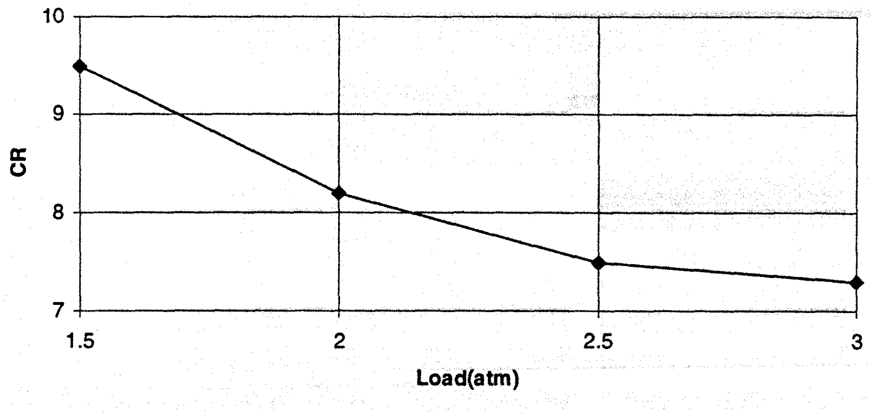

Figure 6.1: Alvar compression ratio-load schedule for turbocharged case study

Figure 6.1, above, can be thought of as a continuation of the compression ratio-load schedule show in Figure 5.2. One may imagine the Alvar engine quickly targeting low compression ratios as the intake pressure increases. So while the compression-ratio schedule lingered at high compression ratios at part loads, the appropriate boost schedule should strive to predominantly maintain low compression ratios at high loads. Figure 6.1 reflects this.

6.6 Results of Comparison

The table below includes the results of the induction time comparison. The loads are represented in terms of intake pressures and in atmospheres to accommodate the convention of the relations used (see section 6.4). The three cases are represented in Table 6.1 with the compression ratio schedule shown in Figure 6.1 included for the variable-compression-ratio Alvar case (i.e. "scheduled" Alvar case in Table 6.1).

Pu and Tu are the unburned gas pressure and temperature at the start of combustion, and τ is the induction time calculated from the integral involving the instantaneous end-gas temperature and pressure, assuming adiabatic compression of the end gas by the flame front. P_b is the brake power of the engine.

Table 6.1 Induction Time Comparison

engine speed = 3000 rpm burn duration = 60 deg.

	Conventional(CR=10.1)				Alvar(CR=7.3)				Alvar(scheduled)				
Load	Tu	Pu	τ_t	P_b	Tu	Pu	τ_t	P_b	CR	Tu	Pu	τ_t	Pb
atm	K	atm	ms	kW	K	atm	ms	kW		K	atm	ms	kW
1.5	799.8	24.2	7.1	78.6	727.6	17.2	20.3	77.6	9.5	799.4	23.2	7.6	78.5
2.0	890.7	31.2	2.8	89.8	813.6	22.3	7.5	89.0	8.3	854.0	26.0	4.7	88.8
2.5	963.3	38.1	1.5	99.8	882.4	27.3	3.7	99.2	7.5	894.0	28.3	3.3	99.4
3.0	1024.3	44.9	0.9	108.8	940.3	32.1	2.2	108.5	7.3	940.8	32.1	2.2	108.5

Figure 6.2 shows the induction times for the unburned gases in the set-compression ratio Alvar case. Note that this set compression ratio case does not imply that the Alvar engine maintains the 7.3 compression ratio throughout the course of operation, instead the compression ratio schedule is set to target different final loads at the same compression ratio of 7.3

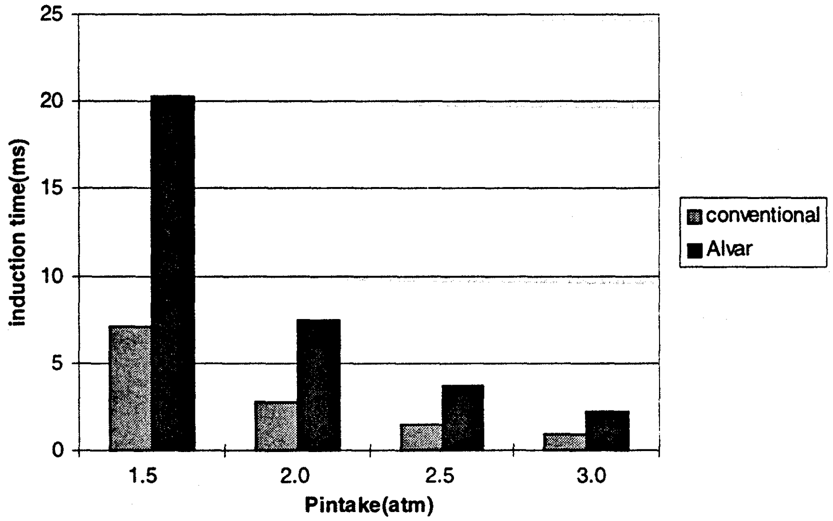

Figure 6.2: Time required to autoignite versus boost pressure for conventional and Alvar (CR=7.3) engines at 3000 RPM, with MBT

The scheduled (variable CR) Alvar case can be compared with the conventional case at individual loads and in the aggregate sense. Figure 6.3 shows that the conventional case matched best with the scheduled Alvar case at a boosted pressure of 1.5 atmospheres directly because the compression ratios are not very different. The improvement widens as the Alvar engine sweeps through the compression ratio-load schedule.

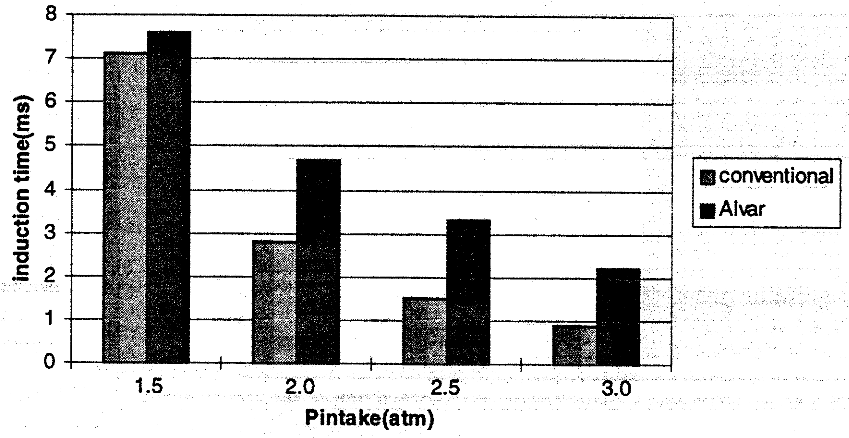

Figure 6.3: Time required to autoignite versus boost pressure for conventional and scheduled (variable CR) Alvar engines at 3000 rpm, with MBT

It is reasonable to expect that knock occurs when the induction time is shorter than the flame travel time. Assume that the flame travel time remains constant at 3.3 ms at 3000 rpm for all loads, it is apparent from Table 6.1 that knock occurs at a much lower power output (boost pressure) for the conventional engine than the Alvar engine.

Figure 6.4 illustrates the increase in unburned gas temperatures for both the scheduled Alvar and conventional engines at brake powers achieved from boosting. Additionally, this chart incorporates the induction times at each resulting brake power point. Note that the results in Figure 6.4 correspond to a boost-pressure range of 1.5 - 3.0 atm. Also note that tc and ta are the induction times for the conventional and Alvar engines respectfully.

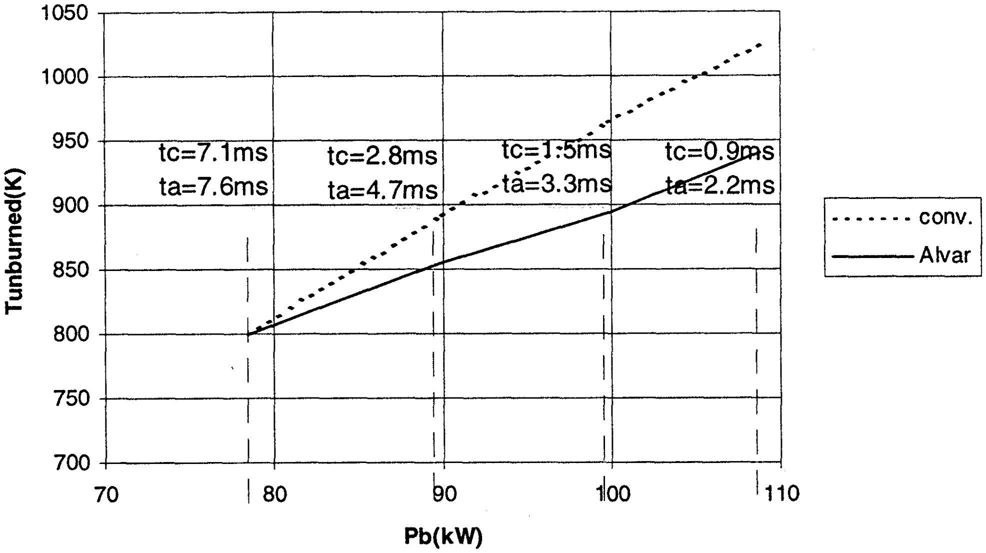

Figure 6.4 In-cylinder unburned gas temperature versus brake power for scheduled Alvar and conventional engines at 3000 rpm, MBT

Figure 6.5 shows the induction times for the Alvar and the conventional engine versus brake power output. Also note that the flame travel time, assuming complete combustion, for both engines at the given speed and burn duration is 3.3 milliseconds. This serves as a lower limit to the induction time since knock prevention maintains that the induction times remain above the flame travel time; assuming knock conditions exist. From Figure 6.5 it can be seen that knock occurs in the Alvar engine at 99.4 kW while knock occurs at 87.5 kW in the conventional engine. The Alvar engine therefore provides an improved power production of 13.6 percent at the above conditions since the conventional engine falls below this limit at a brake power of 87.5 kiloWatts and the scheduled Alvar case meets this constraint at 99.4 kiloWatts, each at a speed of 3000 rpm.

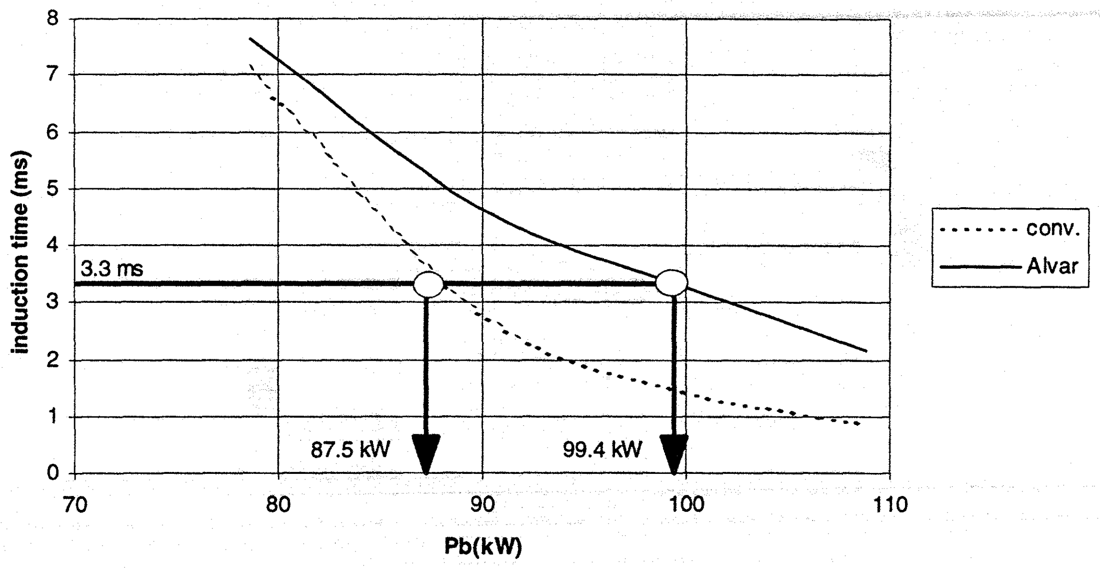

Figure 6.5: Knock induction time versus brake power for Alvar and Conventional engines

6.7 Summary

From the comparison of results for the Alvar and conventional engines, it can be concluded that the Alvar engine has specific benefits, in terms of power density and knock avoidance, over the conventional engine. This conclusion is supported by the fact that there exist an advantage in autoignition induction time for the Alvar engine over the conventional engine. The longer induction time for the Alvar engine allows the Alvar engine to achieve higher boost and higher power output.

Chapter 7

Variable Engine Displacement

7.1 Introduction

A characteristic of the Alvar variable compression ratio engine is that the movement of the secondary piston plays a role in the swept volume(s), or displacement volume(s), of the reciprocating engine. The effective displacement ("size") of an engine can be changed; a "2-liter" engine can be operated with a displacement greater than two liters. Recall that the movement of the secondary piston distinguishes the Alvar engine from other variable compression ratio engines that change the volume of the cylinder chamber by changing the phasing between the primary and secondary pistons. In the Alvar case, the displacement volumes are all different for the intake, compression, expansion, and exhaust strokes. Note that the definition of displacement volume is required in the calculation of the mean effective pressures; in previous chapters, the primary piston displacement volume has been used. The objective of this chapter is to evaluate the effect this variance of displaced volume has on mean effective pressures.

7.2 Definition of Displaced Volumes

The displaced volume of a conventional internal combustion reciprocating engine is normally taken to be the volume swept by the piston with no regard to a particular stroke of the four-stroke cycle. The Alvar engine, however, has four distinct displaced volumes since the primary and secondary pistons move with a phase difference. This occurs because the secondary piston moves at a speed half that of the primary piston. If the pistons moved at the same speed the relative motion would be constant for each stroke. For a given valve timing, the movement of the secondary piston relative to the primary piston dictates the volume displaced on any given stroke. It is therefore necessary to define the displaced volume for each particular stroke. Below, the four distinct displaced volumes are defined.

Intake displaced volume (ivd) = ivmax - evmin (maximum intake stroke volume - minimum exhaust stroke volume)

Compression displaced volume (cmvd) = vivc - cvmin (volume at ivc - minimum compression stroke volume)

Expansion displaced volume (epvd) = vevo - cvmin (volume at evo - minimum compression stroke volume)

Exhaust displaced volume (exvd) = vevo - evmin (volume at evo - minimum exhaust stroke volume)

The schematic below, Figure 7.1, illustrates the differences among the displaced volumes for an Alvar four stroke engine. Note that the schematics are simplified as they do not include the detailed design features. This schematic depicts the relative motion at a phase of 0 degrees; pistons reach the "TDC"s together.

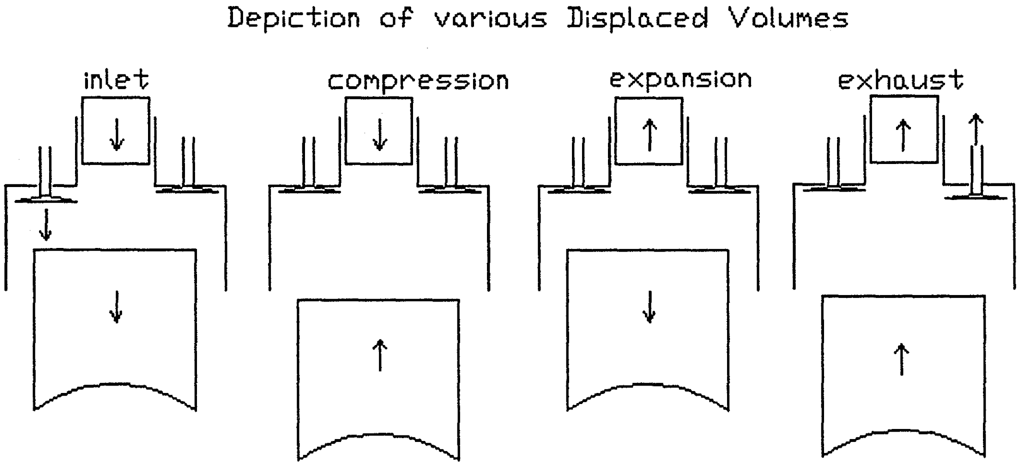

Figure 7.1 Depiction of intake, compression, expansion, and exhaust displaced volumes for the Alvar engine at 0 degrees phase shift

7.3 Mean Effective Pressures

The effect of displaced volume variation on mean effective pressure (mep) is straight forward as mean effective pressure is defined as,

$$\text{mep} = Pn_r/V_dN = W/V_d$$

where P is the engine power, n_r is the number of crank revolutions per power stroke, N is the engine speed, V_d is the displacement volume, and W is the engine work.

To this point, mep calculations have been used with the standard displaced volume excluding secondary effect. Now we can evaluate the differences in mep values, given a particular V_d. To clarify this report, it is necessary to understand the difference caused by phase shift. Figures 7.2 and 7.3 illustrate the chamber volume versus crank angle relationship for a phase of 0 degrees (nominal compression ratio of 13:1) and a phase of 180 degrees (nominal compression ratio of 7:1). Envision a sinusoidal progression between the two cases.

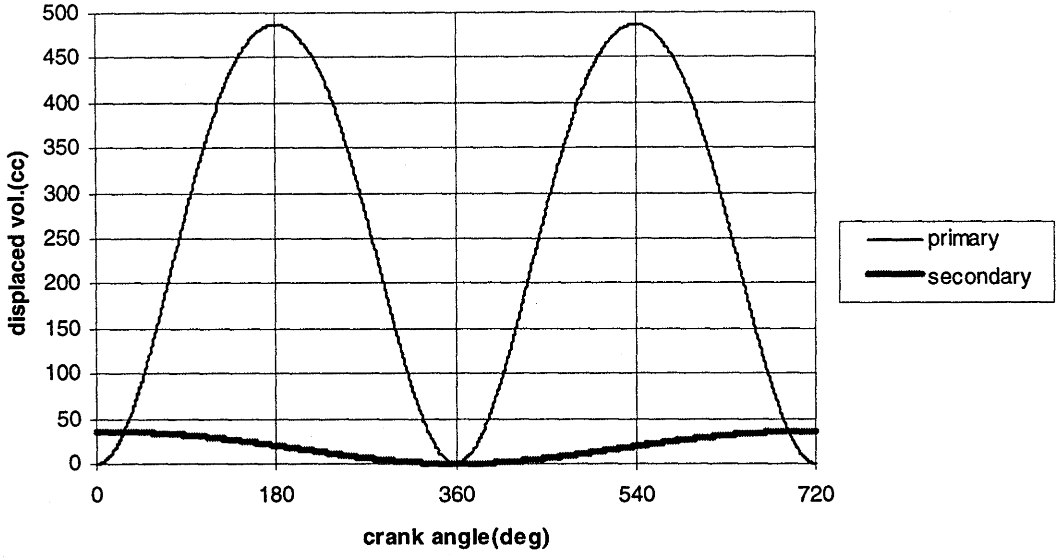

Figure 7.2: Displaced volume versus crank angle, with phase of 0 degrees and nominal compression ratio of 13:1

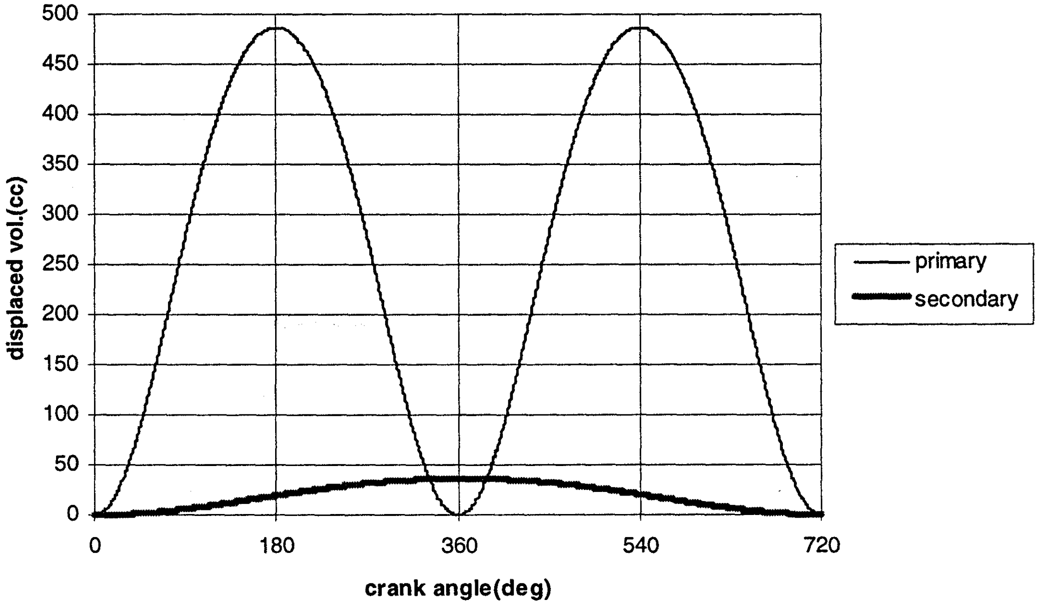

Figure 7.3: Displaced volume versus crank angle, with phase of 180 degrees and nominal compression ratio of 7:1

The results in Table 7.1 relate BMEPs with different displaced volumes.

Table 7.1 Effect of Compression Ratio on BMEPs via Alvar Simulation

BMEP vs. Phase Shift for different Displaced Volumes

phase (deg)	ncr	IBMEP kPa	CMBMEP kPa	EPBMEP kPa	EXBMEP kPa
0	13.0	851.5	791.1	802.8	865.1
60	10.7	825.3	783.5	741.2	778.5
120	7.8	785.8	805.7	749.0	731.7
180	7.0	760.3	819.2	806.4	749.2
240	7.5	752.4	794.5	842.3	799.6
300	10.1	804.3	785.8	843.7	865.1
360	13.0	851.5	791.1	802.8	865.1

Note that the most consistent BMEP values exist for the compression displacement volume with the largest range reached by the exhaust-stroke displacement volume. The case used to generate the values for Table 7.1 includes the primary bore specifications used throughout this thesis, a secondary bore of 34.0 mm, secondary stroke of 39.9 mm, secondary connecting rod length of 101.1 mm, a secondary offset of 20.0 mm, and a clearance volume of 42.27 cc at 3000 rpm, WOT, and MBT. See how each BMEP varies with phase in Figure 7.4.

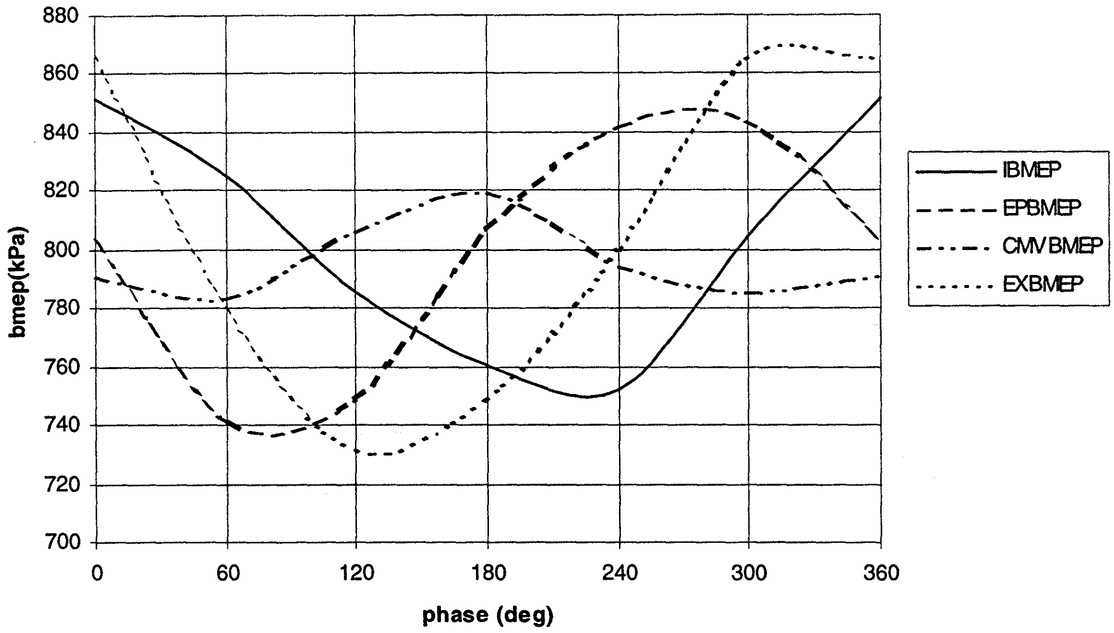

Figure 7.4: BMEP versus phase for given displaced volumes, with engine speed of 3000 RPM, WOT operation, and MBT

The mean effective pressure therefore depends on the definition of the displaced volume over a complete four-stroke cycle. For instance, for a five-cylinder engine each cylinder experiences one exhaust stroke per cycle. The total displaced volume over the exhaust stroke is therefore the combined exhaust displaced volumes of the five cylinders.

7.4 Variable Engine Displacement

The variable-displacement feature of the Alvar engine implies that the effective "size" of the engine can be changed. A 2-liter engine can operate as a 2.5-liter engine if the secondary bore is sufficiently large. The quantity of air in the fuel-air mixture that is inducted into the engine probably depends on the intake displacement. The compression displacement controls the compression ratio. The expansion volume governs the power extracted , and the exhaust displacement affects the residual fraction. All of these can be manipulated to the engine's advantage.

7.5 Summary

This analysis shows how the displaced volume varies with phase shift. The differences among the displaced volumes are evident from the variance in BMEP. Each displaced volume affects a different aspect of engine performance. The intake displacement can change to allow for additional charge or air to be inducted. Therefore the effective displacement of the engine can actually be increased from its nominal value in the Alvar engine configuration.

Chapter 8

Summary and Conclusions

Geometric specifications for a combustion chamber of an Alvar engine system, especially those of the secondary chamber, have been developed using the Alvar (Hoglund) simulation. The Alvar simulation has been compared against a conventional engine simulation (MIT version), and the Alvar simulation was found to be a very powerful tool in the analysis and design of the Alvar engine. Using the Alvar simulation and its adaptation to a turbocharged engine, the effects of different design parameters on engine performance have been studied extensively, and a recommended design for the Alvar combustion chamber has been developed.

The combustion chamber is intended to be incorporated into a cylinder head that would fit onto an existing Volvo 850 engine. Therefore, the dimensions of the primary piston (bore and stroke) are given. Accordingly, the design parameters considered include only the secondary piston bore, stroke, compression ratio, clearance volume, relative locations of piston and valves, etc. The performance parameters studied include the criteria and likelihood of knock, engine heat transfer, efficiency, and engine power density.

Considerations of engine knock and the eventual turbocharging of the Alvar engine led to the determination of a compression ratio range of 13 to 7, which corresponds to light and full load operating conditions respectively. This is a primary design requirement. Adequate flame propagation into the secondary chamber is another criterion in determining the design of the secondary chamber, namely the secondary bore-to-stroke ratio. In addition to these constraints, physical space requirements in the cylinder head dictate the final design details.

While the design approach was iterative, much was gained from each facet of the design study. To this point, several valid possibilities were found in terms of secondary chamber geometrical flexibility. This study suggests that a geometry that includes the primary specifications from the conventional Volvo 850, a secondary bore of 34.0 mm, secondary stroke of 39.9 mm, secondary connecting rod length of 101.1 mm, and a clearance volume of 42.27 cc will be best for the Alvar engine.

The evaluation of the Alvar engine's potential for reducing fuel consumption through increased efficiency, by operating at higher compression ratios at part loads, showed a modest advantage from the Alvar engine. This study shows that an improvement of close to six percent at light loads, and 3.8 percent or higher in energy-weighted-average efficiency over an urban driving cycle, can be expected. While this may appear to be a small advantage, improvements of this magnitude serve to effectively reduce fuel consumption over the total engine life. Fuel economy benefits from reduced engine size at a given power output, and thus vehicle weight, could translate into substantial additional gains.

An area of significant optimism is the capability of the Alvar engine to operate at much higher boost levels before encountering knock. This is due to the capability of the engine to selectively vary the compression ratio according to engine load and intake boost. When compared with a conventional engine, the Alvar engine showed a substantial advantage in its ability to operate at higher intake pressures before knock occurs and thereby increase its power output for a given geometry.

The Alvar engine has been shown to exhibit variable displacement volumes. Thus the effective "size" (engine displacement) of the engine can be changed to some extent by controlling the relative motion between the primary and secondary pistons.

Finally, it is concluded from this work that the Alvar engine is a viable approach to benefit from varying the compression ratio of the internal combustion engine. The advantages outlined in this project include improvements from the Alvar engine in both engine efficiency and power density, during both part loads and at boosted driving conditions. Physical testing of the Alvar engine will serve to confirm, and expand upon, the findings of this work.

References

1. Heywood, John ,Fundamentals of Internal Combustion Engine, McGraw-Hill, Inc. © 1988

2. Hatamura, Kouichi et.al. "Development of Miller Cycle Gasoline Engine - Miller Cycle Engine with Late Intake Valve Closing and Lysholm Compressor" SAE Paper 938051

3. Adams, W.H. et.al. "Analysis of the Combustion Process of a Spark Ignition Engine with a Variable Compression Ratio" SAE Paper 870610

4. Rychter, T.J. et.al. "VR/LE Engine with Variable R/L During A Single Cycle" SAE Paper 850206

5. Wirbeleit, F.G. et.al. "Development of Piston with Variable Compression Height for Increasing Efficiency and Specific Power Output of Combustion Engines" SAE Paper 900229

6. Ashley, Cedric "Variable Compression Pistons" SAE Paper 901539

7. Lia, T.A. "The "Alvar" Engine Concept. A Variable Compression Ratio Spark Ignition Engine" SAE Paper 825106

8. Patton, Kenneth J. "Development and Evaluation of a Performance and Efficiency Model for Spark-Ignition Engines" © MIT, M.S. Thesis, Mechanical Engineering Department, 1989

9. A.M. Douaud and P.Eyzat "Four - Octane - Number Method for Predicting the Anti - knock Behavior of Fuels and Engines" SAE Paper 780080

10. Rychter, T.J. et.al. "A Theoretical Study of a Variable Compression Ratio Turbocharged Diesel Engine" Journal of Power and Energy, Vol. 206, No. A4, p. 227, 1992

11. Blakey, S.C. et.al. "A Design and Experimental Study of an Otto Atkinson Cycle Engine Using Late Intake Valve Closing" SAE Paper 910451

12. Thring, R.H. "The Flexible Diesel Engine" SAE Paper 900175

13. Ma, T.H. & Rajabu, H. "Computer Simulation of an Otto - Atkinson Cycle Engine with Variable Timing Multi - Intake Valves and Variable Compression Ratio" SAE Paper 884053

14. Ladommatos, N. & Stone, C.R. "Developments for Direct Injection Diesel Engines" SAE Paper 864948

15. Mansouri, S.H., Heywood, J.B., and Radhakrishnari, K., "Divided - Chamber Diesel Engine, Part 1: A Cycle - Simulation Which Predicts Performance and Emissions" SAE Paper 820273

16. Ueda, Naoharu et.al. "A Naturally Aspirated Miller Cycle Gasoline Engine - Its Capability of Emission, Power and Fuel Economy" SAE Paper 960589

17. Rychter, T.J. & Teodorczyk, "A Economy and NO Emission Potential of an SI Variable R/L Engine" SAE Paper 850207

18. Zafer Duvsunkaya and Rifat Keriber "Simulation of Secondary Dynamics of Articulated and Conventional Piston Assemblies" SAE Paper 920484

19. D. Bradley, G.T. Kalghatgi and M. Golombok "Fuel Blend and Mixture Strength Effects on Autoignition Heat Release Rates and Knock Intensity in SI Engines" SAE Paper 962105

20. Pyongwan Park and James C. Keck "Rapid Compression Machine Measurements of Ignition Delays for Primary Reference Fuels" SAE Paper 900027

21. W.Lee and H.J. Schaefer "Analysis of Local Pressure, Surface Temperature and Engine Damages Under Knock Conditions" SAE Paper 830508

22. H. Schapertons and W.Lee "Multidimensional Modeling of Knocking Combustion in SI Engines" SAE Paper 841337

23. Philip M. Dimpelfeld and D.E. Foster "The Prediction of Autoignition in Spark Ignited Engine" SAE Paper 841337

24. C.V. Ferraro, M. Marzano and P. Nuccio "Knock - Limit Measurement in High - Speed SI Engines" SAE Paper 850127

Appendices

Appendix A: Alvar Simulation Variables
Appendix B: Alvar Patent

Appendix A: Alvar Simulation Variables

```
  I  to Initialize menu
  C  to Calculate menu
  S  to Show Results
  P  to Plot
  RE to Recall Engine
  SE to Store Engine
  RS to Recall Setup
  SS to Store Setup
  H  for Help in all menus
  Use commands for speed
Alvar 5.7
```

```
     Initialize

  IG to Geometry Menu
  IM to Masses Menu
  ID to Diameters Menu
  IF to Friction Menu
  IC to Conditions Menu
  IH to Heat Release Menu
  IS to Screen Menu
  A  to engine A
  B  to engine B
  Use commands for speed
Alvar 5.7
```

```
    Calculate

 CG to Calculate Geometry

 CE to Calculate Energy

 CF to Calculate Friction

 CP to Calculate Pressure and friction

 CA to Calculate All

 Use commands for speed




Alvar 5.7

    Geometry

    Primary:
 1  BOR1 = Cylinder Bore
 2  CRA1 = Crank Radius
 3  CRL1 = Conrod Length
 4  CSO1 = Crankshaft Offset
    Secondary:
 5  BOR2 = Cylinder Bore
 6  CRA2 = Crank Radius
 7  CRL2 = Conrod Length
 8  CSO2 = Crankshaft Offset

 9  CLV  = Clearance Volume
10  NCR  = Nominal Compression Ratio
11  ECR  = Effective Compression Ratio
    Secondary:
12  CSR  = Crankshaft Speed Ratio
13  CPS  = Crankshaft Phase Shift, TDC

14  IVC  = Intake Valve Closing
15  EVO  = Exhaust Valve Opening

Alvar 5.7
```

Masses

1 PIM1 = Primary Piston Mass
2 CRM1 = Primary Conrod Mass

3 PIM2 = Secondary Piston Mass
4 CRM2 = Secondary Conrod Mass

5 NCY = Number of Cylinders

Alvar 5.7

Diameters

Primary:
1 GPD1 = Gudgeon Pin Diameter
2 CPD1 = Crank Pin Diameter
3 MBD1 = Main Bearing Diameter
Secondary:
4 GPD2 = Gudgeon Pin Diameter
5 CPD2 = Crank Pin Diameter
6 MBD2 = Main Bearing Diameter

7 CSD = Camshaft Diameter

Alvar 5.7

Friction

Primary:
1 PFC1 = Piston Friction Coefficient
2 RFC1 = Top Ring Friction Coeff.
3 GFC1 = Gudgeon Pin Friction Coeff.
4 CFC1 = Crank Pin Friction Coeff.
5 MFC1 = Main Bearing Friction Coeff.
Secondary:
6 PFC2 = Piston Friction Coefficient
7 RFC2 = Top Ring Friction Coeff.
8 GFC2 = Gudgeon Pin Friction Coeff.
9 CFC2 = Crank Pin Friction Coeff.
10 MFC2 = Main Bearing Friction Coeff.

11 CFC = Camshaft Friction Coeff.

12 TBT = Transmission Belt Tension
13 VSF = Valve Spring Force

Alvar 5.7

Conditions

1 ESP = Engine Speed
2 BRT = Brake Torque
3 BRP = Brake Power

4 PAMB = Ambient Pressure (abs.)
5 PDRY = Dry Air Pressure (abs.)
6 PIVC = Cyl. Pressure at IVC (abs.)
7 PEXB = Exhaust Backpressure (abs.)

8 TAMB = Ambient Air Temperature
9 TCHA = Charge Gas Temperature
10 TWAL = Chamber Wall Mean Temp

11 HLC = Wall Heat Loss Constant
12 EGR = Exhaust Gas Recirc. (vol%)

13 CGK = Charge Gas Kappa Value
14 EGK = Exhaust Gas Kappa Value
15 KAT = Kappa Activation Temp (K)

Alvar 5.7

Heat Release

1 A0 = 0 % Energy Release Angle
2 A50 = 50 % Energy Release Angle

3 D90 = 10-90% Energy Rel. Duration
4 D99 = 1-99 % Energy Rel. Duration
5 D100 = 0-100% Energy Rel. Duration

6 FHC = Fuel Heat of Combustion
7 FMW = Fuel Vapor Mean Mole Weight

8 AFR = Air Fuel Ratio
9 SAF = Stoichiometric A/F Ratio
10 FI = (F/A)/(F/A)stoich

Alvar 5.7

Display

1 Set screen for EGA or VGA mode

2 Set foreground color

3 Set background color

4 Set text size

5 Set calculation ready signal

Alvar 5.7

Results 1

ESP = Engine Speed
BRT = Brake Torque
BRP = Brake Power

Mean effective pressure

GMEP = Gross (Ind.) Mean Eff. Pressure
IMEP = Ind. Mean Effective Pressure
BMEP = Brake Mean Eff. Pressure

Specific fuel consumption

GSFC = Gross (Ind.) Spec. Fuel Co.
ISFC = Indicated Specific Fuel Co.
BSFC = Brake Specific Fuel Consumption

Alvar 5.7

Results 2

STR1 = Primary Piston Stroke
STR2 = Secondary Piston Stroke

PDV1 = P. Piston Displacement Volume
PDV2 = S. Piston Displacement Volume

PMS1 = Primary Piston Mean Speed
PMS2 = Secondary Piston Mean Speed

Ratios

NIR = Nominal Intake Ratio
EIR = Effective Intake Ratio

NCR = Nominal Compression Ratio
ECR = Effective Compression Ratio

NER = Nominal Expansion Ratio
EER = Effective Expansion Ratio

Alvar 5.7

Results 3

Angles

AEVMIN = Angle at EVMIN

AIVMAX = Angle at IVMAX

IVC = Angle at Int. Valve Closing

ACVMIN = Angle at CVMIN

APMAX = Angle at Peak Pressure

ATMAX = Angle at Peak Mean Temp.

EVO = Angle at Exh. Valve Opening

AEVMAX = Angle at EVMAX

Alvar 5.7

Results 4

Temperatures

TAMB = Ambient Air Temperature

TCHA = Charge Gas Temperature

TIVC = Cylinder Gas Temp. at IVC

TWAL = Comb. Chamber Surf. Temp

TMAX = Peak Mean Gas Temperature

TEVO = Cylinder Gas Temp. at EVO

TRES = Residual Gas Temperature

Alvar 5.7

Results 5

Pressures

PAMB = Ambient Pressure (abs.)

PDRY = Dry Air Pressure (abs.)

PIVC = Cyl. Pressure at IVC (abs.)

PMAX = Peak Cyl. Pressure (abs.)

PEVO = Cyl. Pressure at EVO (abs.)

PEXB = Exhaust Backpressure (abs.)

Alvar 5.7

Results 6

TER = Total Energy Release
WHL = Wall Heat Loss
EHL = Exhaust Heat Loss

WG = Gross (Indicated) Work
WP = Pumping Work (Valves open)
WI = Indicated Work
WF = Friction Work
WE = Effective (Brake) Work

Efficiency

GEF = Gross (Indicated) Efficiency
IEF = Indicated Efficiency
BEF = Brake Efficiency
MEF = Mechanical Efficiency
NVE = Nominal Volumetric Efficiency
EVE = Effective Volumetric Efficiency

Alvar 5.7

Results 7

Friction work
Primary:
PFW1 = Piston Friction Work
RFW1 = Piston Ring Friction Work
GFW1 = Gudgeon Pin Friction Work
CFW1 = Crank Pin Friction Work
MFW1 = Main Bearing Friction Work
Secondary:
PFW2 = Piston Friction Work
RFW2 = Piston Ring Friction Work
GFW2 = Gudgeon Pin Friction Work
CFW2 = Crank Pin Friction Work
MFW2 = Main Bearing Friction Work

SUM1 = Sum of Friction 1, % of IW
SUM2 = Sum of Friction 2, % of IW
SUM12 = Sum of Friction 1 and 2

TFW = Transmission Friction Work

Alvar 5.7

Results 8

Volumes

EVMIN = Min. Exhaust Stroke Volume
IVMAX = Max. Intake Stroke Volume
VIVC = Volume at IVC
CVMIN = Min. Compression Stroke Volume
VEVO = Volume at EVO
EVMAX = Max. Expansion Stroke Volume

CLV = Clearance Volume

NIV = Nom. Intake Displac. Volume
EIV = Eff. Intake Displac. Volume

NCV = Nom. Compression Displ. Volume
ECV = Eff. Compression Displ. Volume

NEV = Nom. Expansion Displ. Volume
EEV = Eff. Expansion Displ. Volume

Alvar 5.7

```
Results 9

Cylinder gas composition at IVC

MCYL    =  Moles of gas in cylinder

MAIR    =  Moles of air,     % of MCYL

MFUEL   =      "      fuel          "

MWATER  =      "      water         "

MRES    =      "   residual gas     "

MEGR    =      "      EGR           "

AFR   = Air Fuel Ratio

FI    = (F/A)/(F/A)stoich
```

Alvar 5.7

```
Results 10

CA1 = Primary Crankangle
CA2 = Secondary Crankangle
PP1 = Primary Piston Position
PP2 = Secondary Piston Position
VOL = Combustion Chamber Volume
ARE = Combustion Chamber Area
ENE = Combustion Energy Released
RER = Rate of Energy Release
PRE = Combustion Chamber Pressure
RPR = Rate of Pressure Rise
TEM = Combustion Chamber Temp
IW1 = Primary Indicated Work
EW1 = Primary Effective Work
FW1 = Primary Friction Work
IW2 = Secondary Indicated Work
EW2 = Secondary Effective Work
FW2 = Secondary Friction Work

M  to Main Menu
```

Alvar 5.7

```
    Plot Menu


    Current setup

 GM Grid Menu
 SM Scales Menu
 OM Offsets Menu
 PM Positions Menu
 CM Colors Menu
 TM Types Menu
 DM Display Menu
 RS Recall Setup
 SS Store Setup
 PC Plot Curves
 SC Store Curves

 Use commands for speed
```

Alvar 5.7

```
    Grid Menu


  1 PBA= Plot Begin Angle
  2 PEA= Plot End Angle (<=720)
  3 XSC= X-scale
  4 XDI= X-divisions
  5 YDI= Y-divisions
  6 GPA= Grid on/off (1/0)
  7 CPA= Cross parameter (0-3)
  8 GSI= Grid Size (<= 640)
```

Alvar 5.7

```
     Scales Menu


   1 PPS= Piston Position Scale
   2 VOS= Volume Scale
   3 ARS= Area Scale
   4 ENS= Energy Scale
   5 RES= Rate of Energy Scale
   6 PRS= Pressure Scale
   7 RPS= Rate of Pressure Scale
   8 TES= Temperature Scale
   9 IWS= Indicated Work Scale
  10 EWS= Effective Work Scale
  11 FWS= Friction Work Scale
  12 YSC= Y-Scale
```

```
Alvar 5.7
```

```
     Offsets Menu


   1 PPO= Piston Position Offset
   2 VOO= Volume Offset
   3 ARO= Area Offset
   4 ENO= Energy Offset
   5 REO= Rate of Energy Offset
   6 PRO= Pressure Offset
   7 RPO= Rate of Pressure Offset
   8 TEO= Temperature Offset
   9 IWO= Indicated Work Offset
  10 EWO= Effective Work Offset
  11 FWO= Friction Work Offset
```

```
Alvar 5.7
```

Positions Menu

1 PPP= Piston Position Position
2 VOP= Volume Position
3 ARP= Area Position
4 ENP= Energy Position
5 REP= Rate of Energy Position
6 PRP= Pressure Position
7 RPP= Rate of Pressure Position
8 TEP= Temperature Position
9 IWP= Indicated Work Position
10 EWP= Effective Work Position
11 FWP= Friction Work Position

Alvar 5.7

Colors Menu

1 PPC= Piston Position Color
2 VOC= Volume Color
3 ARC= Area Color
4 ENC= Energy Color
5 REC= Rate of Energy Color
6 PRC= Pressure Color
7 RPC= Rate of Pressure Color
8 TEC= Temperature Color
9 IWC= Indicated Work Color
10 EWC= Effective Work Color
11 FWC= Friction Work Color
12 GFC= Grid Foreground Color
13 GBC= Grid Background Color
14 GCC= Grid Cross Color

Alvar 5.7

```
   Types Menu


1 CUA= (1 or 2) Curve A
2 CUB= (1 or 2) Curve B
3 COA= (0 - 15) Color A
4 COB= (0 - 15) Color B
5 PSL= (1 - 8) Stepsize

  CU* = 1 Continuous
  CU* = 2 Dotted
  CO* = 0 Menu colors
  CO* = 1-15 Override
```

Alvar 5.7

```
   Display Menu


1 Choice to plot A
2 Choice to plot B
3 Choice to plot A and B
4 Choice to plot A - B
5 PV-plot setting
```

Alvar 5.7

Appendix B: Alvar Patent

US005188066A

United States Patent [19]

Gustavsson

[11] **Patent Number:** **5,188,066**

[45] **Date of Patent:** **Feb. 23, 1993**

[54] **INTERNAL COMBUSTION ENGINE**

[75] Inventor: **Alvar Gustavsson**, Skärblacka, Sweden

[73] Assignee: **Skarblacka Bil & Motor AB**, Skarblacka, Sweden

[21] Appl. No.: **777,564**

[22] PCT Filed: **Jun. 19, 1990**

[86] PCT No.: **PCT/SE90/00439**

§ 371 Date: **Dec. 5, 1991**

§ 102(e) Date: **Dec. 5, 1991**

[87] PCT Pub. No.: **WO90/15919**

PCT Pub. Date: **Dec. 27, 1990**

[51] **Int. Cl.**^{5} **F02B 75/04**

[52] **U.S. Cl.** .... **123/48 A**; 123/78 A; 123/51 BB

[58] **Field of Search** .... 123/48 A, 48 AA, 78 A, 123/48 R, 51 R, 51 BB, 51 B

[56] **References Cited**

U.S. PATENT DOCUMENTS

1,099,576	6/1914	Slaby	123/78 A
1,162,054	11/1915	Hansen	123/78 A
1,590,940	6/1926	Hallett	123/78 A
1,707,005	3/1929	Hall	123/48 A
1,719,752	7/1929	Brown	123/78 A
4,104,995	8/1978	Steinbock	123/78 A
4,143,628	3/1979	Gustavsson	123/78 A
4,169,435	10/1979	Faulconer	123/78 A
4,625,684	12/1986	Van Avermarte	123/78 A
4,708,096	11/1987	Mroz	123/78 A
5,007,384	4/1991	Blair	123/48 A

FOREIGN PATENT DOCUMENTS

3107382	10/1982	Fed. Rep. of Germany	123/78 A
WO80/00095	1/1980	PCT Int'l Appl.	123/78 A

Primary Examiner—David A. Okonsky
Attorney, Agent, or Firm—Baker & Daniels

[57] **ABSTRACT**

The present invention relates to an arrangement for an internal combustion engine. The engine is of the kind which has a number of working cylinders (1, 2, 3, 4), each of which communicating with a corresponding auxiliary cylinder (5, 6, 7, 8). Each working cylinder has a working piston (9, 10, 11, 12) which is so arranged as to execute a reciprocating motion and, via a connecting rod (9*a*, 10*a*, 11*a*, 12*a*), the working piston is operatively connected to a first crankshaft (17). Each auxiliary cylinder (5–8) has an auxiliary piston (13, 14, 15, 16) which is so arranged as to execute a reciprocating motion and via a connecting rod (9*a*–12*a*), the auxiliary piston is operatively connected to a second crankshaft (18). Acting between the aforementioned crankshafts is a device (19, 20, 21) to ensure that the motion of the auxiliary piston (13–16) occurs in a relation to the motion of the working piston (9–12), and to provide angular displacement between the shafts (20, 21).

13 Claims, 3 Drawing Sheets

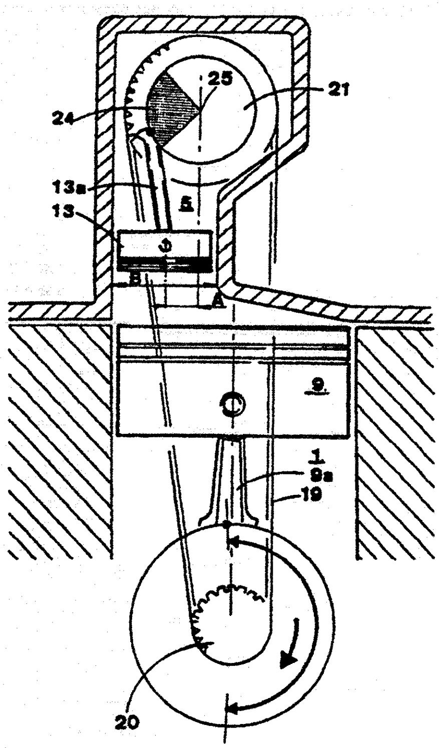

INTERNAL COMBUSTION ENGINE

The present invention relates to an arrangement for an internal combustion engine of the kind which has a number of working cylinders, a corresponding number of auxiliary cylinders, each of which communicates with an associated working cylinder, and in each working cylinder a working piston which is so arranged as to execute a reciprocating motion inside the working cylinder and which, via a connecting rod, is operatively connected to a first crankshaft, in each auxiliary cylinder an auxiliary piston which is so arranged as to execute a reciprocating motion inside the auxiliary cylinder and which, in a similar fashion to the working piston, is operatively connected to a second crankshaft and a device acting between the aforementioned crankshafts to ensure that the reciprocating motion of the auxiliary piston occurs at a frequency related to the frequency of the reciprocating motion of the working piston, and to provide angular displacement between the shafts with a view to the creation of a compression ratio in the respective working cylinders and auxiliary cylinders which is dependent upon the loading on the engine at any given time.

An engine of this construction is previously disclosed, for example, in SE A 7806909-3. Also described here are the advantages which are achieved in respect of thermal efficiency and the nature of the exhaust gases in an engine which exhibits a variable compression ratio. A common feature of previously disclosed engines with a variable, load dependent compression ratio is that energy is taken from the working piston for the purpose of controlling the motion of the auxiliary piston and its instantaneous position in the auxiliary cylinder via the aforementioned device acting between the crankshafts.

Although the engine disclosed through SE A 7806909-A thus exhibits positive features with regard to its efficiency and the composition of the exhaust gases as far as their effect on the environment is concerned, the object of the present invention is to make available an engine of even greater efficiency, in particular in the low-load range of the engine, with this being achieved in accordance with the invention in that the aforementioned device is so arranged as to transmit energy originating from the effect of the combustion on the respective auxiliary piston from the second crankshaft to the first crankshaft, and in that the operative connection between the respective auxiliary piston and the second crankshaft is so arranged as to allow the expansion motion of the auxiliary piston, that is to say its motion away from the working piston, to extend over more than 180° of the rotation of the second crankshaft, and to reduce the lateral forces of the auxiliary piston against the wall of the auxiliary cylinder, which generate frictional losses.

A further object, which is met by an engine in accordance with the invention, is to make available variable piston displacements which reduce the pumping and compression work of the engine.

In accordance with one particular characteristic of the invention, a preferred embodiment of the aforementioned device comprises toothed belt pulleys on the respective crankshafts, a toothed belt running around the belt pulleys, and means of a previously disclosed kind so arranged as to lengthen or shorten one section of the belt at the expense of the other section, in conjunction with which the aforementioned lengthening/-shortening is executed so that the desired angular displacement is achieved, whereby an especially functional and economical construction is obtained.

An operative connection which imparts an expansion motion to the auxiliary piston over more than 180° of the rotation of the second crankshaft, and at the same time reduces its frictional losses, can be appreciated from a second particular characteristic, and in this case means that the operative connection between the respective auxiliary piston and the aforementioned second crankshaft is a connecting rod, and that the axis of rotation of the second crankshaft is displaced in parallel for a certain distance relative to an imaginary line connecting the central axes of the auxiliary cylinders, in conjunction with which the displacement takes place in a direction which coincides with that in which the crank web of the second shaft faces when the auxiliary piston is on its way into the auxiliary cylinder. The aforementioned distance of parallel displacement should preferably lie within the area of 15-35% of the diameter of the auxiliary cylinder, as can be appreciated from a particular characteristic of the invention.

An alternative embodiment of an operative connection of this kind can be appreciated from yet another particular characteristic of the invention, and in this case means that the operative connection between the respective auxiliary piston and the aforementioned second crankshaft is a rocker arm mechanism of a previously disclosed kind.

The invention is explained in greater detail below with reference to the accompanying drawings, in which

FIG. 1 is a perspective view in diagrammatic form of a four-cylinder engine with an arrangement in accordance with the present invention.

FIG. 2 shows a section in diagrammatic form through an engine according to FIG. 1, with a first embodiment of an operative connection between an auxiliary piston and said second crankshaft.

FIG. 3 shows similarly to FIG. 2 an alternative embodiment of the aforementioned operative connection.

The engine in accordance with FIG. 1 exhibits four working cylinders **1**, **2**, **3** and **4**, each of which communicates with a corresponding auxiliary cylinder **5**, **6**, **7** and **8**. In each of the working cylinders **1-4**, and similarly in the auxiliary cylinders **5-8**, working pistons **9**, **10**, **11** and **12** and auxiliary pistons **13**, **14**, **15** and **16** are able to execute reciprocating axial motion. The working pistons **9-12** are operatively connected via connecting rods **9*a*-12*a*** to a working crankshaft **17**. The auxiliary pistons **13-16** are similarly operatively connected via connecting rods **13*a*-16*a*** to an auxiliary crankshaft **18**. Arranged between the crankshafts **17** and **18** are devices which, for the reasons described in the patent specification referred to by way of introduction, cause the reciprocating motion of the auxiliary pistons **13-16** to take place at a frequency related to the reciprocating motion of the working pistons **9-12**, and cause an angular displacement between the crankshafts **17**, **18**, such as to produce in the working cylinders and in the auxiliary cylinders a compression ratio which is dependent on the loading on the engine at any given time. In the case of a four-stroke engine, the frequency of the reciprocating motion of the auxiliary pistons is one half of the frequency of the working pistons. In the case of a two-stroke engine, the aforementioned frequencies are identical. The invention is now explained below in more detail in relation to a four-stroke engine application, with reference to the drawings.

The dependence referred to above is in this case such that the compression ratio is at its lowest under high loading, and at its highest under low loading, that is to say the respective positions of the working pistons and the auxiliary pistons at the moment of ignition, are closest to one another under low load and are furthest away from one another under high load. During the cycle of the working piston 9, which comprises the induction, compression, power and exhaust strokes, during which strokes the working piston 9 moves down, up, down and up, the associated auxiliary piston 13 moves up both during parts of the induction stroke and during the compression and expansion strokes. As will be appreciated from the following, this has been made possible in accordance with the invention in that an operative connection of the kind referred to by way of introduction between the auxiliary piston and the second crankshaft 18, which connection permits the expansion motion of the auxiliary piston 13, that is to say its upward motion during the induction stroke of the working piston, to extend over more than 180° of the rotation of the second crankshaft 18.

A characteristic feature of the invention is that the aforementioned devices acting between the crankshafts are able to transmit energy originating from the effect of the combustion on the respective auxiliary piston 13-16, from the crankshaft 18 to the crankshaft 17. This transmission of energy is effective in particular in the low load range of the engine and contributes to an improved degree of efficiency relative to previously disclosed engines.

The reason why this transmission of energy from the effect of combustion on the auxiliary pistons to the crankshaft 17 contributes in such a particularly effective manner to the high degree of efficiency of the four stroke engine in accordance with the invention is that the auxiliary pistons move at a comparatively low speed, which in itself leads to low frictional losses. Compared with the working pistons, the auxiliary pistons take energy from the combustion process during a much larger proportion of the cycle of the engine than is the case for the working pistons. The reduced induction and compression work and the lower maximum combustion temperature also contribute to lower losses in both four-stroke and two-stroke engines It was thus possible, in a four-stroke test engine in accordance with the invention and at a certain degree of loading, to measure a generated effect on the auxiliary crankshaft 18 as high as approximately 1/5 of the effect generated on the working crankshaft 17, in conjunction with which, however, the frictional losses via the auxiliary crankshaft 18 were only 1/15 of the frictional loss via the working crankshaft 17.

In the embodiment illustrated in the drawings, the aforementioned device consists of a toothed belt 19 which runs around toothed belt pulleys 20, 21 arranged on the crankshafts 17 and 18. The toothed belt pulley 21, in this case for a four-stroke engine, has a diameter which is twice as large as the diameter of the toothed belt pulley 20, in order for the auxiliary pistons 13-16 to execute their reciprocating motion in the manner described above, that is to say at a frequency which is one half as great as the frequency of the working pistons 9-12. In the case of a two-stroke engine the toothed belt pulleys 20, 21 have identical diameters, so that the frequency of the reciprocating motion of both the working pistons and the auxiliary pistons is identical.

The aforementioned angular or phase displacement between the crankshafts can thus by produced by some previously disclosed method, for example by lengthening one section of the belt 19 at the expense of the other section, as described in U.S. Pat. No. 4,104,995. The actual angular or phase displacement can be seen in FIG. 2 as a sector 24 of a circle marked with a pattern of dots. Otherwise this Figure and FIG. 3 use the same reference designations as are used in FIG. 1 for the cylinder 1 nearest the belt 19 and the associated parts of the engine.

A second characteristic feature of the internal combustion engine in accordance with the present invention is that the centre of rotation 23 of the auxiliary crankshaft 18 is displaced by a certain distance A relative to an imaginary line 24 connecting the central axes of the auxiliary cylinders 5-8. The displacement in this case is such that the distance A amounts to 15-35% of the diameter B of the auxiliary cylinder 5. This lateral parallel displacement, known as the offset, contributes to reduced lateral forces acting on the auxiliary pistons and consequently to reduced frictional losses in relation to what is achieved in a conventional engine, and thus to a further improvement in the degree of efficiency of the engine in accordance with the invention. The lateral parallel displacement also contributes to an increased length of stroke for the auxiliary pistons 13-16, and to an expansion motion for the auxiliary pistons over more than 180° of the rotation of the working crankshaft 17.

With regard to the positive effect of the displacement A on the degree of efficiency of the engine in accordance with the invention, the lower frictional losses can be attributed first and foremost to the low guide forces acting on the auxiliary pistons which have been achieved.

An alternative embodiment of an engine in accordance with the invention to achieve low guide forces and an even higher degree of expansion motion over an even greater proportion of the rotation of the working crankshaft 17 than has previously been disclosed is shown in FIG. 3. The operative connection between the auxiliary piston 13 and the second crankshaft 18 is a rocker arm 26 which is pivotally mounted on a shaft 27, and one end of which is attached to the connecting rod 13*a*. The other end of the rocker arm 26 is connected to the auxiliary crankshaft 18 via a link arm 26*a*. The rocker arm 26 has been given a design such that a pivot point 26*a* between the rocker arm 26 and the connecting rod 13*a* lies essentially above the centre of the auxiliary piston 13 during the up-and-down motion of the piston 13, which means that this is subjected to only small guide forces. Another advantage associated with the rocker arm mechanism is that the lateral displacement, which takes place to a higher degree than that previously described, provides automatic adaptation of the volumetric efficiency of the engine to the load imposed on it. What this means is that, under a low engine load, the respective auxiliary piston moves towards the associated working piston and in so doing reduces the volumetric efficiency, whereas under a high engine load the auxiliary piston moves away from the working piston during its induction stroke so that the volumetric efficiency is increased

It is obvious that the invention can be implemented in various ways within the scope of the idea of invention. This is particularly true of the embodiment of the operative connection between the crankshafts 17 and 18, which can also be provided, for example, by an hydraulic transmission of a previously disclosed kind, but also of the size ratios between the respective volumes of the working and auxiliary cylinders and the respective diameters of the working and auxiliary pistons.

It should be noted that the arrangement in accordance with the invention is not restricted to internal combustion engines of the two-stroke or Otto-cycle type, but can be applied to similar engines of the fuel-injection or Diesel type.

I claim:

1. Arrangement for an internal combustion engine of the kind which has a number of working cylinders, a corresponding number of auxiliary cylinders, each of which communicates with an associated working cylinder, and in each working cylinder a working piston which is so arranged as to execute a reciprocating motion inside the working cylinder and which, via a connecting rod, is operatively connected to a first crankshaft, in each auxiliary cylinder an auxiliary piston which is so arranged as to execute a reciprocating motion inside the auxiliary cylinder and which, in a similar fashion to the working piston, is operatively connected to a second crankshaft, and a device acting between the aforementioned crankshafts to ensure that the reciprocating motion of the auxiliary piston occurs at a frequency related to the frequency of the reciprocating motion of the working piston, and to provide angular displacement between the shafts, with a wherein a compression ratio in the respective working cylinders and auxiliary cylinders is dependent upon the loading on the engine at any given time, characterized in that the aforementioned devices are so arranged as to transmit energy originating from the effect of the combustion on the respective auxiliary piston from the second crankshaft to the first crankshaft, and in that the operative connection between the respective auxiliary piston and the second crankshaft, is so arranged so to allow the expansion motion of the auxiliary piston, that is to say its motion away from the working piston, to extend over more than 180° of the rotation of the second crankshaft, and to reduce the lateral forces of the auxiliary piston against the wall of the auxiliary cylinder, which generate frictional losses.

2. Arrangement in accordance with claim 1, characterized in that the aforementioned device comprises toothed belt pulleys on the respective crankshafts, a toothed belt disposed about the belt pulleys, and means for lengthening and shortening one section of the belt at the expense of the other section, in conjunction with which the aforementioned lengthening/shortening is executed so that the desired angular displacement is achieved.

3. Arrangement in accordance with claim 1, characterized in that the operative connection between the respective auxiliary piston and the aforementioned second crankshaft is a connecting rod, and in that the axis of rotation of the second crankshaft is displaced in parallel for a certain distance relative to an imaginary line connecting the central axes of the auxiliary cylinders, in conjunction with which the displacement takes place in a direction which coincides with that in which the crank web of the second shaft faces when the auxiliary piston is on its way into the auxiliary cylinder.

4. Arrangement in accordance with claim 3, characterized in that the aforementioned distance of parallel displacement lies preferably within 15-35% of the diameter of the auxiliary cylinder.

5. Arrangement in accordance with claim 1, characterized in that the operative connection between the respective auxiliary piston and the aforementioned second crankshaft is a rocker arm mechanism of a previously disclosed kind.

6. An internal combustion engine, comprising:

a working cylinder;

an auxiliary cylinder in communication with said working cylinder;

a working piston reciprocatingly disposed within said working cylinder and operatively connected to a first crankshaft via a connecting rod;

an auxiliary piston reciprocatingly disposed within said auxiliary cylinder and operatively connected to a second crankshaft; and

a timing device for establishing a relative rotational frequency between said first and second crankshafts and for providing an angular phase displacement between the said first and second crankshafts, said device adapted to transmit rotational energy from said second crankshaft to said first crankshaft, wherein a compression ratio in said working cylinder and in said auxiliary cylinder is dependent upon the loading of the engine at any given time;

wherein said operative connection is such that upon movement of said auxiliary piston away from said working piston, said auxiliary piston causes said second crankshaft to rotate more than 180 degrees.

7. The engine of claim 6, wherein said device comprises a toothed belt pulley on each of said respective crankshafts, a toothed belt disposed around said belt pulleys, sand means for lengthening and shortening a section of said belt at the expense of the other section so that a desired angular displacement is achieved.

8. The engine of claim 6, wherein the operative connection between said respective auxiliary piston and said second crankshaft is a second connecting rod, wherein the axis of rotation of said second crankshaft is displaced in parallel for a given distance relative to an imaginary line connecting the central axis of said auxiliary cylinder, wherein the displacement takes place in a direction which coincides with that in which said crank web of said second shaft faces when said auxiliary piston moves into said auxiliary cylinder.

9. The engine of claim 8, wherein said distance of parallel displacement ranges from about 15% to about 35% of the diameter of said auxiliary cylinder.

10. The engine of claim 6, wherein the operative connection between said respective auxiliary piston and said second crankshaft is a rocker arm mechanism.

11. The engine of claim 6, wherein said auxiliary piston is substantially smaller than said working piston.

12. The engine of claim 6, wherein the frequency at which said auxiliary cylinder reciprocates is at one-half of the frequency at which said working cylinder reciprocates.

13. The engine of claim 6, wherein the frequency at which said auxiliary cylinder reciprocates is the same as that of said working cylinder.

* * * * *

FIG 1

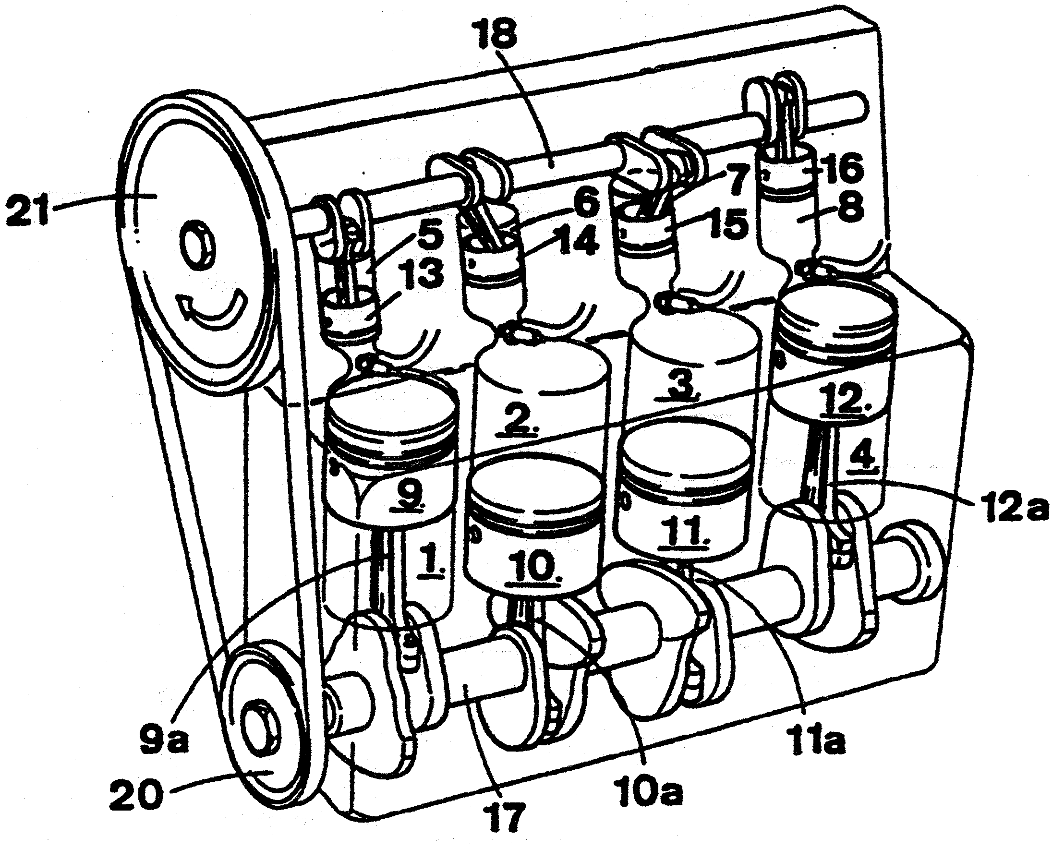
18
21
5
6
7
16
8
15
14
13
2.
3.
12.
9.
4.
12a
1.
10.
11.
9a
20
17
10a
11a

FIG 2

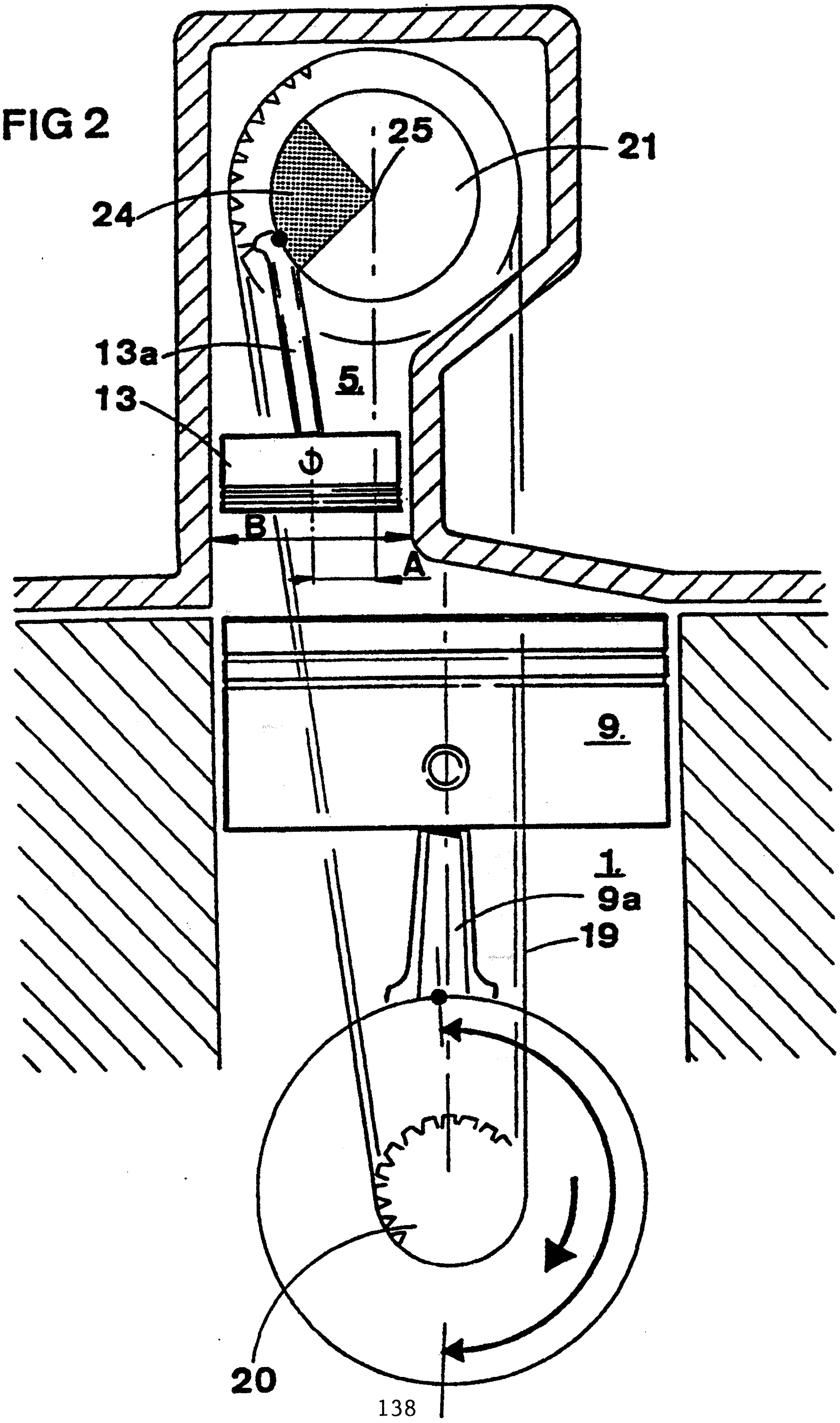
25
21
24
13a
5
13
B
A
9
1
9a
19
20

FIG 3

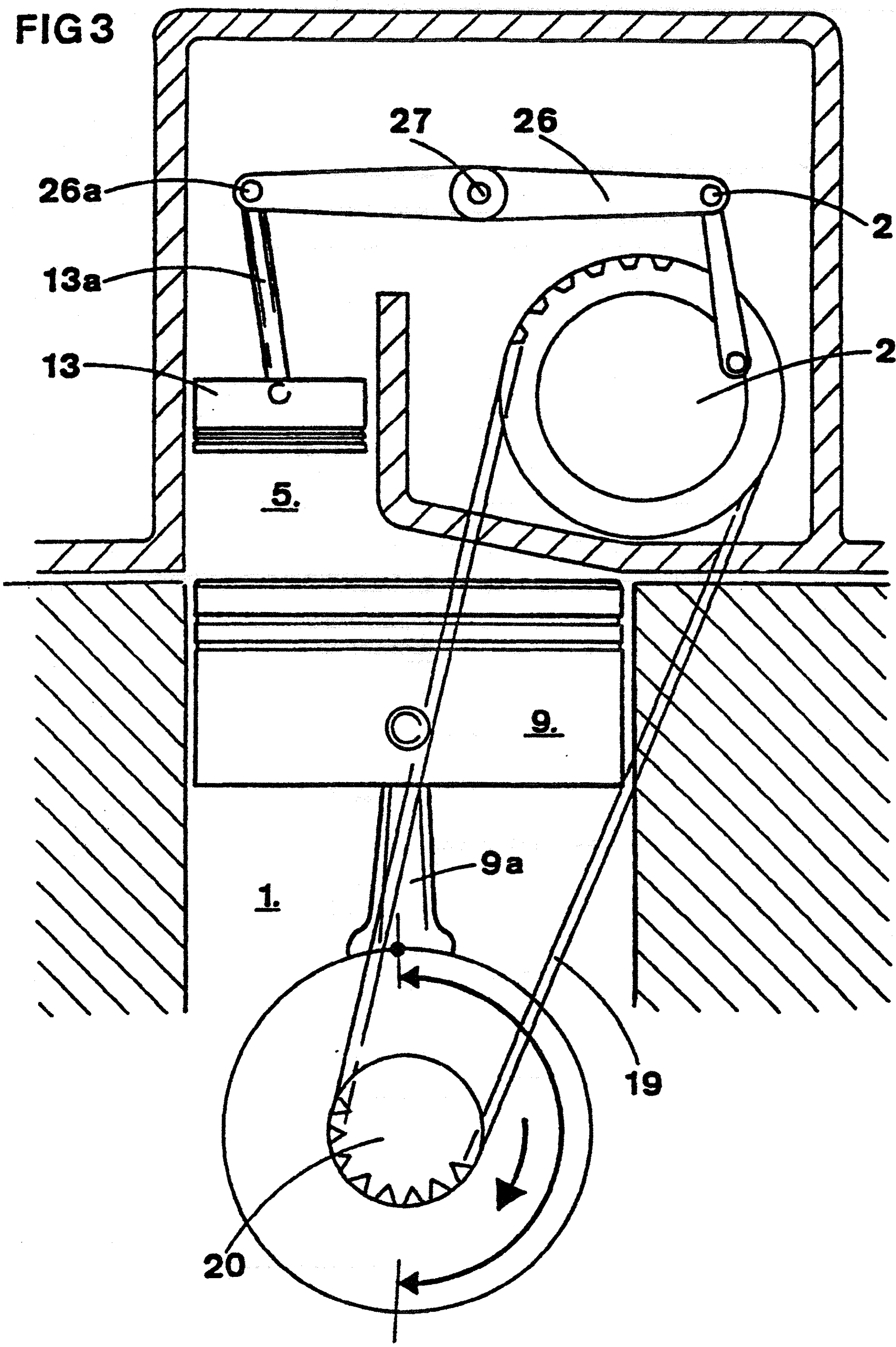
27
26
26a
26b
13a
13
21
5.
9.
9a
1.
19
20